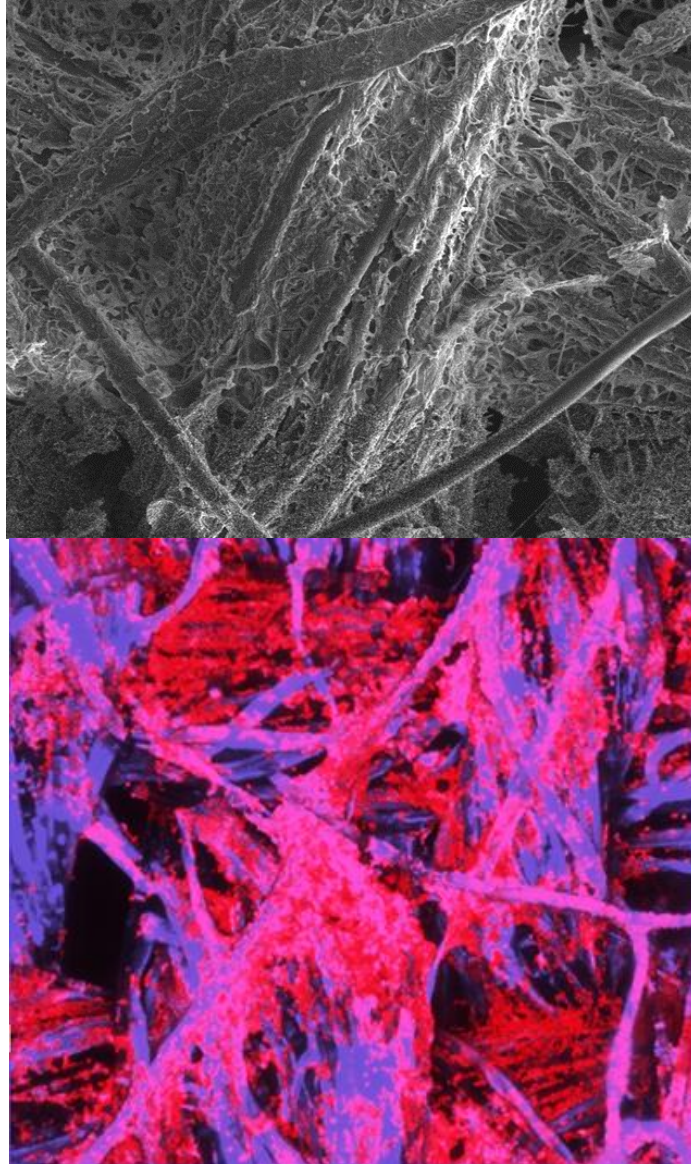


# DEVELOPING A HARVESTING PROCESS FOR ALGAL BIOMASS PRODUCTION



**Oksana Vronska**  
BEng, MEng

*Thesis submitted in fulfilment of the requirements for the award of Doctor  
of Philosophy degree, Faculty of Science/Climate Change Cluster  
(UTS:C3)*

University of Technology Sydney

June 2019

## **CERTIFICATE OF ORIGINAL AUTHORSHIP**

I, Oksana Vronska, declare that this thesis is submitted in fulfilment of the requirements for the award of Doctor of Philosophy degree, in the Faculty of Science/School of Life Sciences at the University of Technology Sydney.

This thesis is wholly my own work unless otherwise reference or acknowledged. In addition, I certify that all information sources and literature used are indicated in the thesis.

This document has not been submitted for qualifications at any other academic institution.

This research is supported by the Australian Government Research Training Program.

Production Note:

Signature removed  
prior to publication.

Signed: Oksana Vronska (PhD Candidate)

Date: 23.06.2019

## ACKNOWLEDGEMENTS

I would like to express my deepest gratitude to my primary supervisor, **Professor Peter Ralph**, for the opportunity to carry out this exciting and challenging research. His constant support and wise leadership helped me progress and develop.

I am forever thankful to my co-supervisor **Dr Bojan Tamburic** for his guidance, motivation, never-ending enthusiasm and setting high standards. His door was always open, his feedback was structured and constructive, and his trust in my abilities inspired me to keep moving, conquering, and never stop achieving in all aspects of life.

I would also like to thank **Max Garavaglia**, my industry collaborator, for the support, advice, useful discussions, and being incredibly helpful in both professional and personal matters.

I am grateful to **Dr Audrey Commault** for her cheerful attitude, helpfulness and openness.

This part of my life's journey was made enjoyable, easy, fun-filled and unforgettable by the people who were next to me every day. I am most grateful to **Ben** and **Liz Evans** for becoming my second true family in Sydney.

Finally, no words can describe how thankful I am to my mother **Iryna Vronska** and my grandmother **Lydia Mandryka** for their eternal and unconditional love.

## **PREFACE**

In my thesis, **Chapter 1**, **Chapter 2** and **Chapter 4** are intended to be submitted for publication in peer-reviewed journals. A certain degree of repetition is present.

In association with my PhD, I have been a co-author on a publication that is relevant to my thesis, but does not contribute to it. The work presented in Chekli et al. (2017) used titanium-based coagulants for microalgae removal from freshwaters as an alternative method of biomass harvesting.

Chekli, L., Eripret, C., Park, S.H., Tabatabai, S. A. A., **Vronska, O.**, Tamburic, B., Kim, J.H. & Shon, H.K. 2017, 'Coagulation performance and floc characteristics of polytitanium tetrachloride (PTC) compared with titanium tetrachloride (TiCl<sub>4</sub>) and ferric chloride (FeCl<sub>3</sub>) in algal turbid water', *Separation and Purification Technology*, vol. 175, pp. 99–106.

## CONTENTS

CERTIFICATE OF ORIGINAL AUTHORSHIP .....	ii
ACKNOWLEDGEMENTS .....	iii
PREFACE .....	iv
LIST OF FIGURES .....	ix
LIST OF TABLES .....	xiv
ABSTRACT .....	xv
<b>CHAPTER 1. GENERAL INTRODUCTION .....</b>	<b>17</b>
1.1 Microalgal biomass .....	17
1.2 Cultivation and harvesting of microalgae .....	17
1.3 Science of biofilm formation.....	19
1.4 Existing biofilm systems .....	22
1.5 Thin-layer cascade systems .....	29
1.6 Biofilm attachment materials .....	34
1.7 Operational conditions of biofilm systems.....	36
1.8 Imaging of biofilms .....	37
1.9 References .....	39
<b>CHAPTER 2. SELECTION OF A BIOFILM ATTACHMENT MATERIAL .....</b>	<b>48</b>
2.1 Introduction .....	48
2.2 Aim and objectives .....	51
2.3 Research methodology .....	52
2.3.1 Experimental procedure.....	52
2.3.2 Initial cell attachment test. Stock culture of <i>Dunaliella tertiolecta</i> .....	52
2.3.3 Experimental culture of <i>Dunaliella tertiolecta</i> .....	52
2.3.4 Fabrics for microalgal biofilms formation.....	52
2.3.5 Initial attachment experimental setup and sampling.....	55

2.3.6 Biofilm development on liquid-air interface. Stock culture of <i>Chlorella vulgaris</i> .....	55
2.3.7 Experimental setup and conditions .....	56
2.3.8 Scanning electron microscopy – fabric structure.....	57
2.3.9 Confocal laser scanning microscopy – biofilm structure.....	58
2.3.10 Quantification of attached microalgal density on the fabrics .....	59
2.3.11 Confocal laser scanning microscopy – biofilm thickness.....	59
2.4 Results and discussion.....	61
2.5 Summary .....	81
2.6 References .....	83
<b>CHAPTER 3. DEVELOPMENT OF A BIOFILM SYSTEM TO BE INSTALLED IN RACEWAY PONDS.....</b>	<b>87</b>
3.1 Introduction .....	87
3.2 Aim and objectives .....	88
3.3 Research methodology .....	88
3.3.1 Growth conditions and limitations in a raceway pond. Stock culture of <i>Nannochloropsis oceanica</i> .....	88
3.3.2 Experimental culture of <i>Nannochloropsis oceanica</i> .....	88
3.3.3 Design and equipment of the rooftop raceway pond .....	89
3.3.4 Volumetric oxygen mass transfer .....	91
3.3.5 Evaporative loss in the raceway pond.....	91
3.3.6 Monitoring of microalgal growth conditions.....	92
3.3.7 Sampling protocol.....	92
3.3.8 Dry weight .....	93
3.3.9 Automated cell density determination .....	93
3.3.10 Chlorophyll <i>a</i> extraction .....	93
3.3.11 Nitrate concentration.....	94
3.3.12 Light attenuation in the raceway pond.....	94

3.3.13 Biofilm system design .....	95
3.3.14 Biofilm system operation. Stock culture of <i>Chlorella vulgaris</i> .....	96
3.3.15 Experimental culture of <i>Chlorella vulgaris</i> .....	96
3.3.16 Raceway pond inoculation.....	97
3.3.17 Raceway pond dilutions.....	97
3.3.18 Mounting of fabrics on paddlewheels.....	97
3.4 Results and discussion.....	99
3.5 Summary .....	115
3.6 References .....	116
Supplement 3.1 .....	119
<b>CHAPTER 4. DEVELOPMENT OF A MODIFIED CASCADE SYSTEM FOR ATTACHED BIOMASS PRODUCTION .....</b>	<b>121</b>
4.1 Introduction .....	121
4.2 Aim and objectives .....	124
4.3 Research methodology .....	125
4.3.1 Stock and experimental cultures of <i>Nannochloropsis oceanica</i> .....	125
4.3.2 Experimental setup – cascade system.....	125
4.3.3 Optical density .....	127
4.3.4 Biomass sampling and harvesting.....	127
4.3.5 Biofilm imaging and quantitative image processing .....	128
4.3.6 Mass fraction of biomass to water and biomass productivity.....	130
4.3.6 Statistical analysis.....	130
4.4 Results and discussion.....	131
4.5 Summary .....	139
4.6 References .....	140
Supplement 4.1 .....	145
Supplement 4.2.....	147

<b>CHAPTER 5. GENERAL CONCLUSIONS AND PERSPECTIVES FOR FUTURE RESEARCH</b> .....	148
5.1 References .....	156

## LIST OF FIGURES

<b>Figure 1.1</b> Biofilm formation process: <i>A</i> – surface conditioning with organic molecules followed by microorganism attachment; <i>B</i> – stable biofilm formation in a matrix of EPS .....	21
<b>Figure 1.2</b> Existing pilot-scale biofilm systems: <i>A</i> – twin-layer system; <i>B</i> – Rotating Algal Biofilm Reactor (RABR); <i>C</i> – Algadisk system; <i>D</i> – Revolving Algal Biofilm (RAB) reactor.....	29
<b>Figure 2.1</b> A fabric sample partially submerged in <i>C. vulgaris</i> suspension.....	57
<b>Figure 2.2</b> Experimental setup – flasks containing fabrics with biofilms submerged in microalgal suspension: blue stripes – coated blend samples; red stripes – cotton samples; green stripes – uncoated blend samples .....	57
<b>Figure 2.3</b> Top view of a 3-dimensional CLSM image of <i>C. vulgaris</i> biofilm on a fabric: <i>A</i> – before compression with ImageJ (Fiji) software; <i>B</i> – after compression with ImageJ (Fiji) software .....	59
<b>Figure 2.4</b> Microalgal cell diffusion in agarose with time .....	60
<b>Figure 2.5</b> Change in fabric colour due to <i>D. tertiolecta</i> biofilm formation between the first day (Day 0) and the last day (Day 7) of the initial attachment experiment.....	64
<b>Figure 2.6</b> OD of suspended <i>D. tertiolecta</i> culture: <i>A</i> – OD in the Petri dishes with cotton (C) and hessian (H) samples; <i>B</i> – OD in the Petri dishes with coated blend (CB) and polar fleece (F) samples; <i>C</i> – OD in the Petri dishes with hemp & linen blend (HL) and linen (L) samples .....	66
<b>Figure 2.7</b> Coated blend structure imaged with SEM at different magnifications.....	69
<b>Figure 2.8</b> Cotton structure imaged with SEM at different magnifications .....	70
<b>Figure 2.9</b> Uncoated blend structure imaged with SEM at different magnifications.....	72
<b>Figure 2.10</b> <i>C. vulgaris</i> biofilm development with time on coated blend, uncoated blend and cotton fabrics imaged by CLSM (red channel – microalgal chlorophyll	

autofluorescence, blue channel – Hoechst 33342 stained fabric fibres fluorescence; imaged square size 636 $\mu\text{m}$ x 636 $\mu\text{m}$ , variable depths): <b>A</b> – imaged biofilms after 7 days of attached growth; <b>B</b> – imaged biofilms after 14 days of attached growth; <b>C</b> – imaged biofilms after 21 days of attached growth; <b>D</b> – imaged biofilms after 28 days of attached growth .....	75
<b>Figure 2.11</b> Quantitative analysis of CLSM images: microalgal chlorophyll autofluorescence for two images (measurement 1 and measurement 2) at each datapoint: <b>A</b> – coated blend; <b>B</b> – cotton; <b>C</b> – uncoated blend.....	76
<b>Figure 2.12</b> Microalgal biofilm cross-sections on coated blend, cotton and uncoated blend for biofilm thickness measurements .....	79
<b>Figure 3.1</b> Rooftop raceway pond: <b>A</b> – raceway pond; <b>B</b> – microalgal culture in the raceway pond .....	90
<b>Figure 3.2</b> Air diffusers with metal loads.....	90
<b>Figure 3.3</b> HOBO Data Loggers positions in the raceway pond: (1) above the microalgal culture surface; (2) in the top layer of the culture; (3) close to the bottom of the pond; (4) microalgal suspension in the pond .....	92
<b>Figure 3.4</b> Nitrate analysis standard.....	94
<b>Figure 3.5</b> Schematic design of a biofilm device in the form of a paddlewheel (dimensions in mm) .....	95
<b>Figure 3.6</b> Schematic diagram of the paddlewheels with the fabrics in the raceway pond .....	98
<b>Figure 3.7</b> Light intensity measured in the rooftop raceway pond.....	99
<b>Figure 3.8</b> Temperature measured in the rooftop raceway pond.....	100
<b>Figure 3.9</b> Daily variations in environmental conditions in the rooftop raceway pond: <b>A</b> – daily light intensity; <b>B</b> – daily temperature.....	102
<b>Figure 3.10</b> OD of <i>N. oceanica</i> in the rooftop raceway pond .....	103

<b>Figure 3.11</b> Comparison between OD and automated cell density of <i>N. oceanica</i> in the rooftop raceway pond.....	104
<b>Figure 3.12</b> DW per cell of the microalgal culture in the rooftop raceway pond .....	105
<b>Figure 3.13</b> Relationship between attenuation coefficient ( <i>a</i> ) and OD of the microalgal culture in the rooftop raceway pond; shaded section marks light limitation .....	107
<b>Figure 3.14</b> Relationship between pH and OD measured in the rooftop raceway pond; shaded section marks CO <sub>2</sub> limitation .....	108
<b>Figure 3.15</b> Relationship between nitrate concentration and OD measured in the rooftop raceway pond; shaded section marks nitrate limitation .....	109
<b>Figure 3.16</b> Microalgal culture growth limitations identified in the raceway pond.....	110
<b>Figure 3.17</b> The 4 paddlewheels in the rooftop raceway pond .....	111
<b>Figure 3.18</b> Microalgal culture growth determined by OD and turbidity measurements in the raceway pond .....	112
<b>Figure 3.19</b> Higher microalgal cell accumulation at the liquid-air interface on an attachment material mounted on a vane of a paddlewheel .....	113
<b>Figure 3.20</b> Dense microalgal biofilm at the liquid-air interface grown in the laboratory .....	114
<b>Figure 4.1</b> Cascade reactors: <i>A</i> – reactor A (left) and reactor B (right) components, 1 – media distribution tubes, 2 – channels for biofilm formation, 3 – collection flasks with pumps; <i>B</i> – <i>N. oceanica</i> biofilm formation on coated blend fabric in the reactor channels.....	127
<b>Figure 4.2</b> Confocal image compression for the quantification of attached microalgal autofluorescence and stained fibre fluorescence in reactor A after 14 days (2 weeks) of cascade system operation: red stacks represent layers covered by algal cells; blue stacks represent underlying fibres.....	129

<b>Figure 4.3</b> Compressed confocal images of a biofilm before and after harvesting: red colour – chlorophyll autofluorescence; blue colour – Hoechst 33342 stained fabric fluorescence; <b>A</b> – reactor A, 14 days/2 weeks of cascade system operation, before harvesting; <b>B</b> – reactor B, 21 days/3 weeks of cascade system operation, after harvesting .....	129
<b>Figure 4.4</b> <i>N. oceanica</i> biofilm in reactor B at different timepoints of cascade system operation: <b>A</b> – initial cell settlement immediately after inoculation on Day 0; <b>B</b> – initial attachment (7 days, week 1); <b>C</b> – third biofilm growth/harvesting cycle (28 days, week 4) .....	131
<b>Figure 4.5</b> Cotton fabric damage after 4 weeks of growing <i>N. oceanica</i> biofilms in a cascade system under laboratory conditions .....	134
<b>Figure 4.6</b> Spatial distribution of microalgal cells on the coated blend fibres in reactor B: red colour – chlorophyll autofluorescence; blue colour – Hoechst 33342 stained fabric fluorescence; imaged square size 600 µm x 600 µm, variable depths; <b>A</b> – <i>N. oceanica</i> biofilm after 7 days/1 week of cascade system operation; <b>B</b> – <i>N. oceanica</i> biofilm after 14 days/2 weeks of cascade system operation; <b>C</b> – <i>N. oceanica</i> biofilm after 28 days/4 weeks of cascade system operation; <b>D</b> – <i>N. oceanica</i> biofilm after 35 days/5 weeks of cascade system operation .....	135
<b>Figure 4.7</b> Quantification of Hoechst 33342 stained fabric fluorescence ( <b>A</b> ) and attached microalgal fluorescence ( <b>B</b> ), and the ratio between these values ( <b>C</b> ). *p < 0.05; **p < 0.01; ***p < 0.001. ....	137
<b>Figure S4.1</b> 65% polyester and 35% cotton with plastic polymer coating fabric (coated blend).....	145
<b>Figure S4.2</b> 65% polyester and 35% cotton without coating .....	146
<b>Figure S4.3</b> Cell density of the suspended biomass during the first week of the cascade system operation. The steady decrease in the suspended biomass density was recorded due to cell attachment to the fabrics and biofilm formation .....	147

**Figure 5.1** Steps undertaken in my thesis to select the most beneficial fabric for microalgal cell attachment ..... 149

## LIST OF TABLES

Table 1.1 Summary of the developed biofilm systems performance.....	22
Table 1.2 Summary of cascade systems operation.....	33
Table 2.1 Fabrics used in the experiment and their cost.....	53
Table 2.2 Properties of fabrics .....	54
Table 2.3 Performance of the fabrics in the experiment .....	67
Table 2.4 Summary of experimental procedure and main outputs of fabric attachment material selection .....	80
Table S3.1 Experimental run attempts in the rooftop raceway pond retrofitted with the microalgal biofilm system.....	119
Table 4.1 Mass fractions of biomass to water ( $f_x/w$ ) and aerial productivity ( $P_x$ ) of the biofilms in the cascade system.....	133
Table 4.2 Percentage of attached biofilm biomass harvested by scraping.....	137
Table 5.1 Main results from biofilm systems operation .....	151

## ABSTRACT

Microalgal biomass is a promising alternative energy feedstock. Its commercial production currently entails suspended cultivation of microscopic cells in large liquid volumes. Microalgal harvesting, *i.e.* separation of the cells from the liquid, is an energy-intensive and expensive process that makes large-scale biomass production economically challenging. In my thesis, an alternative technique for microalgal biomass cultivation and harvesting was developed. The cells were grown in biofilm systems attached to fabrics, thus being naturally concentrated and easy to harvest by simple mechanical scraping.

The selection of fabrics used for microalgal attachment remains an open question, and it is a critical factor in overall performance of a biofilm system. In my thesis, a durable fabric with a special web-like coating that promoted microalgal cell attachment was identified and tested. This fabric is being successfully used by an industry collaborator for bacterial biofilm cultivation and wastewater treatment. The distinctive features, fibre structure and arrangement of this fabric were compared with other fabrics commonly used in the literature to determine possible reasons for its improved performance. Gradual biofilm formation process was imaged by confocal laser scanning microscopy to analyse the specifics of cell attachment and development of a mature biofilm. A method for quick and easy biofilm thickness measurement was developed. Two microalgal biofilm systems were designed and custom-built for attached biomass growth and harvesting at laboratory scale and at pilot scale.

The maximum surface productivity achieved during attached microalgal cultivation was  $25.2 \text{ g m}^{-2} \text{ d}^{-1}$ . The mass fraction of biomass to water of the harvested microalgal sludge was above  $150 \text{ g kg}^{-1}$ , which was comparable to dewatered and concentrated biomass from suspended biomass systems. The experiments also revealed a pattern of biofilm development, where the liquid-air interface of the fabrics was characterised by the highest cell attachment. This observation could be valuable for future design of attached systems. Mechanical scraping proved to be an efficient method of biofilm harvesting, with 95.2-98.7% biomass removed. The above-average algal productivity, together with the high dry biomass concentration and efficient harvesting, indicates that the growth and harvesting technique developed in this thesis represents a promising alternative to

suspended biomass cultivation. It does not require expensive dewatering and drying steps, so it could substantially decrease commercial biomass production costs.

## **CHAPTER 1. GENERAL INTRODUCTION**

### **1.1 Microalgal biomass**

The energy crisis resulting from continuous growth of the world's population (Misra et al. 2016), as well as limited fossil fuel reserves, and the necessity to introduce low greenhouse gas emission fuels, has drawn attention to a diverse group of microscopic photosynthetic organisms – microalgae (Odjadjare, Mutanda & Olaniran 2015). Biomass derived from microalgae is a promising alternative energy source; it can be converted into biodiesel, bioethanol, biohydrogen, methane and bioelectricity (Baicha et al. 2016). The advantages of microalgae as a feedstock for biofuel production are extensive, including: easy cultivation with sunlight and inorganic nutrients; the ability to grow in wastewater; and reduced land area requirements for the same level of productivity compared to other agricultural, aqueous and forestry plants (Mata, Martins & Caetano 2010). Microalgal biomass is also being used in the production of commercial high-value compounds such as pigments and enzymes (Odjadjare, Mutanda & Olaniran 2015).

Microalgal harvesting for commercial, large-scale microalgal biomass production, which involves separation of microscopic cells from large liquid volumes, is energy-intensive, expensive and therefore currently not commercially feasible (Zeng et al. 2016). This thesis will develop alternative cost-effective methods of microalgae cultivation and harvesting for biomass production.

### **1.2 Cultivation and harvesting of microalgae**

Microalgal biomass production usually starts with species selection, depending on the local conditions and the desired product, followed by microalgal cultivation, harvesting and biomass processing (Mata, Martins & Caetano 2010). One of the crucial steps in obtaining microalgal biomass for commercial applications is the design of an economical and reliable microalgal cultivation system (Voloshin et al. 2016). In order to generate microalgal biomass, a number of factors that influence microalgal growth should be considered including: abiotic (light availability, temperature, nutrient and carbon dioxide concentration, pH, salinity), biotic (competing microorganisms and

pathogens) and production (shear stress, harvesting, dilution rate) (Mata, Martins & Caetano 2010).

At laboratory scale, microalgal cultivation can be carried out in fermenters, internally-illuminated photobioreactors (PBRs) or tanks (Amin 2009). For large scale production, microalgae are grown in open-air and closed systems (Voloshin et al. 2016). There are four main types of open-air cultivation systems in use: shallow large ponds, tanks, circular ponds and raceway ponds; these systems have various advantages and disadvantages (Borowitzka 1999).

Among the existing variety of PBR designs, tubular PBRs are considered suitable for outdoor commercial microalgal biomass production (Ugwu, Aoyagi & Uchiyama 2008). As for the open systems, only raceway ponds are capable of producing large enough volumes of microalgal biomass at commercial scale (Grobelaar 2012). PBRs are expensive and hard to scale-up, which is why raceway ponds are the most common operating commercial system for biomass production (Borowitzka & Moheimani 2013).

A typical raceway pond is comprised of closed loop recirculation channels 0.2–0.5 m deep (Brennan & Owende 2010); it can be made of concrete or compacted soil, sometimes with white plastic lining (Chisti 2008). A paddlewheel installed in the raceway pond serves multiple purposes, including maintaining cell suspension, eliminating thermal stratification, promoting nutrient and gas transportation, and improving light utilisation (Terry & Raymond 1985). The major advantages of microalgal cultivation in raceway ponds include low energy requirements in comparison with tubular PBRs (Norsker et al. 2011) and relative simplicity in design and maintenance (Brennan & Owende 2010). The drawbacks include considerable evaporative losses, poor mixing, relatively low biomass density and high risk of contamination (Chisti 2008).

Another essential step in microalgal biomass production is harvesting, which involves microalgal biomass recovery from the growth medium. This process requires microscopic cell separation from large volumes of water, and thus accounts for 20–30% of the total production cost (Molina Grima et al. 2003). In general, harvesting is performed by centrifugation, sedimentation or (ultra-)filtration, sometimes with an additional flocculation step (Mata, Martins & Caetano 2010); these methods are usually

not only energy expensive, but also time-consuming (Chen et al. 2011). Unfortunately, there is no universally affordable harvesting method for commercialised microalgal biomass production (Laamanen, Ross & Scott 2016), and intensive research efforts need to be directed at enhancing existing harvesting methods as well as introducing new ones.

For commercial water and wastewater treatment purposes, microalgae are typically removed by the following sequence of processes: pre-oxidation, coagulation and flocculation, and clarification by sedimentation or dissolved air flotation (Henderson, Parsons & Jefferson 2008; Borowitzka & Moheimani 2013). Dissolved air flotation (DAF) is a solid-liquid separation process where microscopic bubbles are introduced to a suspension with microalgal flocs (Yap et al. 2014). The bubbles collide and attach to the flocs bringing them to the liquid surface (Henderson, Parsons & Jefferson 2010) forming a floating layer, which can subsequently be removed mechanically or hydraulically (Yap et al. 2014). Although DAF has been successfully applied at large-scale (Christenson & Sims 2011), further downstream processes may be adversely affected due to the addition of flocculants used to overcome electrostatic repulsion in a microalgal suspension (Molina Grima et al. 2003).

Microalgal growth as a biofilm attached to a solid attachment material, as opposed to a suspended culture, offers advantages in terms of easy biomass harvesting by scraping, which eliminates time-consuming and expensive conventional harvesting methods (Johnson & Wen 2010).

### **1.3 Science of biofilm formation**

A biofilm is a layer of structured microbial communities that accumulate at a solid-liquid interface (Flemming & Wingender 2010). Biofilms can attach to a surface in almost any moist environment provided that a sufficient quantity of nutrients and light is available (Singh, Paul & Jain 2006). The microorganisms can aggregate on a surface as a monolayer biofilm, in which cells attach only to the attachment material, or as a multilayer biofilm, where the microorganisms assemble into clusters that adhere both to the attachment material and to the other cells (Karatan & Watnick 2009). A biofilm usually consists of water and microscopic cells, as well as a mixture of polymers, nutrients, metabolites, cell lysis products, and attachment material components (Singh,

Paul & Jain 2006). Apart from a wide range of environmental and physiological factors, the process of biofilm formation depends on the type and diversity of microorganisms, as it can be formed by a single bacterial species, or a complex community of bacteria, algae, fungi and protozoa (Singh, Paul & Jain 2006). In general, this process can be divided into two stages – initial physicochemical cell adsorption, and secondary cell attachment with production of extracellular polymeric substances (EPS) (Bos, Van Der Mei & Busscher 1999; Dunne 2002). Some studies distinguish another stage in the attachment process, called surface conditioning (Dunne 2002), which occurs in a moist environment with the presence of organic matter (Bos, Van Der Mei & Busscher 1999).

The formation of a ‘conditioning film’ composed of adsorbed organic molecules precedes the initial cell adsorption stage due to the more rapid attachment of organic molecules to an attachment material when compared with microorganism adhesion (**Figure 1.1A**) (Bos, Van Der Mei & Busscher 1999). Planktonic cultures, where cells move freely in the liquid, would normally prefer suspended growth. However, the net sum of attractive and repulsive forces that arise between a microorganism and an attachment material surface determines the initial reversible attachment, which takes place when the microorganism moves towards or is transported to the attachment material (Dunne 2002). The initial adhesion stage is followed by stable secondary attachment in a matrix of secreted EPS (**Figure 1.1B**), which is made up of high molecular weight compounds, such as polysaccharides, proteins, nucleic acids, humic substances, and ionisable functional groups (Shen et al. 2015). The chemical composition of EPS depends on various factors, such as the availability of nutrients, temperature, pH and culture age (Bhaskar & Bhosle 2005). The EPS matrix protects the biofilm from desiccation, shear stress, toxic substances, some protozoan grazers, and is responsible for the biofilm’s architecture and structural stability (Flemming & Wingender 2010; Romaní et al. 2008; Kesaano & Sims 2014).

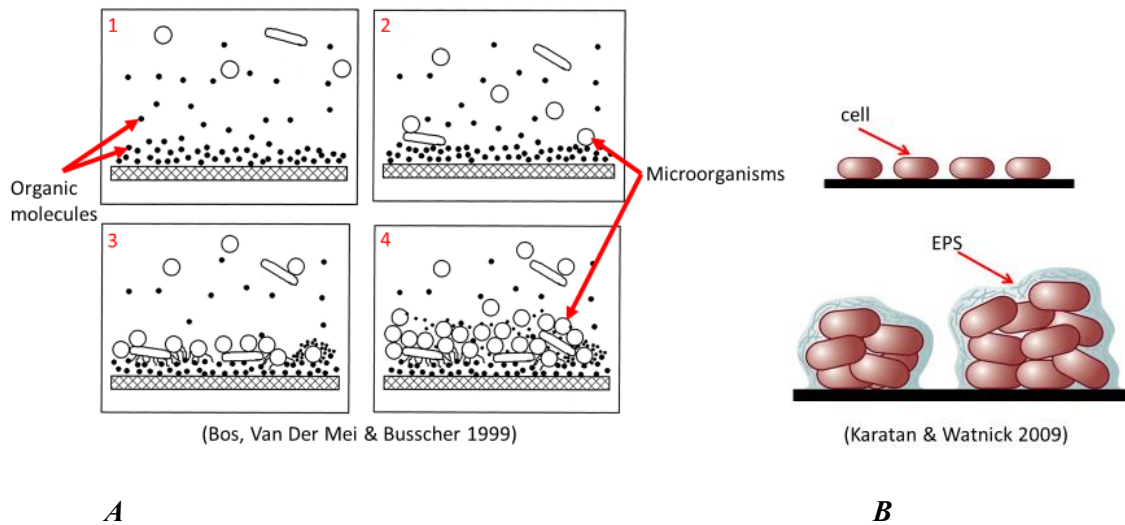


**Figure 1.1** Biofilm formation process: **A** – surface conditioning with organic molecules followed by microorganism attachment; **B** – stable biofilm formation in a matrix of EPS.

In terms of EPS production by microalgal species that were used in this thesis, *Dunaliella tertiolecta* was characterised as a promising candidate to be used industrially within a biorefinery due to its EPS, which was identified as a glucose-based homopolysaccharide (Goo et al. 2013). It was reported that *D. tertiolecta*, with its high production of EPS, may be a suitable candidate for biotechnological production of glucose and bioethanol (Goo et al. 2013). It was concluded from coagulation experiments that *D. tertiolecta* produced a much higher quantity of EPS than *Nannochloropsis* sp. (Eldridge, Hill & Gladman 2012).

There is a larger body of literature that describes bacterial biofilm formation and development, whereas the reports of microalgal biofilms are relatively sparse. The role of bacteria in microalgal attachment and biofilm formation has been thoroughly researched (Holmes 1986; Steinman & Parker 1990; Fukami, Nishijima & Ishida 1997; Sekar et al. 2004; Hodoki 2005; Acs et al. 2007; Irving & Allen 2011). It was experimentally determined that algal settlement on a glass attachment material was proportional to the attached bacteria density (Hodoki 2005). Additionally, a bacterial biofilm of *Alcaligenes* sp. was observed to enhance the growth of the benthic marine diatom *Nitzschia* sp. (Fukami, Nishijima & Ishida 1997). Similarly, it was experimentally determined that the presence of a *Pseudomonas putida* bacterial biofilm

promoted the adhesion of *Nitzschia amphibia* to titanium and glass surfaces (Sekar et al. 2004). A conditioned surface was reported to have a positive influence on microalgal cell attachment after comparing the adhesion of *N. amphibia* to a surface coated with an organic polymer film and to a control surface (Sekar et al. 2004). However, in another study, significant differences between conditioned and unconditioned surfaces of unglazed ceramic cylinders used as attachment materials were observed only during the first nine days of the experimental run. It was concluded that surface conditioning had a short-term effect on early-stage algal biofilm development (Steinman & Parker 1990).

### 1.4 Existing biofilm systems

Algal biofilm systems were initially designed for wastewater treatment purposes. For example, a system for biological wastewater bioremediation with bacteria and algae was originally developed in 1971 by Torpey, Heukelekian & Kaplovsky. The unit consisted of a series of rotating aluminium disks partially submerged in wastewater. Removal of carbonaceous organic matter by bacterial biofilms established on aluminium discs was followed by nutrient uptake performed by attached filamentous algae grown under fluorescent illumination. Biofilm systems of different configurations, both for wastewater treatment and biomass production, have been developed since then. The performance of some of them is summarised in **Table 1.1**.

**Table 1.1** Summary of the developed biofilm systems performance.

Reference	Design	Scale	Alga	Attachment material	Biomass productivity g m <sup>-2</sup> d <sup>-1</sup>	Nutrient removal from wastewater
Shi, Podola & Melkonian (2007)	Twin-layer PBR	Lab	<i>Chlorella vulgaris</i> , <i>Scenedesmus rubescens</i>	Reinforced nitrocellulose membrane on glass fibre fleece	0.86-1.33	Municipal and artificial wastewater: N – 94-96% P – 90%

Wei et al. (2008)	3 plexiglass biofilm chambers for wastewater treatment and 1 precipitation chamber for algal sludge separation	Lab	Mixed culture	PVC filler	Not reported	Artificial wastewater: N – 84-87%, P – 95-98%
Johnson & Wen (2010)	A growth chamber with an attachment material on a rocking mechanism.	Lab	<i>Chlorella</i> sp.	Polystyrene foam	2.57	Dairy manure wastewater: N – 77-78%, P – 71-90%
Ozkan et al. (2012)	Concrete layer on a tilted wooden support with a dripping mechanism	Lab	<i>Botryococcus braunii</i>	Concrete	0.71	NA
Christenson & Sims (2012)	A partially submerged rotating drum wrapped into an algal attachment material with a spool harvester	Lab, Medium, Pilot	Mixed culture	Cotton cording	5.5-31	Municipal wastewater: N – 14.1 g m <sup>-2</sup> d <sup>-1</sup> ; P – 2.1 g m <sup>-2</sup> d <sup>-1</sup>
Zamalloa, Boon & Verstraete (2013)	Rooftop PBR: an inclined parallel plate connected to a pipe in the bottom	Lab	<i>Scenedesmus obliquus</i>	Polycarbonate sheet	2.5	Domestic wastewater: N – 67%, P – 96%
Gross et al. (2013)	A partially submerged rotating triangular system on supporting shafts	Lab, Pilot	<i>Chlorella vulgaris</i>	Cotton duct	8-14	NA
(Liu et al. 2013)	Vertical plate attached PBR (single- and multiple-layer)	Lab	<i>Scenedesmus obliquus</i> , <i>Botryococcus braunii</i> , <i>Nannochloropsis</i> sp.	Filter paper on glass plate	50-80	NA

Shi, Podola & Melkonian (2014)	Twin-layer vertical PBR	Pilot	<i>Halochlorella rubescens</i>	Reinforced glass fibre mesh on nylon filter sheets	6.3	Municipal wastewater: P and N – 70-99%
Gross & Wen (2014)	Triangular and vertical conveyor RAB systems	Pilot	<i>Chlorella vulgaris</i>	Cotton	18.9	NA
Blanken et al. (2014)	Algadisk system: Partially submerged vertical rotating disks	Lab	<i>Chlorella sorokiniana</i>	Stainless steel woven mesh and polycarbonate with polyelectrolyte coating	20.1	NA
Sukačová, Trtílek & Rataj (2015)	Horizontal flat panel PBR	Medium	Mixed culture	Concrete	6-12	Artificial and municipal wastewater: P – 97%
Sebestyén et al. (2016)	Algadisk system: Partially submerged vertical rotating disks (in parallel)	Pilot	<i>Chlorella sorokiniana</i>	Polyvinylchloride roughened with sandpaper	0.5-8.4	NA
Ekelhof & Melkonian (2017)	Twin-layer PBR	Lab	<i>Netrium digitus</i>	Filter disks in transparent test tubes	2-3	NA
de Assis et al. (2017)	Flat acrylic vertical panels wrapped into fabric	Pilot	Mixed culture	Cotton	5.9-10	Pre-treated domestic wastewater: N-NH <sub>3</sub> – 79-84%, P – 20-30%
Zhao et al. (2018)	Vertical conveyor belt partially submerged in medium reservoir	Pilot	Mixed culture	Flexible belt material	1-7 (footprint); 0.3-0.9 (aerial)	Supernatant from sludge sedimentation: N – 87%, P – 80%

In a more recent study, a twin-layer system for wastewater treatment was developed, which comprised of a laboratory-scale tube-type PBR with two vertically oriented layers: a substrate layer for cell immobilisation; and a source layer for culture medium/wastewater recirculation (Shi, Podola & Melkonian 2007). The performance of

this system was analysed, and it was concluded that the twin layers may be advantageous for wastewater treatment. Later, the twin-layer concept was used to assess the potential of cultivating the high EPS-producing alga *Netrium digitus* as a biofilm (Ekelhof & Melkonian 2017). The authors recorded a tenfold increase in cell dry weight and a sixfold increase in EPS dry weight when compared to a suspended culture. It was concluded that growing EPS-producing microalgae in a twin-layer bioreactor is beneficial in terms of efficient harvesting, minimised contamination risk and easier scalability.

An attached microalgal growth system has been proposed for biofuel production (Johnson & Wen 2010). In this small-scale laboratory study, an artificially-illuminated growth chamber with polystyrene foam used as a microalgal supporting material was placed on a rocking shaker. The agitation enabled the cells to alternatively access dissolved nutrients in wastewater and air for photosynthesis. The resulting attached biomass was harvested by scraping, and the remaining cells on the attachment material were used as inoculum for further biofilm cultivation in the system. Improved biomass and fatty acid production for the attached growth system, in comparison with a suspended culture, was reported. However, the aerial biomass productivity of  $2.57 \text{ g m}^{-2} \text{ d}^{-1}$  was quite low compared to other attached microalgal cultivation systems. Importantly, the water content of the biomass harvested by scraping was similar to the water content of a suspended culture after centrifugation (Johnson & Wen 2010). This result is encouraging as it indicates the possibility of eliminating an energy-intensive step such as centrifugation when performing attached microalgal cultivation.

Another microalgal biofilm PBR was also developed and analysed for sustainable and economic production of biofuels (Ozkan et al. 2012). The green algae *Botryococcus braunii* was immobilised on a thick concrete surface and illuminated by fluorescent lamps, with dripping nozzles for delivering nutrient-rich medium to the cells. Although the system required 45% less water and 99.7% less energy for its operation if compared to existing raceway ponds and closed PBRs, the aerial biomass productivity was low ( $0.71 \text{ g m}^{-2} \text{ d}^{-1}$ ), presumably because of the relatively slow doubling time of *B. braunii* and insufficient light availability. Also, the perspectives for system scale-up and integration into existing microalgal cultivation infrastructure were not analysed.

A different design of the microalgal biofilm growth system encompassed a rotating algal biofilm reactor (RABR) that aimed to combine wastewater treatment and microalgae cultivation for the production of bioproducts such as biodiesel (Christenson & Sims 2012). The system used a drum with cotton cords wrapped around it that was partially submerged in wastewater. The cords served as a biofilm attachment material, and a spool harvester was constructed to scrape the biomass from the cords. The system was operated under both indoor and outdoor conditions, and it had a positive energy balance. An aerial biomass productivity of 20–30 g m<sup>-2</sup> d<sup>-1</sup> was reported in this study.

A similar rotating system concept was used for the development of a revolving microalgal biofilm growth system (RAB) consisting of cotton duct stretched around supporting shafts in a triangular configuration and partially submerged into growth medium (Gross et al. 2013). The system operational parameters, such as harvesting frequency and speed of rotation were analysed and adjusted to improve biomass yield. A raceway pond was retrofitted with a pilot-scale rotating biofilm growth system in order to evaluate its scalability. Although the attached microalgal cultivation concept resulted in better biomass productivity (8–14 g m<sup>-2</sup> d<sup>-1</sup>) and similar water content as a suspended culture after centrifugation, the lipid content was rather low (7.7% DW). Unfortunately, energy consumption was not reported in this study. The commercialisation potential of the revolving microalgal biofilm cultivation setup was evaluated in 2014 by a one-year pilot study (Gross & Wen 2014). In addition to the triangular configuration, partially submerged vertical conveyors, operating under the same principle, were tested. Two triangular and six vertical units were installed into an 8.5 m<sup>2</sup> raceway pond situated in a greenhouse facility. The conveyors had higher aerial biomass productivity compared to the triangular units, emphasising the importance of designing biofilm systems that present the highest illuminated surface area for biofilm development. The aerial biomass productivity of the pilot-scale system was better than the laboratory setup, and was equal to 21.5 g m<sup>-2</sup> d<sup>-1</sup>. Later, the conveyor system was used for biofilm cultivation together with bioremediation of municipal wastewater at pilot scale (Zhao et al. 2018). The system operation was dependent on design features, *i.e.* conveyor length, and hydraulic retention time, and resulted in considerably higher nutrient removal than in conventional open ponds.

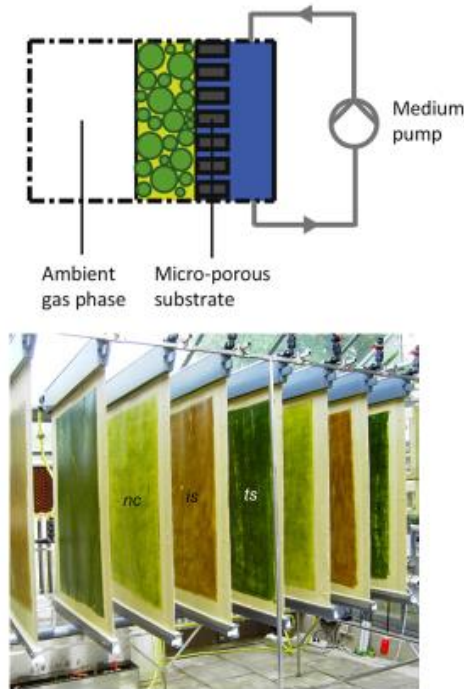
Attached growth of microalgae was also tested by cultivating biofilms on vertical rotating stainless steel woven mesh disks, called Algadisks, that were partially submerged in a growth medium under different operational conditions (Blanken et al. 2014). Biomass productivity of the Algadisks was  $20.1 \text{ g m}^{-2} \text{ d}^{-1}$ , and mass fraction of biomass to water was reported to be  $170 \text{ g kg}^{-1}$ , compared to a mass fraction of biomass to water of  $1\text{--}10 \text{ g kg}^{-1}$  in suspended systems. The solids fraction in a wet biofilm was calculated by dividing the dry biomass weight by the wet biomass weight.

A half-year pilot-scale study was carried out to assess the outdoor performance of the Algadisk system (Sebestyén et al. 2016). The highest *Chlorella sorokiniana* biomass productivity for the pilot-scale Algadisk system was  $8.4 \text{ g m}^{-2} \text{ d}^{-1}$ . This productivity was considerably lower than with the laboratory-scale prototype, which was attributed to a number of physicochemical and mechanical problems incurred during the course of the experiment. Hence, careful experimental design, as well as project planning and management, are key parts of successful biofilm system operation. The Algadisk microalgal bioproductivity results were encouraging: the long-term (more than 20 weeks) operation of the system without re-inoculation was also an important development.

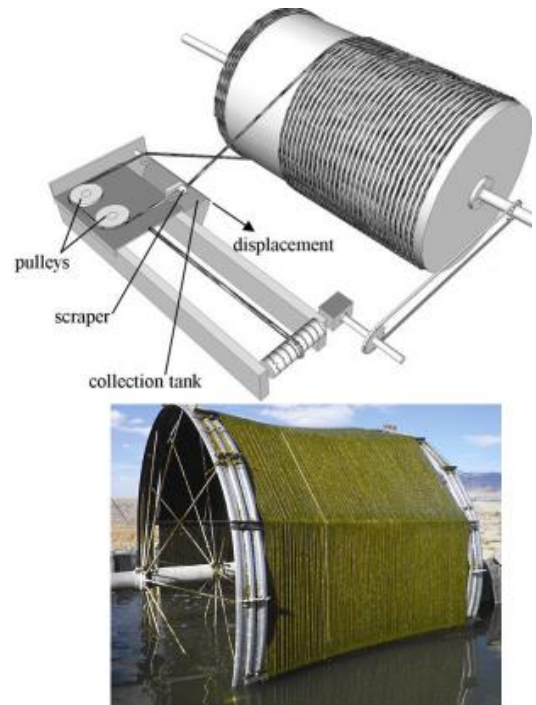
Biomass cultivation in raceway ponds integrated with biofilms growing on cotton attachment materials was tested in the study by de Assis et al. (2017) to determine biomass production potential and to assess wastewater bioremediation efficiency. Growth medium from raceway ponds was recirculated to vertical panels covered with cotton as a cell attachment material. The panels were installed next to the raceways. After the medium was supplied to the panels, it was collected in gutters and returned to the ponds. The performance of these hybrid systems was compared to a conventional raceway pond. No substantial differences in wastewater treatment efficiency were observed. Additionally, the absence of  $\text{CO}_2$  supplementation in one of the hybrid systems did not cause a decrease in total biomass productivity. The authors attributed this result to the direct access of the biofilms to atmospheric gases that lead to  $\text{CO}_2$  saturation of the system. It was suggested that conventional high-rate ponds with  $\text{CO}_2$  supplementation could be replaced with this hybrid system with no  $\text{CO}_2$  supplementation without a reduction in biomass productivity and wastewater

bioremediation efficiency. However, the financial aspects of the hybrid system operation in comparison with a typical raceway pond were not considered.

The configurations of some of the developed pilot-scale biofilm systems are shown in **Figure 1.2**.

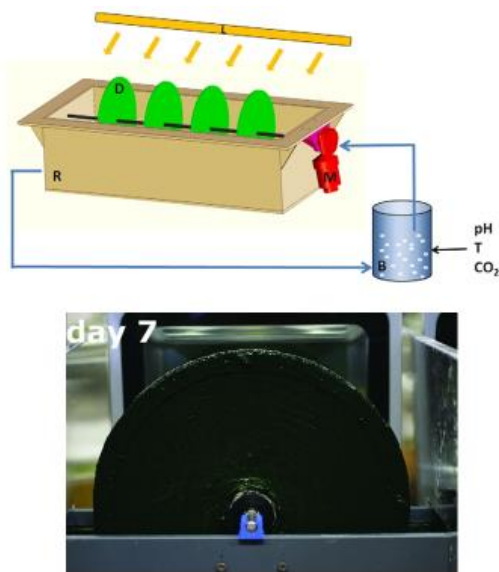


(Naumann et al. 2013; Podola, Li & Melkonian 2017)



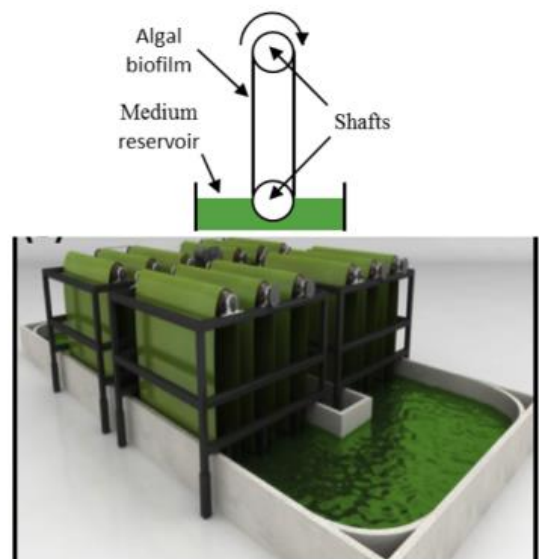
(Christenson & Sims 2012; Bernstein et al. 2014)

**A**



(Blanken et al. 2014; Sebestyén et al. 2016)

**B**



(Zhao et al. 2018)

**C**

**D**

**Figure 1.2** Existing pilot-scale biofilm systems: *A* – twin-layer system; *B* – Rotating Algal Biofilm Reactor (RABR); *C* – Algadisk system; *D* – Revolving Algal Biofilm (RAB) reactor.

Overall, microalgal biomass cultivation and harvesting in biofilm systems has numerous advantages over suspended culture and is a promising way to enhance microalgal productivity and reduce harvesting costs (Hoh, Watson & Kan 2016).

## 1.5 Thin-layer cascade systems

Growing suspended cultures in thin-layer cascade systems improves volumetric biomass productivity and reduces water use. The concept was introduced in the 1960s in the Czech Republic (Šetlík, Šust & Málek 1970). The system design consisted of a thin layer of microalgal suspension (less than 1 cm deep) flowing on an inclined surface under gravity into a retention tank, from which it was pumped back onto the sloped surface. The system could be equipped with a set of baffles installed perpendicularly to the culture flow in order to create turbulence, ensure mixing and prevent cell sedimentation. Although the first thin-layer cascade systems were costly to build and complex to maintain compared to a typical raceway pond, they were successfully operated for more than 30 years, proving reliability of the concept (Doucha & Livansky 1995).

Doucha & Livansky (1995) reported on the operation of a cascade system where the suspended biomass was recirculated only during the daytime and was stored in an aerated container at night. The microalgal cell density in this cascade system considerably exceeded the cell densities obtained in raceway ponds with no decrease in algal growth rate, presumably due to the enhanced mixing and more efficient light utilisation. The threefold increase in final cell density was highly beneficial for harvesting purposes. The authors reported that regular cleaning was necessary to reduce bacterial growth; however, the changes in bacterial communities and their impact on system performance were not studied. Microalgal cultivation in cascade systems as opposed to raceway ponds resulted in substantial reduction in energy input required for mixing, aeration and harvesting of microalgal biomass.

Two decades ago, microalgal growth in cascade systems was perceived as one of the most promising and advantageous methods of open-air microalgal biomass production

in terms of maintaining high cell densities together with high growth rates (Borowitzka 1999). A more considerate approach to the selection of construction materials and system locations was required in order to make the cascade system performance competitive with a paddlewheel-driven raceway pond, the only large-scale industrial means of biomass production (Borowitzka 1999). At the time, the operation of existing cascade systems was economically unfeasible due to glass used as a sloping surface material and the systems being located in colder climate that shortened annual cultivation period of microalgae.

A decade ago, studies on cascade systems were mainly driven by the potential to optimise light utilisation efficiency of microalgal cells grown in thin-layer systems, and thus to increase biomass productivity.

Becerra-Dórame, López-Elías & Martínez-Córdova (2010) slightly modified the design of a cascade system, replacing the smooth sloped surface traditionally used for culture circulation with plastic sheets arranged in a ladder-like manner above the medium collection container. The primary aim of their experimental study was to enhance light availability in order to improve microalgal biomass production for aquaculture feed in shrimp hatcheries. A 35-40% increase in the final cell density was reported for *Chaetoceros muelleri* cultivated in the ladder-like cascade system compared to a traditional aerated plastic container. Although microalgal growth rates were improved in the cascade system, the economics of system operation were not considered.

Torzillo et al. (2010) attempted to reduce light saturation effect in suspended microalgal cultures by building and operating a 5 m<sup>2</sup> corrugated cascade system. The light saturation effect inhibits growth in open ponds and PBRs when incident light intensity considerably exceeds cell saturation values (Torzillo et al. 2010). The authors aimed to enhance the efficiency of light utilisation in their system by creating a thin, but dense culture layer. A fluid dynamic analysis for this cascade system was conducted, and maximum aerial biomass productivity of 5.8 g m<sup>-2</sup> d<sup>-1</sup> was reported. These low biomass yields were attributed to high temperature stress (up to 35°C) experienced by the microalgal culture.

Figueroa, Jerez & Korbee (2013) grew *Chlorella fusca* culture in a 4 m<sup>2</sup> thin-layer reactor and performed chlorophyll fluorescence measurements to determine electron

transport rate and to estimate biomass productivity. This approach was also used in a similar study by Jerez et al. (2016). The researchers used *in vivo* chlorophyll *a* fluorescence measurements to assess microalgal biomass productivity in an outdoor cascade system. Light intensity, photosynthetic activity and hydrodynamics of *C. fusca* suspension were also studied based on retention time at different points of culture medium flow in an outdoor fiberglass cascade system with variable suspension depths.

In cascade systems, photosynthetic efficiency depends on the absorbed irradiance, which decreases at low ratio between the surface exposed to irradiation and the total culture volume (Jerez et al. 2016). The light regime in a cascade reactor is influenced by the residence time of microalgal culture in different sections of the reactor, which is determined by the system hydrodynamics (Jerez et al. 2014). Extending the duration of retention time on the sloping surface of a cascade reactor with the short light path can be achieved by mounting a baffle at the edge of the sloping surface. This adjustment increases the suspension layer thickness, which prevents photoinhibition (Jerez et al. 2014).

In contrast, Prokop, Bajpai & Zappi (2015) suggested that the future development of cascade systems must be focused on decreasing the depth of the suspended culture layer for enhanced microalgal biomass yields and productivity. However, the authors did not suggest ways of addressing possible adverse effects of evaporation and photoinhibition in such ultrathin-layer systems.

De Marchin, Erpicum & Franck (2015) operated two 35 m<sup>2</sup>, 4,000 L outdoor cascade systems to test the influence of CO<sub>2</sub> availability on *Scenedesmus obliquus* performance in a thin-layer bioreactor. The sloped surfaces were equipped with baffles to increase the suspension layer depths and to enhance mixing. The systems were operated for 12 days at the suspension layer thicknesses of 26-44 mm and at reduced biomass concentrations to avoid a decrease in productivity due to cell shading. One of the systems was supplied with CO<sub>2</sub> through periodic injections based on pH measurements. CO<sub>2</sub> availability was found to be the limiting factor for enhancing microalgal biomass productivity in this cascade system. The highest aerial productivity achieved in this study under CO<sub>2</sub>-replete conditions was approximately 24 g m<sup>-2</sup> d<sup>-1</sup>.

Apel et al. (2017) identified several constraints limiting the further development of cascade systems, including absence of systems for marine microalgae cultivation and the use of expensive construction materials. The authors attempted to address these issues by developing a pilot-scale economical thin-layer system for saltwater microalgal species cultivation. Very high volumetric productivity of  $4 \text{ g L}^{-1} \text{ d}^{-1}$  was achieved (aerial productivity  $25 \text{ g m}^{-2} \text{ d}^{-1}$ ) for *Nannochloropsis salina*. However, the average calculated evaporation rate was  $7.4 \text{ L m}^{-2} \text{ d}^{-1}$ . It could be beneficial for fast increase in salinity to be aimed at contamination reduction and production of specific compounds, and disadvantageous in terms of expensive freshwater requirement.

Benavides et al. (2017) grew the cyanobacterium *Arthrospira platensis* in an outdoor cascade system and in a circular open pond under different temperature regimes to compare diurnal changes of photosynthetic activity and biomass productivity in these systems. The productivity of *A. platensis* culture grown in the 10 mm deep thin-layer cascade at optimal temperature reached  $20 \text{ g m}^{-2} \text{ d}^{-1}$  (volumetric productivity  $1.7 \text{ g L}^{-1} \text{ d}^{-1}$ ), approximately one third higher than in the pond. Photosynthetic activity of the microalgal suspension grown in the cascade system was also 20% higher than the one measured in the open pond. The superior performance of the cascade system was attributed to culture being circulated as a thin layer that enabled faster cell movement between photic and dark zones and more rapid culture warming in the mornings, if compared to the 100 mm deep open pond.

**Table 1.2** Summary of cascade systems operation.

Reference	Depth (mm)	Aerial productivity (g m <sup>-2</sup> d <sup>-1</sup> )	Volumetric productivity (g L <sup>-1</sup> d <sup>-1</sup> )	Dry fraction (g DW L <sup>-1</sup> )
Šetlík, Šust & Málek (1970)	6-10	25	2-3	15
Torzillo et al. (2010)	3.6	3.2-5.8	0.1-0.3	-
Figueroa, Jerez & Korbee (2013)	10; 20	3.7; 5.6	0.1; 0.2	0.07; 0.05 mg DW L <sup>-1</sup>
De Marchin, Erpicum & Franck (2015)	26-44	7-24	0.06-0.21	0.7-2.3
Apel et al. (2017)	5.6	15-25	2.4-4	≤ 50
Benavides et al. (2017)	10	20	1.7	-

Overall, growing microalgal biomass in cascade systems (summarised in **Table 1.2**) is primarily beneficial in terms of volumetric productivity, which is usually equal to 0.12-0.48 g L<sup>-1</sup> d<sup>-1</sup> for a raceway pond (Kumar et al. 2015). It is a promising method of biomass cultivation, which requires further engineering improvements in regards to system design and material construction. In this thesis, a cascade system was retrofitted for microalgal biofilms cultivation, thus combining the benefits of these two biomass production systems.

## 1.6 Biofilm attachment materials

The selection of a biofilm attachment material, which is the material used for microalgae immobilisation (Nowack, Podola & Melkonian 2005), is a critical factor that influences overall performance of a biofilm system (Gross, Jarboe & Wen 2015). Currently, there is no specific material or group of materials recommended for attached microalgal cultivation (Kesaano & Sims 2014). Microalgal attachment materials are usually selected based on their ability to promote and sustain biofilm formation under specific experimental conditions, which are different for every reported study. For example, Xu et al. (2017) used household polyester mops for *Scenedesmus sp.* attachment in their capillary-driven bioreactor. This type of vertically-oriented attachment material showed aerial biomass productivity as high as  $10 \text{ g m}^{-2} \text{ d}^{-1}$ , which was dependent on the mop fibre density. The cell harvesting procedure involved squeezing the mops, washing the fibres with deionised water, and biomass filtration. One of the main advantages of attached biomass cultivation, *i.e.* the harvesting of concentrated sludge with the elimination of dewatering processes (Blanken et al. 2014) was not utilised. Lan et al. (2017) used shifting sand as an attachment material to grow cyanobacterial biofilms at laboratory scale in order to test the concept of biomass cultivation in desert environments. The resulting biofilms could be easily removed from the sand with a sharp shovel. However, the amount of sand particles in the biofilms and their influence on the properties of the harvested biomass were not discussed. It was reported that polystyrene foam proved to be the most favourable of six materials for *Chlorella sp.* attached cultivation (Johnson & Wen 2010). The same study concluded that porous materials were unsuitable for biofilm cultivation due to complicated harvesting of biomass. In another experimental study, eight materials were investigated for cell adhesion, and the highest cell accumulation was found on cotton fabric (Christenson & Sims 2012). A similar result with cotton fabric showing the highest cell attachment was achieved after screening 16 potential attachment materials (Gross et al. 2013). The experimental data demonstrated that cotton fabric with a specific weave (cotton duct) supported excellent biofilm growth. Overall, cotton fabric was used as a favourable attachment material for biofilm formation in multiple studies (Christenson & Sims 2012; Gross et al. 2013; Bernstein et al. 2014; Kesaano et al. 2015; Gross et al. 2016).

Several cell attachment studies have been carried out in order to determine the influence of a material's physicochemical properties, composition, surface roughness, microalgal culture density and growth phase on the adhesion capacity of attachment materials. Acid-base interactions were reported to be important for the selection of a biofilm attachment material after conducting experiments with 10 microalgal species and six attachment materials (Ozkan & Berberoglu 2013). Electron transfer interactions between polar components of cell and attachment material surfaces caused acid-base reactions, which were expressed as hydrophobic attraction or hydrophilic repulsion between the interacting surfaces based on the free energy of cohesion. In fact, one of the physicochemical properties that characterises a material is its free surface energy, which is an energy excess of the atoms or molecules at the material surface in comparison with the energy distribution in the bulk of the material. The correlation between surface energies of microalgal cells and biofilm attachment materials has been proposed as an important parameter for cell adhesion (Cui & Yuan 2013; Genin, Aitchison & Allen 2014). However, an in-depth analysis of 34 materials with different physicochemical properties and surface textures reported no influence of surface energy on microalgal attachment (Gross et al. 2016).

A considerable amount of biofilm attachment material research is directed at the analysis of surface roughness as an indication of an attachment material's performance. Increasing surface roughness reduces shear force, prevents biofilm washing off and decreases fluid velocity giving cells more time to settle (Cao et al. 2009; Gross, Jarboe & Wen 2015). Roughening the surface texture of glass with 10  $\mu\text{m}$  grooves led to an increase in *S. obliquus* biofilm thickness within the first few days of the experiment, but did not have a long-term influence on attachment material performance in terms of biofilm growth and development capacity (Irving & Allen 2011). The size and shape of textures was shown to be important for cell settlement, with maximum attachment gained when the cell diameter matched the size of the opening (Cui, Yuan & Cao 2014). In addition, V-shaped textures resulted in the highest cell settlement (Cui, Yuan & Cao 2014). Also, mesh materials with 0.50–1.25 mm openings were reported to be the most favourable for cell adhesion; nylon and polypropylene mesh performed well as long-term attachment materials in biofilm systems (Gross et al. 2016).

The influence of the microalgal culture used for biofilm inoculation has also been discussed in the literature. It was concluded that species selection and control have an impact on microalgal biofilm cultivation (Irving & Allen 2011). The microalgal growth phase was found to be important for biofilm formation, and a higher adhesion of cells was observed in the exponential growth phase than in the stationary phase (Sekar et al. 2004). Microalgal cell settlement was also found to be directly proportional to culture density (Sekar et al. 2004). Gross et al. (2016) emphasised that the impact of flocculation on biofilm formation must be studied in future attachment tests, and that the average floc size must be taken into consideration when selecting a favourable texture size of an attachment material, as a microalgal floc may not fit into an opening that accommodates a single cell.

In general, the choice of a biofilm attachment material must be based on such properties as material cost, durability in wet environments and local availability (Kesaano & Sims 2014). Conducting attachment experiments for a specific biofilm system is important because vertical orientation of a biofilm, as opposed to horizontal orientation, may have an influence on an attachment material performance, although this parameter has not been covered in the literature (Genin, Aitchison & Allen 2014).

## **1.7 Operational conditions of biofilm systems**

The configuration of a biofilm system may have a considerable impact on microalgal biomass productivity (Gross, Jarboe & Wen 2015). For example, a 187% increase in biomass productivity was measured in a 1-year pilot study after increasing the total surface area of the biofilm attachment material (Gross & Wen 2014). The average biomass productivity of the initial triangular system was  $5.3 \text{ g m}^{-2} \text{ d}^{-1}$ , and the productivity of the improved system configuration that used vertical conveyors was  $11.4 \text{ g m}^{-2} \text{ d}^{-1}$ .

Another important operational parameter applicable to microalgal biofilm systems is harvesting frequency (Gross et al. 2013), which means the time period between biomass scraping (Gross et al. 2013). Excessively frequent harvesting keeps attached microalgal cells in the lag phase, while overly long intervals between harvests lead to the formation of an extremely thick biofilm (Gross et al. 2013). Increased biofilm thickness may cause limited nutrient and mass transfer rates within the biofilm, as well as reduce its integrity

(Gross, Jarboe & Wen 2015). Algal biomass growth is often limited by self-shading, which emphasises the importance of timely biomass scraping (Gross & Wen 2014). The harvesting frequencies reported in the literature are different, but in general most research teams allow biofilms to grow longer for initial attachment (microalgal colonisation of a fresh attachment material), when compared with re-growth cycles (repeated biofilm growth on an attachment material after harvesting). In a pilot study on a partially-submerged rotating disks system (Sebestyén et al. 2016) the attached biomass was harvested approximately once every 14 days. However, the highest productivity was reached with a 5–7 day interval between scraping both for the triangular and for the vertical conveyor rotating biofilm systems (Gross & Wen 2014).

The speed of rotation selected for an axial biofilm system determines the shear stress that the biofilm has to withstand (Gross, Jarboe & Wen 2015). Rotation speed must be carefully adjusted to prevent biofilm drying as a result of slow rotation (Gross et al. 2013) and sloughing at excessively high speeds (Kadu & Rao 2012). Another negative consequence of operating a biofilm system at low rotation frequency is the possibility for the accumulation of toxic compounds in the biofilm (Blanken et al. 2014). In fact, the health of a biofilm is crucial, especially in its bottom layers since they serve as an inoculum for the following growth cycle, and their damage or decay may result in an extended lag phase (Gross, Jarboe & Wen 2015). On the other hand, increasing the speed of rotation leads to exponential increase in the energy consumption for the motor drive (Hassard et al. 2015). Biomass productivity of a biofilm cultivated on partially submerged disks at rotation speeds ranging from 3 to 20 rpm was experimentally assessed by Blanken et al. (2014). Significantly higher productivity at 11 rpm was reported when compared to higher rotational speeds, which sets an upper limit for rotation speed.

## **1.8 Imaging of biofilms**

Microscopic imaging of biofilms is a proven method of examining their formation, development and structure (Eighmy, Maratea & Bishop 1983; Sich & Van Rijn 1997). In order to obtain high resolution 2- and 3-dimensional images of biofilms on surfaces with detailed visualisation of particular biofilm components, modern techniques such as

scanning electron microscopy (SEM) and confocal laser scanning microscopy (CLSM) have been employed (Doiron et al. 2012).

SEM offers a number of advantages compared to light microscopy, generating high-contrast images with improved resolution, higher level of magnification and enhanced depth of focus (Yau et al. 2016). In the research on attached microalgal cultivation, SEM has been extensively used for studying various biofilm components. For example, Schnurr, Espie & Allen (2013) and Genin, Aitchison & Allen (2014) used SEM to detect the presence of microbes and EPS in microalgal biofilms. The structure of the biofilms was preserved by sample preparation that involved treatment with osmium tetroxide solution and sample freezing. Both environmental SEM and CLSM techniques were employed in the study on microalgal biofilm attachment materials by Zhang et al. (2017). Environmental SEM was used to visualise microalgal cell distribution on the growth materials after 1 day of biofilm cultivation. 3-dimensional images of attachment material surface geometry were obtained using CLSM, which allowed examination of the material roughness and correlating it with biomass productivity. However, the quality and precision of microalgal cell images are highly influenced by sample pre-treatment, which must remove volatile matter, enhance conductivity and radiation resistance, whilst maintaining cell morphology (Yau et al. 2016).

CLSM is one the most functional and practical methods of studying microalgal biofilms that allows simultaneous visualisation of multiple biofilm parameters, including its surface distribution and thickness. Microalgae can be detected by autofluorescence, whereas EPS and bacterial cells can be labelled with specific dyes, including species-specific dyes in the case of fluorescence in-situ hybridisation. The amount of microalgae, EPS and bacteria can thus be quantified digitally (Lawrence, Neu & Swerhone 1998). Doiron et al. (2012) used CLSM to image living and dead microalgal and bacterial cells within a biofilm. Irving & Allen (2011) measured approximate biofilm thickness with CLSM. The authors also emphasised the ability of CLSM to capture comprehensive morphology of a biofilm surface.

In this thesis, SEM was used to visualise the structures of fabrics used for microalgal cell attachment, and to assess their roughness. CLSM was employed to observe biofilm formation and development on the fabrics, and to characterise cell distribution on the attachment material surfaces with time.

## 1.9 References

- Acs, E., Borsodi, K.A., Kropfl, K., Vladoar, P. & Zaray, G. 2007, 'Changes in the algal composition, bacterial metabolic activity and element content of biofilms developed on artificial substrata in the early phase of colonization', *Acta Botanica Croatica*, vol. 66, no. 2, pp. 89–100.
- Amin, S. 2009, 'Review on biofuel oil and gas production processes from microalgae', *Energy Conversion and Management*, vol. 50, no. 7, pp. 1834–40.
- Apel, A.C., Pfaffinger, C.E., Basedahl, N., Mittwollen, N., Göbel, J., Sauter, J., Brück, T. & Weuster-Botz, D. 2017, 'Open thin-layer cascade reactors for saline microalgae production evaluated in a physically simulated Mediterranean summer climate', *Algal Research*, vol. 25, pp. 381–90.
- de Assis, L.R., Calijuri, M.L., do Couto, E.D.A. & Assemany, P.P. 2017, 'Microalgal biomass production and nutrients removal from domestic sewage in a hybrid high-rate pond with biofilm reactor', *Ecological Engineering*, vol. 106, pp. 191–9.
- Baicha, Z., Salar-García, M.J., Ortiz-Martínez, V.M., Hernández-Fernández, F.J., De los Rios, A.P., Labjar, N., Lofti, E. & Elmahi, M. 2016, 'A critical review on microalgae as an alternative source for bioenergy production: A promising low cost substrate for microbial fuel cells', *Fuel Processing Technologies*, vol. 154, pp. 104–116.
- Becerra-Dórame, M., López-Elías, J.A. & Martínez-Córdova, L.R. 2010, 'An alternative outdoor production system for the microalgae *Chaetoceros muelleri* and *Dunaliella* sp. during winter and spring in Northwest Mexico', *Aquacultural Engineering*, vol. 43, pp. 24–8.
- Benavides, A.M.S., Ranglová, K., Malapascua, J.R., Masojídek, J. & Torzillo, G. 2017, 'Diurnal changes of photosynthesis and growth of *Arthrospira platensis* cultured in a thin-layer cascade and an open pond', *Algal Research*, vol. 28, pp. 48–56.
- Bernstein, H.C., Kesaano, M., Moll, K., Smith, T., Gerlach, R., Carlson, R.P., Miller, C.D., Peyton, B.M., Cooksey, K.E., Gardner, R.D. & Sims, R.C. 2014, 'Direct measurement and characterization of active photosynthesis zones inside wastewater remediating and biofuel producing microalgal biofilms', *Bioresource Technology*, vol. 156, pp. 206–15.
- Bhaskar, P.V. & Bhosle, N.B. 2005, 'Microbial extracellular polymeric substances in marine biogeochemical processes', *Current Science*, vol. 88, no. 1, pp. 45–53.

- Blanken, W., Janssen, M., Cuaresma, M., Libor, Z., Bhaiji, T. & Wijffels, R.H. 2014, 'Biofilm growth of *Chlorella sorokiniana* in a rotating biological contactor based photobioreactor', *Biotechnology and Bioengineering*, vol. 111, no. 12, pp. 2436–45.
- Borowitzka, M.A. 1999, 'Commercial production of microalgae: ponds, tanks, tubes and fermenters', *Journal of Biotechnology*, vol. 70, no. 1–3, pp. 313–21.
- Borowitzka, M.A. & Moheimani, N.R. (eds) 2013, *Algae for Biofuels and Energy*, vol. 5, Springer Netherlands, Dordrecht.
- Bos, R., Van Der Mei, H.C. & Busscher, H.J. 1999, 'Physico-chemistry of initial microbial adhesive interactions - Its mechanisms and methods for study', *FEMS Microbiology Reviews*, vol. 23, no. 2, pp. 179–229.
- Brennan, L. & Owende, P. 2010, 'Biofuels from microalgae - A review of technologies for production, processing, and extractions of biofuels and co-products', *Renewable and Sustainable Energy Reviews*, vol. 14, no. 2, pp. 557–77.
- Cao, J., Yuan, W., Pei, Z.J., Davis, T., Cui, Y. & Beltran, M. 2009, 'A preliminary study of the effect of surface texture on algae cell attachment for a mechanical-biological energy manufacturing system', *Journal of Manufacturing Science and Engineering*, vol. 131, no. 6, p. 064505.
- Chen, C.Y., Yeh, K.L., Aisyah, R., Lee, D.J. & Chang, J.S. 2011, 'Cultivation, photobioreactor design and harvesting of microalgae for biodiesel production: A critical review', *Bioresource Technology*, vol. 102, no. 1, pp. 71–81.
- Chisti, Y. 2008, 'Biodiesel from microalgae beats bioethanol', *Trends in Biotechnology*, vol. 26, no. 3, pp. 126–31.
- Christenson, L.B. & Sims, R.C. 2011, 'Production and harvesting of microalgae for wastewater treatment, biofuels, and bioproducts', *Biotechnology Advances*, vol. 29, no. 6, pp. 686–702.
- Christenson, L.B. & Sims, R.C. 2012, 'Rotating algal biofilm reactor and spool harvester for wastewater treatment with biofuels by-products', *Biotechnology and Bioengineering*, vol. 109, no. 7, pp. 1674–84.
- Cui, Y. & Yuan, W. 2013, 'Thermodynamic modeling of algal cell-solid substrate interactions', *Applied Energy*, vol. 112, pp. 485–92.
- Cui, Y., Yuan, W.Q. & Cao, J. 2014, 'Effect of surface texturing on microalgal cell attachment to solid carriers', *International Journal of Agricultural and Biological*

- Engineering*, vol. 7, no. 2, pp. 82–91.
- De Marchin, T., Erpicum, M. & Franck, F. 2015, 'Photosynthesis of *Scenedesmus obliquus* in outdoor open thin-layer cascade system in high and low CO<sub>2</sub> in Belgium', *Journal of Biotechnology*, vol. 215, pp. 2–12.
- Doiron, K., Linossier, I., Fay, F., Yong, J., Abd Wahid, E., Hadjiev, D. & Bourgougnon, N. 2012, 'Dynamic approaches of mixed species biofilm formation using modern technologies', *Marine Environmental Research*, vol. 78, pp. 40–7.
- Doucha, J. & Livansky, K. 1995, 'Novel outdoor thin-layer high density microalgal culture system: productivity and operational parameters', *ARCHIV FUR HYDROBIOLOGIE-SUPPLEMENT*, vol. 106, p.129.
- Dunne, W.M. 2002, 'Bacterial adhesion: seen any good biofilms lately?', *Clinical microbiology reviews*, vol. 15, no. 2, pp. 155–66.
- Eighmy, T.T., Maratea, D. & Bishop, P.L. 1983, 'Electron microscopic examination of astewater biofilm formation and structural components', *Applied and environmental microbiology*, vol. 45, no. 6, pp. 1921–31.
- Ekelhof, A. & Melkonian, M. 2017, 'Enhanced extracellular polysaccharide production and growth by microalga *Netrium digitus* in a porous substrate bioreactor', *Algal Research*, vol. 28, pp. 184–91.
- Eldridge, R.J., Hill, D.R. & Gladman, B.R. 2012, 'A comparative study of the coagulation behaviour of marine microalgae', *Journal of Applied Phycology*, vol. 24, no. 6, pp. 1667–79.
- Figueroa, F.L., Jerez, C.G. & Korbee, N. 2013, 'Use of in vivo chlorophyll fluorescence to estimate photosynthetic activity and biomass productivity in microalgae grown in different culture systems', *Latin American Journal of Aquatic Research Journal of Aquatic Research*, vol. 41, no. 5, pp. 801–19.
- Flemming, H. & Wingender, J. 2010, 'The biofilm matrix', *Nature reviews. Microbiology*, vol. 8, no. 9, pp. 623–33.
- Fukami, K., Nishijima, T. & Ishida, Y. 1997, 'Stimulative and inhibitory effects of bacteria on the growth of microalgae', *Hydrobiologia*, vol. 358, no. 1–3, pp. 185–91.
- Genin, S.N., Aitchison, S.J. & Allen, G.D. 2014, 'Design of algal film photobioreactors: Material surface energy effects on algal film productivity, colonization and lipid content', *Bioresource Technology*, vol. 155, pp. 136–43.

- Goo, B.G., Baek, G., Choi, D.J., Park, Y. I., Synytsya, A., Bleha, R., Seong, D.H., Lee, C.G. & Park, J.K. 2013, 'Characterization of a renewable extracellular polysaccharide from defatted microalgae *Dunaliella tertiolecta*', *Bioresource Technology*, vol. 129, pp. 343–50.
- Grobbelaar, J.U. 2012, 'Microalgae mass culture: the constraints of scaling-up', *Journal of applied phycology*, vol. 24, no. 3, pp. 315-8.
- Gross, M., Henry, W., Michael, C. & Wen, Z. 2013, 'Development of a rotating algal biofilm growth system for attached microalgae growth with in situ biomass harvest', *Bioresource Technology*, vol. 150, pp. 195–201.
- Gross, M., Jarboe, D. & Wen, Z. 2015, 'Biofilm-based algal cultivation systems', *Applied Microbiology and Biotechnology*, vol. 99, no. 14, pp. 5781–9.
- Gross, M. & Wen, Z. 2014, 'Yearlong evaluation of performance and durability of a pilot-scale Revolving Algal Biofilm (RAB) cultivation system', *Bioresource Technology*, vol. 171, pp. 50–8.
- Gross, M., Zhao, X., Mascarenhas, V. & Wen, Z. 2016, 'Effects of the surface physico-chemical properties and the surface textures on the initial colonization and the attached growth in algal biofilm', *Biotechnology for Biofuels*, vol. 9, no. 1, p. 38.
- Hassard, F., Biddle, J., Cartmell, E., Jefferson, B., Tyrrel, S. & Stephenson, T. 2015, 'Rotating biological contactors for wastewater treatment - A review', *Process Safety and Environmental Protection*, vol. 94, pp. 285–306.
- Henderson, R., Parsons, S.A. & Jefferson, B. 2008, 'The impact of algal properties and pre-oxidation on solid–liquid separation of algae', *Water Research*, vol. 42, no. 8, pp. 1827–45.
- Henderson, R.K., Parsons, S.A. & Jefferson, B. 2010, 'The impact of differing cell and algogenic organic matter (AOM) characteristics on the coagulation and flotation of algae', *Water Research*, vol. 44, no. 12, pp. 3617–24.
- Hodoki, Y. 2005, 'Bacteria biofilm encourages algal immigration onto substrata in lotic systems', *Hydrobiologia*, vol. 539, no. 1, pp. 27–34.
- Hoh, D., Watson, S. & Kan, E. 2016, 'Algal biofilm reactors for integrated wastewater treatment and biofuel production: A review', *Chemical Engineering Journal*, vol. 287, pp. 466–73.
- Holmes, P.E. 1986, 'Bacterial enhancement of vinyl fouling by algae', *Applied and Environmental Microbiology*, vol. 52, no. 6, pp. 1391–3.

- Irving, T.E. & Allen, D.G. 2011, 'Species and material considerations in the formation and development of microalgal biofilms', *Applied Microbiology and Biotechnology*, vol. 92, no. 2, pp. 283–94.
- Jerez, C.G., Malapascua, J.R., Sergejevová, M., Masojídek, J. & Figueroa, F.L. 2016, 'Chlorella fusca (Chlorophyta) grown in thin-layer cascades: Estimation of biomass productivity by in-vivo chlorophyll a fluorescence monitoring', *Algal Research*, vol. 17, pp. 21–30.
- Jerez, C.G., Navarro, E., Malpartida, I., Rico, R.M., Masojídek, J., Abdala, R. & Figueroa, F.L. 2014, 'Hydrodynamics and photosynthesis performance of Chlorella fusca (Chlorophyta) grown in a thin-layer cascade (TLC) system', *Aquatic Biology*, vol. 22, pp. 111–22.
- Johnson, M.B. & Wen, Z. 2010, 'Development of an attached microalgal growth system for biofuel production', *Applied Microbiology and Biotechnology*, vol. 85, no. 3, pp. 525–34.
- Kadu, P.A. & Rao, Y.R.M. 2012, 'Rotating biological contactors : A critical review', *Journal of Scientific and Engineering Research*, vol. 3, no. 9, pp. 1–6.
- Karatan, E. & Watnick, P. 2009, 'Signals, regulatory networks, and materials that build and break bacterial biofilms', *Microbiology and Molecular Biology Reviews*, vol. 73, no. 2, pp. 310–47.
- Kesaano, M., Gardner, R.D., Moll, K., Lauchnor, E., Gerlach, R., Peyton, B.M. & Sims, R.C. 2015, 'Dissolved inorganic carbon enhanced growth, nutrient uptake, and lipid accumulation in wastewater grown microalgal biofilms', *Bioresource Technology*, vol. 180, pp. 7–15.
- Kesaano, M. & Sims, R.C. 2014, 'Algal biofilm based technology for wastewater treatment', *Algal Research*, vol. 5, no. 1, pp. 231–40.
- Kumar, K., Mishra, S.K., Shrivastav, A., Park, M.S. & Yang, J.W. 2015, 'Recent trends in the mass cultivation of algae in raceway ponds', *Renewable and Sustainable Energy Reviews*, vol. 51, pp. 875–85.
- Laamanen, C.A., Ross, G.M. & Scott, J.A. 2016, 'Flotation harvesting of microalgae', *Renewable and Sustainable Energy Reviews*, vol. 58, pp. 75–86.
- Lan, S., Wu, L., Yang, H., Zhang, D. & Hu, C. 2017, 'A new biofilm based microalgal cultivation approach on shifting sand surface for desert cyanobacterium *Microcoleus vaginatus*', *Bioresource Technology*, vol. 238, pp. 602–8.

- Lawrence, J.R., Neu, T.R. & Swerhone, G.D.W. 1998, 'Application of multiple parameter imaging for the quantification of algal, bacterial and exopolymer components of microbial biofilms', *Journal of Microbiological Methods*, vol. 32, no. 3, pp. 253–61.
- Liu, T., Wang, J., Hu, Q., Cheng, P., Ji, B., Liu, J., Chen, Y., Zhang, W., Chen, X., Chen, L., Gao, L., Ji, C. & Wang, H. 2013, 'Attached cultivation technology of microalgae for efficient biomass feedstock production', *Bioresource Technology*, vol. 127, pp. 216–22.
- Mata, T.M., Martins, A.A. & Caetano, N.S. 2010, 'Microalgae for biodiesel production and other applications: A review', *Renewable and Sustainable Energy Reviews*, vol. 14, no. 1, pp. 217–32.
- Misra, N., Panda, P.K., Parida, B.K. & Mishra, B.K. 2016, 'Way forward to achieve sustainable and cost-effective biofuel production from microalgae: a review', *International Journal of Environmental Science and Technology*, vol. 13, no. 11, pp. 2735–56.
- Molina Grima, E., Belarbi, E.H., Acien Fernández, F., Robles Medina, A. & Chisti, Y. 2003, 'Recovery of microalgal biomass and metabolites: process options and economics', *Biotechnology Advances*, vol. 20, no. 7, pp. 491–515.
- Naumann, T., Çebi, Z., Podola, B. & Melkonian, M. 2013, 'Growing microalgae as aquaculture feeds on twin-layers: A novel solid-state photobioreactor', *Journal of Applied Phycology*, vol. 25, no. 5, pp. 1413–20.
- Norsker, N.H., Barbosa, M.J., Vermue, M.H. & Wijffels, R.H. 2011, 'Microalgal production - A close look at the economics', *Biotechnology Advances*, vol. 29, no. 1, pp. 24–7.
- Nowack, E.C.M., Podola, B. & Melkonian, M. 2005, 'The 96-well twin-layer system: A novel approach in the cultivation of microalgae', *Protist*, vol. 156, no. 2, pp. 239–51.
- Odjadjare, E.C., Mutanda, T. & Olaniran, A.O. 2015, 'Potential biotechnological application of microalgae: a critical review', *Critical Reviews in Biotechnology*, vol. 37, no. 1, pp. 37–52.
- Ozkan, A. & Berberoglu, H. 2013, 'Cell to substratum and cell to cell interactions of microalgae', *Colloids and Surfaces B: Biointerfaces*, vol. 112, pp. 302–9.
- Ozkan, A., Kinney, K., Katz, L. & Berberoglu, H. 2012, 'Reduction of water and energy

- requirement of algae cultivation using an algae biofilm photobioreactor’, *Bioresource Technology*, vol. 114, pp. 542–8.
- Prokop A., Bajpai R.K. & Zappi M.E. (eds) 2015, ‘Thin-layer systems for mass cultivation of microalgae: flat panels and sloping cascades’, in J. Masojidek, M. Sergejevova, J.R. Malapascua, J. Kopecky, *Algal Biorefineries: Volume 2: Products and Refinery Design*, Springer, pp. 237–63.
- Romaní, A.M., Fund, K., Artigas, J., Schwartz, T., Sabater, S. & Obst, U. 2008, ‘Relevance of polymeric matrix enzymes during biofilm formation’, *Microbial Ecology*, vol. 56, no. 3, pp. 427–36.
- Schnurr, P.J., Espie, G.S. & Allen, D.G. 2013, ‘Algae biofilm growth and the potential to stimulate lipid accumulation through nutrient starvation’, *Bioresource Technology*, vol. 136, pp. 337–44.
- Sebestyén, P., Blanken, W., Bacsa, I., Tóth, G., Martin, A., Bhajji, T., Dergez, Á., Kesserű, P., Koós, Á. & Kiss, I. 2016, ‘Upscale of a laboratory rotating disk biofilm reactor and evaluation of its performance over a half-year operation period in outdoor conditions’, *Algal Research*, vol. 18, pp. 266–72.
- Sekar, R., Venugopalan, V.P., Satpathy, K.K., Nair, K.V.K. & Rao, V.N.R. 2004, ‘Laboratory studies on adhesion of microalgae to hard substrates’, *Hydrobiologia*, vol. 512, pp. 109–16.
- Šetlík, I., Šust, V. & Málek, I. 1970, ‘Dual purpose open circulation units for large scale culture of algae in temperate zones. I. Basic design considerations and scheme of a pilot plant’, *Algological Studies/Archiv für Hydrobiologie, Supplement Volumes*, pp. 111–64.
- Shen, Y., Zhang, H., Xu, X. & Lin, X. 2015, ‘Biofilm formation and lipid accumulation of attached culture of *Botryococcus braunii*’, *Bioprocess and Biosystems Engineering*, vol. 38, no. 3, pp. 481–8.
- Shi, J., Podola, B. & Melkonian, M. 2007, ‘Removal of nitrogen and phosphorus from wastewater using microalgae immobilized on twin layers: An experimental study’, *Journal of Applied Phycology*, vol. 19, no. 5, pp. 417–23.
- Shi, J., Podola, B. & Melkonian, M. 2014, ‘Application of a prototype-scale twin-layer photobioreactor for effective N and P removal from different process stages of municipal wastewater by immobilized microalgae’, *Bioresource Technology*, vol. 154, pp. 260–6.

- Sich, H. & Van Rijn, J. 1997, 'Scanning electron microscopy of biofilm formation in denitrifying, fluidised bed reactors', *Water Research*, vol. 31, no. 4, pp. 733–42.
- Singh, R., Paul, D. & Jain, R.K. 2006, 'Biofilms: implications in bioremediation', *Trends in Microbiology*, vol. 14, no. 9, pp. 389–97.
- Steinman, A.A.D. & Parker, A.A.F. 1990, 'Influence of substrate conditioning on periphytic growth in a heterotrophic woodland stream', *Journal of the North American Benthological Society*, vol. 9, no. 2, pp. 170–9.
- Sukačová, K., Trtílek, M. & Rataj, T. 2015, 'Phosphorus removal using a microalgal biofilm in a new biofilm photobioreactor for tertiary wastewater treatment', *Water Research*, vol. 71, pp. 55–63.
- Terry, K.L. & Raymond, L.P. 1985, 'System design for the autotrophic production of microalgae', *Enzyme and Microbial Technology*, vol. 7, no. 10, pp. 474–87.
- Torpey, W., Heukelekian, H. & Kaplovsky, A. 1971, 'Rotating disks with biological growths prepare wastewater for disposal or reuse', *Journal (Water Pollution Control Federation)*, pp. 2181–8.
- Torzillo, G., Giannelli, L., Martinez-Poldan, A., Verdone, N., De Filippis, P., Scarsella, M. & Bravi, M. 2010, 'Microalgal culturing in thin-layer photobioreactors', *Chemical Engineering*, vol. 20, pp. 265–70.
- Ugwu, C.U., Aoyagi, H. & Uchiyama, H. 2008, 'Photobioreactors for mass cultivation of algae', *Bioresource Technology*, vol. 99, no. 10, pp. 4021–8.
- Voloshin, R.A., Rodionova, M.V., Zharmukhamedov, S.K., Nejat Veziroglu, T. & Allahverdiev, S.I. 2016, 'Review: Biofuel production from plant and algal biomass', *International Journal of Hydrogen Energy*, vol. 41, no. 39, pp. 17257–73.
- Wei, Q., Hu, Z., Li, G., Xiao, B., Sun, H. & Tao, M. 2008, 'Removing nitrogen and phosphorus from simulated wastewater using algal biofilm technique', *Frontiers of Environmental Science and Engineering in China*, vol. 2, no. 4, pp. 446–51.
- Xu, X.Q., Wang, J.H., Zhang, T.Y., Dao, G.H., Wu, G.X. & Hu, H.Y. 2017, 'Attached microalgae cultivation and nutrients removal in a novel capillary-driven photobiofilm reactor', *Algal Research*, vol. 27, pp. 198–205.
- Yap, R.K.L., Whittaker, M., Diao, M., Stuetz, R.M., Jefferson, B., Bulmus, V., Peirson, W.L., Nguyen, A.V. & Henderson, R.K. 2014, 'Hydrophobically-associating cationic polymers as micro-bubble surface modifiers in dissolved air flotation for

- cyanobacteria cell separation', *Water Research*, vol. 61, pp. 253–62.
- Yau, S.K., Yusoff, F.M., Khong, N.M.H., Foo, S.C. & Lai, J.I. 2016, 'Improved pre-treatment protocol for scanning electron microscopy coupled with energy dispersive X-ray spectroscopy analysis of selected tropical microalgae', *Pertanika Journal of Tropical Agricultural Science*, vol. 39, no. 3, pp. 321–42.
- Zamalloa, C., Boon, N. & Verstraete, W. 2013, 'Decentralized two-stage sewage treatment by chemical-biological flocculation combined with microalgae biofilm for nutrient immobilization in a roof installed parallel plate reactor', *Bioresource Technology*, vol. 130, pp. 152–60.
- Zeng, X., Guo, X., Su, G., Danquah, M., Chen, X. & Lin, L. 2016, 'Harvesting of Microalgal Biomass', *Algae Biotechnology*, pp. 77–89.
- Zhang, Q., Liu, C., Li, Y., Yu, Z., Chen, Z., Ye, T., Wang, X., Hu, Z., Liu, S., Xiao, B. & Jin, S. 2017, 'Cultivation of algal biofilm using different lignocellulosic materials as carriers', *Biotechnology for Biofuels*, vol. 10, no. 1, pp. 1–16.
- Zhao, X., Kumar, K., Gross, M. a., Kunetz, T.E. & Wen, Z. 2018, 'Evaluation of revolving algae biofilm reactors for nutrients and metals removal from sludge thickening supernatant in a municipal wastewater treatment facility', *Water Research*, vol. 143, pp. 467–78.

## **CHAPTER 2. SELECTION OF A BIOFILM ATTACHMENT MATERIAL**

### **2.1 Introduction**

Cultivation of microalgal biofilms as a method of biomass production for various industrial applications has been researched extensively. One of the primary benefits of attached cell growth is the increased biomass concentration per unit volume compared to conventional suspended systems (Gross, Jarboe & Wen 2015; Christenson & Sims 2012). The higher solids concentration results in a lower liquid medium requirement, and consequently simpler and more economical harvesting (Berner, Heimann & Sheehan 2014). A biofilm is a layered accumulation of microorganism communities at a solid-liquid interface (Flemming & Wingender 2010) that forms in two stages – an initial reversible cell adsorption to a surface that has been conditioned with organic molecules, and a secondary stable cell attachment in a matrix of extracellular polymeric substances (EPS) (Bos, Van Der Mei & Busscher 1999; Dunne 2002). The process of initial cell attachment to a fresh attachment material usually lasts longer than successive biomass regrowth after the first harvesting (Johnson & Wen 2010; Blanken et al. 2014). The main parameters that influence microalgal biofilm formation on a supporting material include species selection (Irving & Allen 2011), cell growth phase and density (Sekar et al. 2004), harvest frequency (Gross et al. 2013) and attachment material properties (Gross, Jarboe & Wen 2015). The frequency of biomass harvesting has a direct impact on biofilm thickness, which must be monitored to prevent possible biomass sloughing when the biofilm is overly thick (Katarzyna, Sai & Singh 2015). Besides, the formation of an excessively thick biofilm may result in cell shading (Gross & Wen 2014), decrease mass transfer efficiency and reduce biofilm integrity (Gross, Jarboe & Wen 2015). The importance of choosing an appropriate microalgal biofilm attachment material has been stressed and discussed in numerous studies (Johnson & Wen 2010; Gross et al. 2013; Ozkan & Berberoglu 2013; Gross et al. 2016; Melo et al. 2018). Experimental results have indicated that microalgal biofilm formation varies widely with bioreactor setup and operational conditions (Gross et al. 2013; Gross & Wen 2014; Zhao et al. 2018), and there is no preferred type of material recommended for use in every biofilm system.

A number of approaches have been proposed to predict and explain the differences in microalgal cell attachment to various materials. Physicochemical properties of an attachment material have been extensively studied, with variable outcomes (Ozkan & Berberoglu 2013; Cui & Yuan 2013; Genin, Aitchison & Allen 2014; Gross et al. 2016; Christenson & Sims 2012; Zheng et al. 2016). Ozkan & Berberoglu (2013) claimed that acid-base reactions are the predominant mechanism of interaction between microalgal cells as well as between the cells and an attachment material, which determined biomass attachment. Genin, Aitchison & Allen (2014) attributed the efficiency of initial attachment to the polar surface energy of a material. Biofilm productivity showed weak correlation to liquid-attachment material contact angle, supporting the earlier conclusions of Irving & Allen (2011). However, changing the contact angle not only resulted in a 17% increase in *Scenedesmus obliquus* biofilm biomass concentration when compared to an untreated surface, but also caused modifications of the biofilm structure (Zheng et al. 2016). The authors altered glass surface wettability by spraying polytetrafluoroethylene emulsion on the attachment material and reported an increase in the biofilm porosity. The porous biofilm structure could have both positive and negative consequences on the biofilm system performance, such as enhanced mass transfer and lower biofilm stability (Zheng et al. 2016). Shen et al. (2016) reported a correlation between *Chlorella vulgaris* biofilm biomass productivity and adhesion ratio, which was different for cotton rope, canvas and spandex. It was suggested that the characteristics and the productivity of bound EPS determined the adhesion ratio. The influence of attachment surface texture on cell adsorption has also been widely researched. In general, initial cell recruitment on fresh materials with rough surfaces was reported to be higher than for smooth attachment materials (Irving & Allen 2011; Cui, Yuan & Cao 2014; Cao et al. 2009; Gross, Jarboe & Wen 2015). In particular, the geometry of microfeatures on an attachment material surface could have a considerable influence on cell settlement. Biofilm stability could be partially dependent on feature geometry due to cells being sheltered from shear stress in the crevices and openings on the surface of the material (Schnurr & Allen 2015). V-shaped grooves with dimension matching cell size were reported to provide a favourable environment for biomass adsorption (Cui, Yuan & Cao 2014; Sathananthan et al. 2013). Huang et al. (2018) determined the most advantageous size and geometry of microgrooves on a material surface for *S. obliquus* attachment. The V-shaped grooves were reported to decrease shear stress on the surface

compared to U-shaped grooves. The microgrooves also reduced the duration of initial cell attachment >2.5 fold, while also facilitating higher biomass concentration than a smooth attachment material. However, Gross et al. (2016) emphasised that the impact of flocculation must be studied when matching the size of surface features to cell diameter.

The material used for microalgal cell attachment is usually selected experimentally for a specific biofilm system. Melo et al. (2018) evaluated initial adhesion of *C. vulgaris* to six supporting materials and concluded that polyvinyl chloride with a rough surface showed the best performance in terms of promoting cell attachment. Tao et al. (2016) performed an initial *C. vulgaris* adsorption experiment to determine cell settlement efficiency on solid surfaces in order to choose the most favourable material for use in an algal biofilm airlift photobioreactor. Fibre showed the highest biomass adsorption capacity, and the authors attributed this result to increased surface roughness of this material when compared with plastic and terylene, which were also tested. Blersch et al. (2017) used three-dimensional (3D) printing to create surfaces of different topographies and test mixed community biofilm formation on them. The authors concluded that the feature size had an influence on the attachment dynamics of individual microalgal species. Cotton fabric was selected as cell attachment material in multiple microalgal biofilm studies (Christenson & Sims 2012; Gross et al. 2013; Bernstein et al. 2014; Kesaano et al. 2015; Gross et al. 2016). Christenson & Sims (2012) tested eight attachment materials with different weave patterns and material geometries for microalgal attachment, including cotton, nylon, polypropylene, acrylic, jute and polyester. While no biofilms could be harvested from polypropylene and nylon surfaces, cotton showed good performance as a biofilm growth material in domestic wastewater. In the study of Gross et al. (2013), sixteen materials including different fabrics were tested for their capacity to support microalgal biofilm formation. Cotton fabric was selected to support biofilm cultivation in their rotating algal biofilm system due to its ability to promote the highest cell attachment, alongside its durability and affordability. However, Gross et al. (2016) reported cotton degradation after 2-3 months of being submerged in liquid culture medium, and recommended nylon and polypropylene meshes as superior attachment materials. Microscopy proved to be a convenient tool for studying various aspects of microalgal biofilms. For example, Zhang et al. (2017) used environmental scanning electron microscopy (SEM) to produce images of microalgal biofilms on different attachment materials, and confocal laser

scanning microscopy (CLSM) to visualise topographical features of the material surfaces. *S. obliquus* biofilms were imaged with inverted microscopy in the study of Huang et al. (2018) to investigate the influence of different attachment material groove patterns on the microalgal cell attachment.

In this chapter, promising fabrics for attached microalgae cultivation with superior properties to cotton were selected. Fabric structures and surface features were visualised with SEM, and biofilm formation and development process on those surface geometries was studied with CLSM. A novel fabric with plastic polymer coating applied for increased roughness and enhanced cell attachment was also tested.

## **2.2 Aim and objectives**

**Aim:** Select optimal fabrics for microalgal biofilm growth and identify their distinctive features.

**Objective 1:** Assess initial microalgal attachment to different fabrics.

**Objective 2:** Analyse fabric surface structure by scanning electron microscopy.

**Objective 3:** Image biofilm formation and development by confocal laser scanning microscopy.

## 2.3 Research methodology

### 2.3.1 Experimental procedure

The selection process of the optimal fabrics for microalgal biofilm formation started with performing an initial cell attachment test for six promising materials. Based on the results of this test, three superior fabrics were chosen, and their surface structures were studied. Finally, the process of biofilm formation on these three fabrics was visualised using microscopy.

### 2.3.2 Initial cell attachment test. Stock culture of *Dunaliella tertiolecta*

The marine green flagellate *Dunaliella tertiolecta* (CS-321, ANACC, CSIRO) was cultured at 21.5°C in an incubator (Labec Pty Ltd, Australia). Microalgal cells were subjected to a 12/12h light/dark cycle of fluorescent illumination with a photon flux density of 40  $\mu\text{mol photon m}^{-2} \text{s}^{-1}$ . Fortnightly re-inoculations of 50 mL fresh F/2 medium (Guillard & Ryther 1962) took place to maintain the stock cultures.

### 2.3.3 Experimental culture of *Dunaliella tertiolecta*

An 800 mL sample of *D. tertiolecta* culture was used to inoculate 10 L of F/2 medium made with a dry concentrate (Varicon Aqua Solutions, Cell-hi F2P) in a modified transparent carboy. The microalgal culture was grown at 23°C in a temperature-controlled room under an irradiance of 100–200  $\mu\text{mol photon m}^{-2} \text{s}^{-1}$  and a 12/12h light/dark cycle. Gas exchange was facilitated by continuous culture aeration (400 ppm CO<sub>2</sub>) through an air diffuser and release of exhaust gas through an opening in the carboy lid.

The optical density (OD) of *D. tertiolecta* culture in the carboy measured as absorbance at 750 nm (SPECTRONIC 200 spectrophotometer) was 0.11 on the day of the attachment test start (Day 0).

### 2.3.4 Fabrics for microalgal biofilms formation

Six fabrics were selected based on their structural properties for the initial cell attachment test. The fabrics included: 65% polyester and 35% cotton blend with plastic polymer coating (coated blend), polar fleece, cotton, hemp and linen blend, linen, and hessian.

Coated blend is the material used by BioGill Operations Pty Ltd for microbial treatment of wastewater in trickle-bed reactors (Taylor et al. 2005; Taylor 2006). Wastewater is pumped and dispersed onto the coated blend fabric surface allowing a bacterial biofilm to form and digest nutrients from the wastewater. The hypothesis was that coated blend fabric would also promote microalgal cell attachment.

A fabric that served as an intermediate between coated blend and cotton was used in further experimentation. This fabric, referred to as uncoated blend, had the same composition as coated blend (65% polyester and 35% cotton), but with no coating.

The prices of the fabrics are listed in **Table 2.1**, and their properties are summarised in **Table 2.2**.

**Table 2.1** Fabrics used in the experiment and their cost.

<b>Fabric</b>	<b>Price per m<sup>2</sup>, fabric retail stores, Sydney, Australia</b>
Polar fleece	\$7
Hessian	\$9
65% polyester & 35% cotton blend with plastic polymer coating (coated blend)	\$10 (wholesale price, BioGill Pty Ltd)
Linen	\$16
Cotton	\$24
Hemp & linen blend	\$42

Polar fleece, coated blend, and hessian were the most economic materials tested in the initial microalgal attachment experiment.

**Table 2.2** Properties of fabrics.

<b>Fabric</b>	<b>Advantages</b>	<b>Disadvantages</b>	<b>Previous performance</b>	<b>Availability</b>
Coated blend	Lightweight, durable in wet environments.	Coating stability not studied.	Effective attachment material in commercial biofilm wastewater treatment.	Limited
Polar fleece	Durable, does not fray.	Heavy when wet.	Polypropylene fleece showed good performance as an attachment material for biofilm-based ammonium-rich groundwater bioremediation (Jechalke et al. 2010).	Widely available
Cotton	Durable in both wet and dry environments, resistant to alkaline conditions.	Prolonged exposure to sunlight weakens fibres.	Reported as a favorable cell attachment material (Christenson & Sims 2012; Gross et al. 2013); Degrades in 6 months if used as a biofilm attachment material (Gross et al. 2016).	Widely available
Hemp and linen blend	Strong, durable, heat and UV resistant.	-	-	Limited
Linen	Durable, stronger wet than dry, abrasion-resistant, heat resistant.	Breaks if folded repeatedly due to very low fibre elasticity.	-	Widely available
Hessian	Strong, durable in both wet and dry environments.	Heavy.	The beginning of hessian bag degradation was observed after 12-months of operation in seawater for seagrass seedlings recruitment (Irving, Tanner & Collings 2014).	Widely available
Uncoated blend*	Lightweight, tear-, abrasion-resistant, durable, keeps shape.	Flammable.	-	Widely available

\*Uncoated blend was used in further experimentation and was not tested in the initial cell attachment experiment.

### 2.3.5 Initial attachment experimental setup and sampling

Twelve Petri dishes with the six fabrics (coated blend, polar fleece, cotton, hemp and linen blend, linen, and hessian; 2 replicates for each fabric) were placed on an orbital shaker (Bioline Global Pty Ltd, Australia) in an incubator at 23°C under a 12/12h light/dark cycle and a photon flux density of 40  $\mu\text{mol photon m}^{-2} \text{ s}^{-1}$ . The Petri dishes contained a 5 x 5 cm square of fabric and 30 mL of *D. tertiolecta* culture. Magnetic stirrers were positioned on top of the fabric squares to prevent them from floating. The location of the Petri dishes on the orbital shaker was changed every day to decrease the impact of differences in irradiance on microalgal growth.

Measurements and sampling were performed daily at 11:00 h. 0.5 mL of *D. tertiolecta* culture was sampled from each Petri dish and replaced with 0.5 mL of fresh F/2 medium. OD measurements were performed immediately. Dilutions were applied if the value exceeded OD 0.5. In order to visually detect cell attachment, photos of the fabrics were taken daily with the Petri dish lids removed. The following procedure was carried out before taking photos of the fabrics to eliminate the possibility of suspended cells settlement on the surface without attachment:

- Carefully remove the stirring bar and take the fabric out of the liquid with tweezers.
- Allow it to drip for 40 seconds.
- Gently shake the fabric three times to remove drops.
- Carefully place the fabric back into its Petri dish with tweezers.
- Place the stirring bar in its original position on top of the fabric.

A change in fabric colour to green indicated cell attachment to the surface.

### 2.3.6 Biofilm development on liquid-air interface. Stock culture of *Chlorella vulgaris*

After performing the initial attachment test, the alga was changed in order to estimate biofilm formation efficiency in freshwater environment. For this purpose, the unicellular green microalga *C. vulgaris* (CS-42, Australian National Algae Culture Collection, CSIRO) was grown in suspension in MLA medium made from MLA 4-part concentrate (Algaboost™, AusAqua Pty Ltd, Australia) with regular re-inoculations every three weeks. Glass conical flasks (250 mL) containing 100 mL of *C. vulgaris*

suspended culture were kept in an incubator with fluorescent illumination (Labec Pty Ltd, Australia) under a photon flux density of  $40 \mu\text{mol photon m}^{-2} \text{s}^{-1}$  at  $20^\circ\text{C}$  and a 12/12h light/dark cycle.

### 2.3.7 Experimental setup and conditions

The setup described below was used to incorporate larger suspension volumes compared to the initial attachment test, and to prevent possible splashing. The fabric sample geometry was altered for testing two samples per flask under the same conditions, and for ensuring unobstructed access to a sample when it was required for imaging. This setup also allowed investigating the formation of microalgal biofilms at the liquid-air interface.

A 1 L glass conical flask containing 600 mL of MLA medium was inoculated with 60 mL of *C. vulgaris* stock culture and was kept at  $23^\circ\text{C}$  in a temperature-controlled laboratory under LED illumination. The microalgal cells were exposed to 12/12h light/dark cycles and were subjected to an irradiance of  $100\text{--}200 \mu\text{mol photon m}^{-2} \text{s}^{-1}$ .

After 7 days, the microalgal culture was used to fill 12 conical flasks (100 mL capacity) with 50 mL of the suspension in each flask. Samples of coated blend, uncoated blend and cotton with dimensions of  $15 \times 1.5$  cm were cut out and submerged in separate conical flasks (two replicates in each flask) so that half of the sample was soaked in the microalgal suspension, and the other half was dry, as shown in **Figure 2.1**. There were 4 flasks containing samples of each fabric to be imaged during 4 consecutive weeks of the experiment (**Figure 2.2**).



**Figure 2.1** A fabric sample partially submerged in *C. vulgaris* suspension.

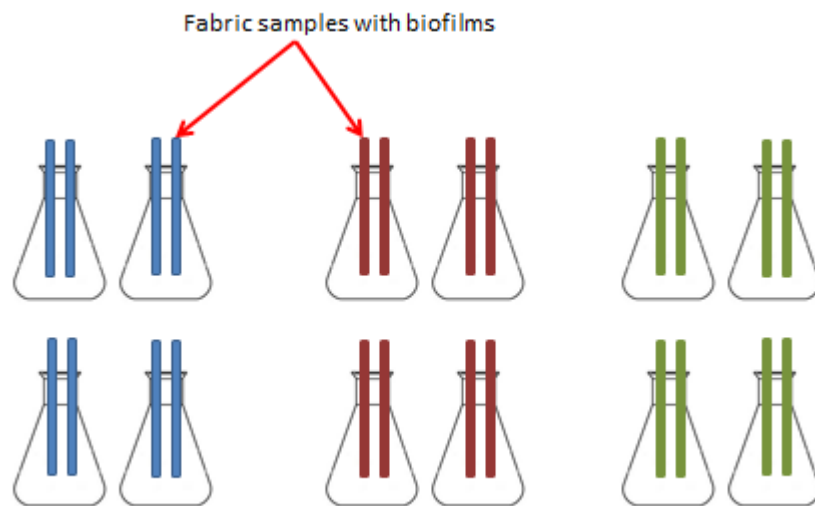


**Figure 2.2** Experimental setup – flasks containing fabrics with biofilms submerged in microalgal suspension: blue stripes – coated blend samples; red stripes – cotton samples; green stripes – uncoated blend samples.

The conical flasks containing microalgal suspension and the fabrics were placed on an orbital shaker (Bioline Global Pty Ltd, Australia) in the temperature-controlled laboratory.

### 2.3.8 Scanning electron microscopy – fabric structure

Structures of the preselected fabrics used for microalgal biofilm development were imaged by SEM. Fabric samples with dimensions of approximately 0.7 x 0.7 mm were

mounted on standard electron microscopy stubs with carbon double-sided adhesive disks. The samples were then placed in the Leica EM ACE600 high vacuum sputtering and carbon thread coater (Leica Microsystems Pty Ltd, Germany), and gold/palladium sputter coating was applied to inhibit charging, reduce thermal damage and improve secondary electron emission. Subsequently, the fabric structures were imaged with the Zeiss Evo LS15 thermionic tungsten electron gun scanning electron microscope (Carl Zeiss, Germany). The imaging was performed in high vacuum mode using a voltage of 10 kV in three different locations within a sample at 50X, 250X, 500X and 1,500X magnifications.

### **2.3.9 Confocal laser scanning microscopy – biofilm structure**

Three-dimensional structures of microalgal biofilms growing on the fabrics were analysed with CLSM. Each fabric sample was imaged once in two different regions and was disposed of after the procedure. The section of fabric with an attached biofilm (1 x 1 cm) in dimension was cut out of every sample and placed into a tissue culture dish (FD35-100, FluoroDish™, World Precision Instruments, USA). The sample was stained with Hoechst 33342 nucleic acid stain solution in water (Invitrogen, Thermo Fisher Scientific Inc., USA) with 1:200 dilution for 20 minutes to label the fibres with the fluorescent dye. The biofilm-covered fabric was subsequently washed twice for 5 minutes with ultrapure water (Arium®pro Ultrapure Water Systems, Sartorius, Germany) to remove any unbound dye. Finally, the fabric sample was placed on a tissue (Kimtech Science Kimwipes delicate task wipers, Kimberly-Clark Professional, USA) and left to dry at room temperature.

The dry biofilm samples were mounted on microscope slides and examined with the Nikon A1 confocal microscope operated by NIS-Elements Microscope Imaging Software, version 4.13 (Nikon, Japan). For the fabric imaging, laser excitation was at 405.6 nm (Hoechst 33342), while emission wavelengths were at 425-475 nm. Excitation wavelength for microalgal autofluorescence detection was at 637.4 nm, and emission signals were collected at 663-738 nm. Three-dimensional images were obtained using a Nikon 20X Plan Fluor NA0.45 objective with long working distance (Nikon, Japan).

### 2.3.10 Quantification of attached microalgal density on the fabrics

The approximate quantification of attached *C. vulgaris* biomass density on the fabrics was performed by processing the CLSM images with ImageJ (Fiji) software. Initially, the depth of the biofilm for every image was determined by multiplying the number of z stacks by the step distance. The common biofilm depth of  $100 \pm 1 \mu\text{m}$  was selected to be processed for all images. Then, the images were compressed across the z-axis, and the microalgal chlorophyll autofluorescence was quantified in the red channel. The quantified autofluorescence for every CLSM image was normalised to the highest obtained autofluorescence value, which was set to unity.

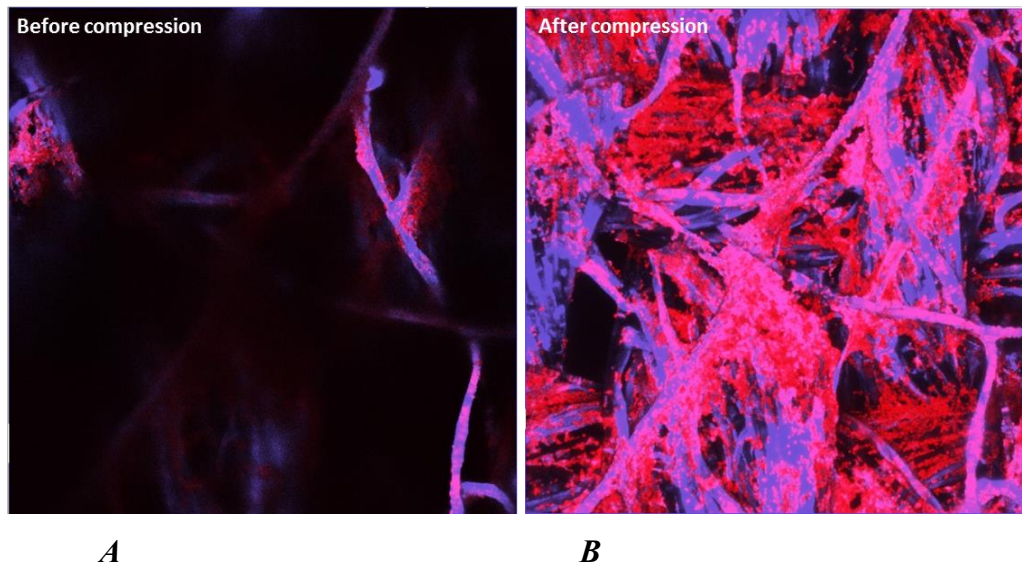


**Figure 2.3** Top view of a 3-dimensional CLSM image of *C. vulgaris* biofilm on a fabric: **A** – before compression with ImageJ (Fiji) software; **B** – after compression with ImageJ (Fiji) software.

**Figure 2.3** shows the image of a microalgal biofilm processed with ImageJ (Fiji) software for attached biomass density quantification.

### 2.3.11 Confocal laser scanning microscopy – biofilm thickness

CLSM was used to estimate the thicknesses of microalgal biofilms attached to each of the fabrics. A dry freshly cut square sample of a fabric with microalgal biofilm at liquid-air interface, pre-stained according to the same procedure as for the biofilm structure imaging, was turned onto its side and placed into a tissue culture dish (FD35-100, FluoroDish™, World Precision Instruments, USA) so that it was standing flat on the

bottom of the dish. The sample was held in place with a paper clip and was immobilised in agarose. The cross-section of the biofilm in the dish was imaged with Nikon A1 Confocal Microscope controlled by NIS-Elements Microscope Imaging Software, version 4.13 (Nikon, Japan) using Nikon 20X Plan APO NA0.75 objective (Nikon, Japan). The imaging protocol for biofilm thickness estimation was similar to the protocol for biofilm structure investigation described above. Finally, the obtained images were analysed to estimate the microalgal biofilm thicknesses.

It was determined that microalgal cell detachment and dissipation in agarose was likely to happen approximately 30 minutes after immobilisation (**Figure 2.4**).

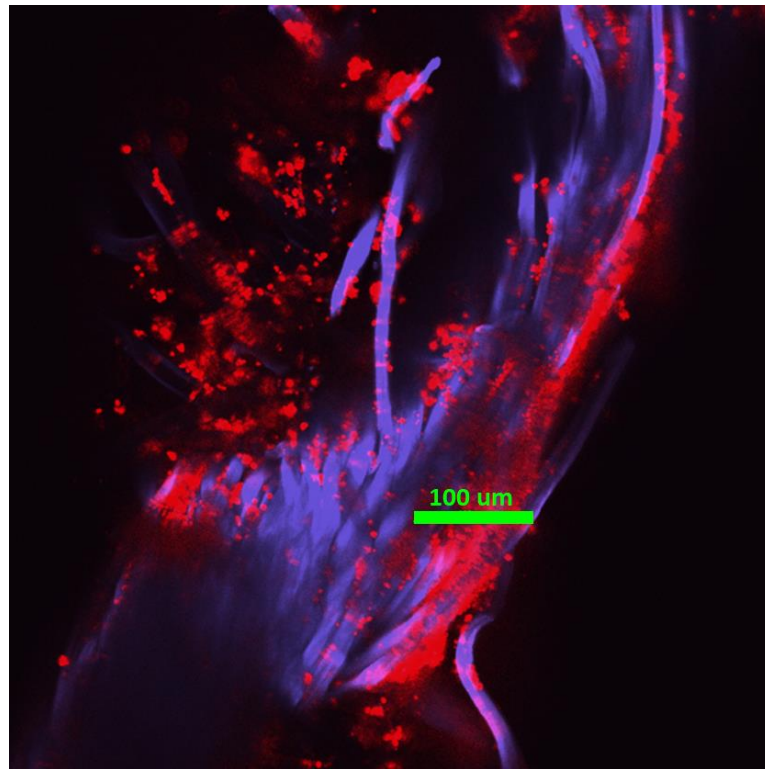


**Figure 2.4** Microalgal cell diffusion in agarose with time.

Thus, samples were prepared one by one and imaged immediately to avoid biofilm structure alterations.

## 2.4 Results and discussion

The selection of a fabric attachment material for microalgal biofilm attachment can have a crucial impact on biofilm system performance (Gross, Jarboe & Wen 2015). There is no universally-accepted material for microalgal biofilm production (Kesaano & Sims 2014), thus the attachment material selection is an open question. The pre-selected fabrics, including 65% polyester and 35% cotton blend with plastic polymer coating (coated blend), polar fleece, hessian, linen, cotton, and hemp and linen blend were tested for their capacity to promote and sustain initial microalgal cell attachment.

The progress of *D. tertiolecta* cell adsorption to the fabrics was assessed by visual observation. Change of fabric colour to green was attributed to microalgal cell attachment. The difference in colour of the material surfaces between the inoculation day (Day 0) and the last day of the experiment (Day 7) is demonstrated in **Figure 2.5**.

**Cotton:**

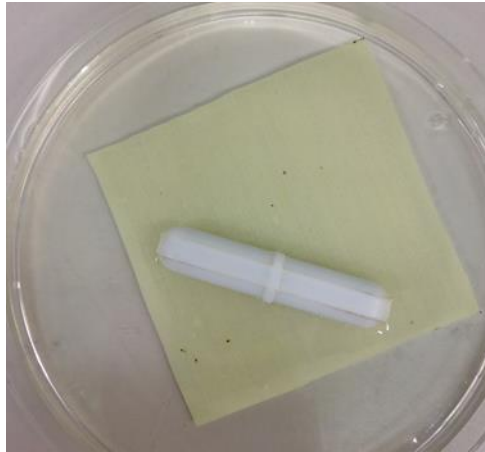


*Day 0*

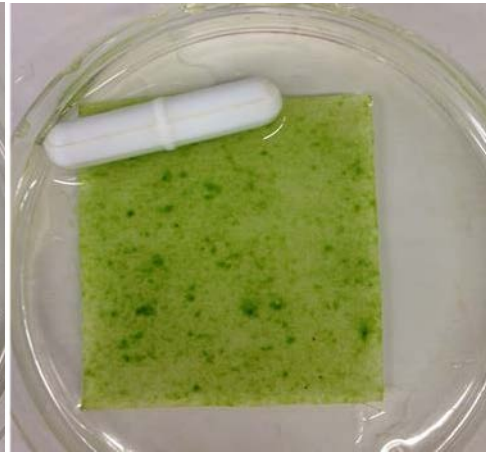


*Day 7*

**Coated blend:**



*Day 0*



*Day 7*

**Polar fleece:**



*Day 0*

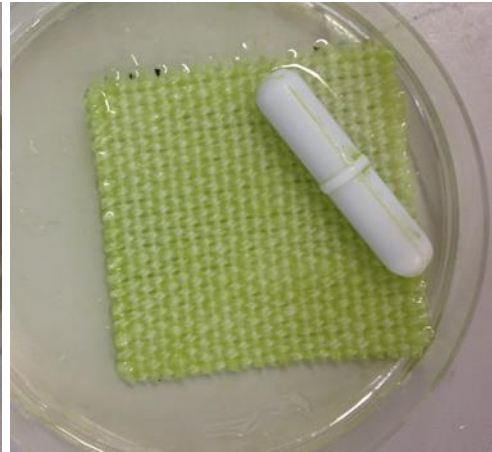


*Day 7*

**Hemp & linen blend:**



*Day 0*



*Day 7*

**Linen:**

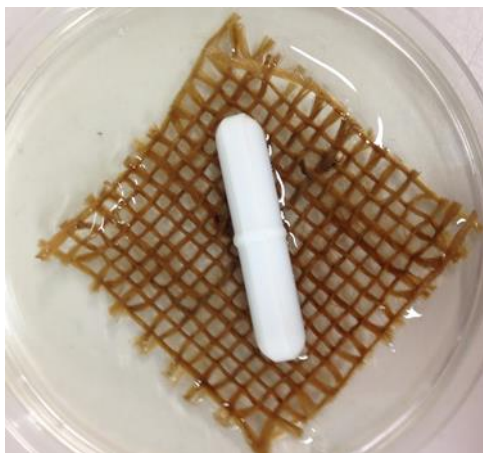


*Day 0*

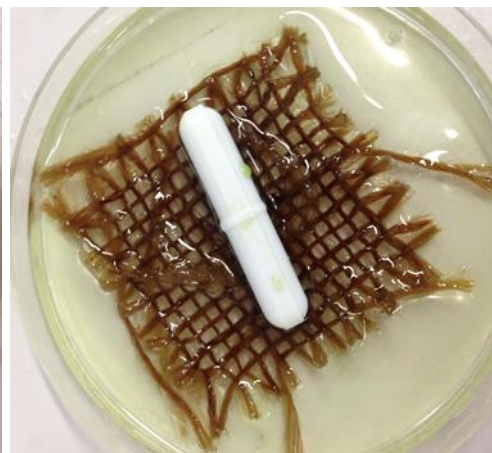


*Day 7*

**Hessian:**



*Day 0*



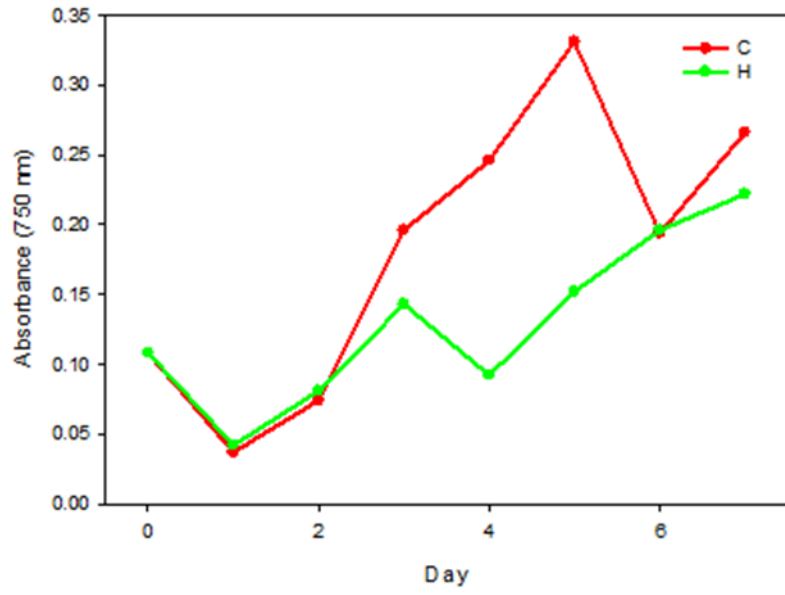
*Day 7*

**Figure 2.5** Change in fabric colour due to *D. tertiolecta* biofilm formation between the first day (Day 0) and the last day (Day 7) of the initial attachment experiment.

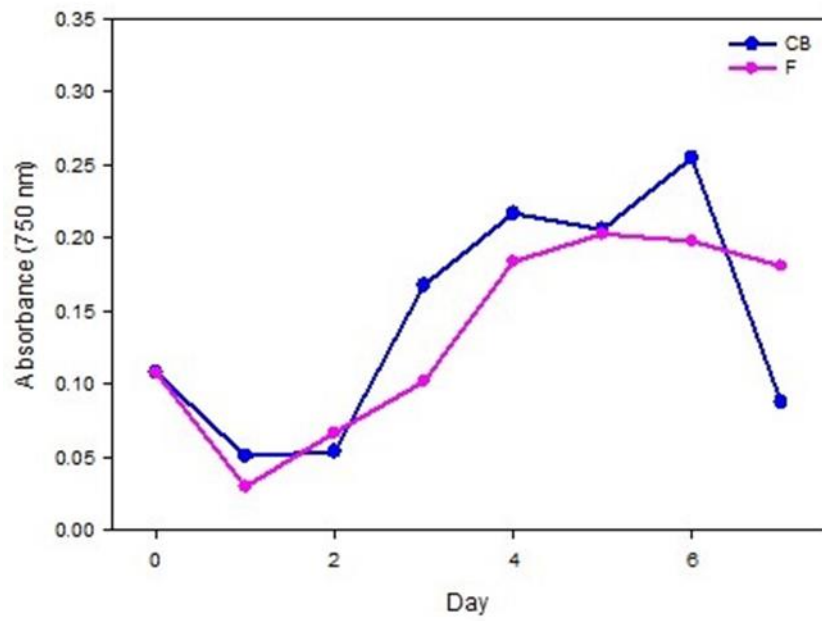
Cotton proved to be a suitable material for microalgal biofilm formation. Cell settlement on cotton was used as a baseline for comparison with the other fabrics because it was previously reported to be a favourable attachment material for biofilm formation (Christenson & Sims 2012; Gross et al. 2013; Bernstein et al. 2014; Kesaano et al. 2015; Gross et al. 2016) due to its flexibility, affordability, wide availability (Kesaano & Sims 2014), cellulose fibres (Christenson & Sims 2012) and surface roughness (Cui, Yuan & Cao 2014; Cao et al. 2009; Huang et al. 2018). Coated blend and polar fleece showed very good *D. tertiolecta* cell attachment. Visually, they had a slightly higher amount of biomass on their surfaces than cotton. Linen, as well as hemp and linen blend, showed moderate results. No microalgal settlement on hessian was observed.

Several fabric-specific patterns of initial biofilm formation were identified. Instant attachment occurred for polar fleece, whereby small areas of the sample surface turned green immediately after inoculation on Day 0. On Day 3, several dark green spots, presumably microalgal conglomerates, were detected on the surface of coated blend fabric. The number of conglomerates grew every day, and on Day 7, they covered the whole sample. A similar pattern was observed for polar fleece and linen, although the spots appeared later (Day 4 for linen and Day 6 for fleece) and in lower numbers.

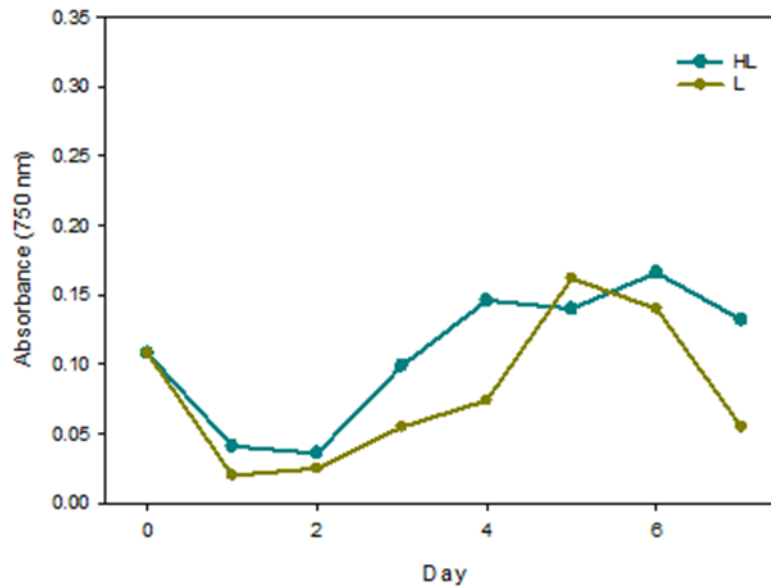
The OD of *D. tertiolecta* cultures (**Figure 2.6**) decreased by > 50% after inoculation on Day 0 in almost all Petri dishes. This could be attributed to the rapid attachment of the cells to the fabrics, or the change in growth conditions from the stock culture, or the combination of both factors. The highest suspended culture density was observed in the Petri dish containing the cotton sample. The OD decrease towards the end of the experiment was not detected for the hessian sample, where cells did not attach. This suggests that the cell density decrease in the Petri dishes, except in the one containing hessian, could either be caused by rapid cell attachment to the fabrics, or by cell death. Active and fast cell attachment to the fabrics is highly desirable for the purpose of biomass harvesting.



*A*



*B*



**C**

**Figure 2.6** OD of suspended *D. tertiolecta* culture: **A** – OD in the Petri dishes with cotton (C) and hessian (H) samples; **B** – OD in the Petri dishes with coated blend (CB) and polar fleece (F) samples; **C** – OD in the Petri dishes with hemp & linen blend (HL) and linen (L) samples.

The changes in OD measured for the suspended cultures in the Petri dishes could also be caused by a number of factors, including small changes in illumination, fabric toxicity, biofilm sloughing and subsequent growth in suspension.

**Table 2.3** summarises key results obtained in the current fabric attachment study.

**Table 2.3** Performance of the fabrics in the experiment.

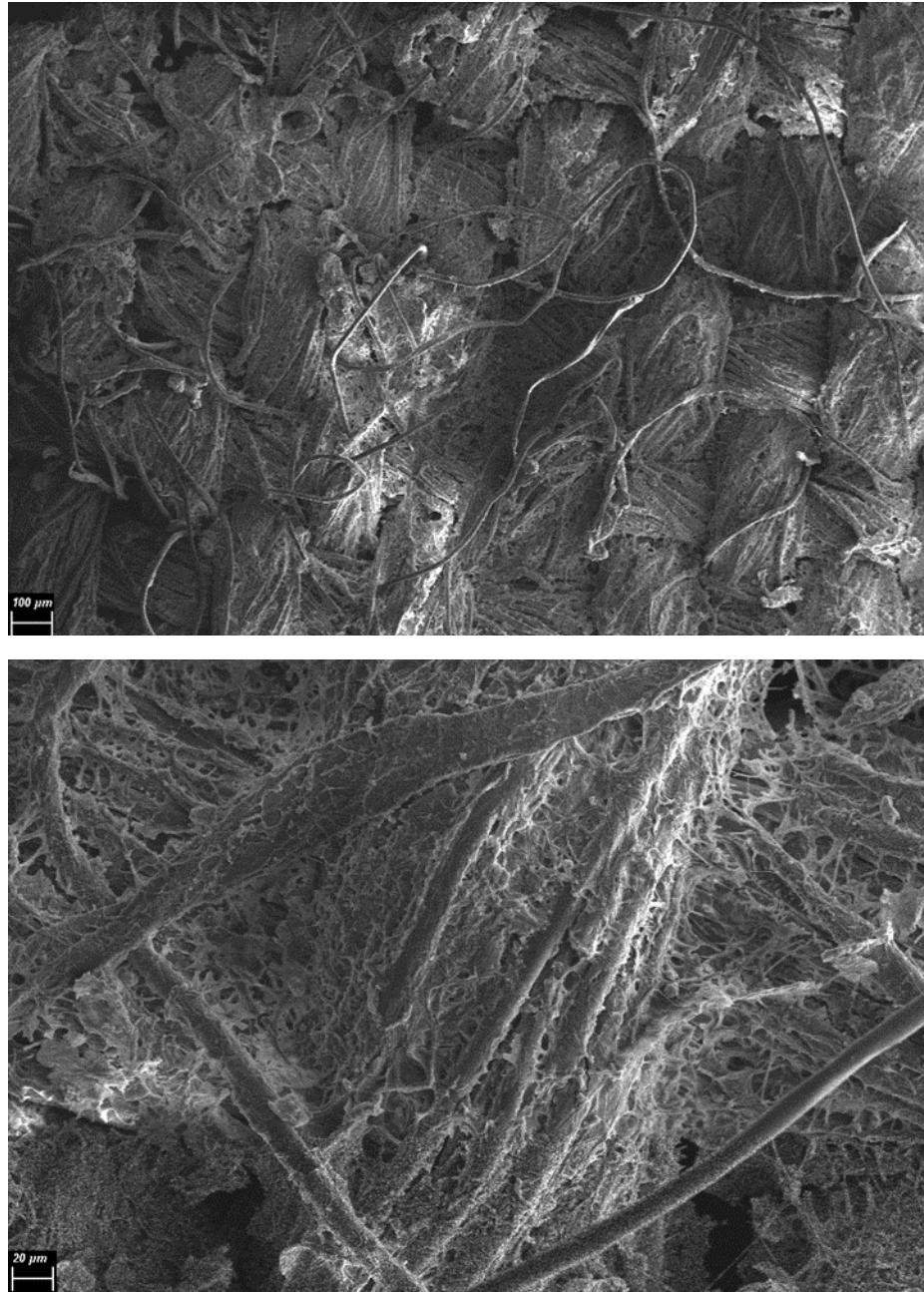
<b>Fabric</b>	<b>Performance</b>	<b>Additional observations</b>
Coated blend	Very good cell attachment; medium suspended culture density.	Fast formation of dark spots (hypothetically cell conglomerates) on the surface.
Polar fleece	Very good cell attachment; medium suspended culture density.	Slow formation of dark spots (hypothetically cell conglomerates) on the surface; immediate attachment on the day of inoculation.
Cotton	Good cell attachment; high suspended culture density.	-
Hemp & linen blend	Moderate cell attachment; low suspended culture density.	-
Linen	Moderate cell attachment; low suspended culture density.	Fast formation of dark spots (hypothetically cell conglomerates) on the surface.
Hessian	No cell attachment; medium suspended culture density.	No OD decrease in suspension towards the end of experiment.

Based on the information presented in **Table 2.3**, coated blend, cotton, and polar fleece were selected for further biofilm formation and development studies. In subsequent experiments, polar fleece demonstrated fast and efficient cell entrapment within its fibres, but no stable biofilm formation was observed on this fabric. Thus, further investigations are recommended to assess the potential of using polar fleece as an affordable and readily available biomass filter for various applications. The primary aim of this study was to develop a biofilm harvesting method with biomass production potential, which involves the development of a multilayer biofilm with stable attachment to a fabric. Polar fleece did not meet these requirements and its performance in biofilm formation was not continued. An intermediate fabric to serve as a control between coated blend and cotton, referred to as uncoated blend (**Table 2.2**), was used for subsequent experimentation.

The material structures of coated blend, cotton and uncoated blend fabrics were imaged with scanning SEM. Surface roughness, which has been identified as a promoting factor

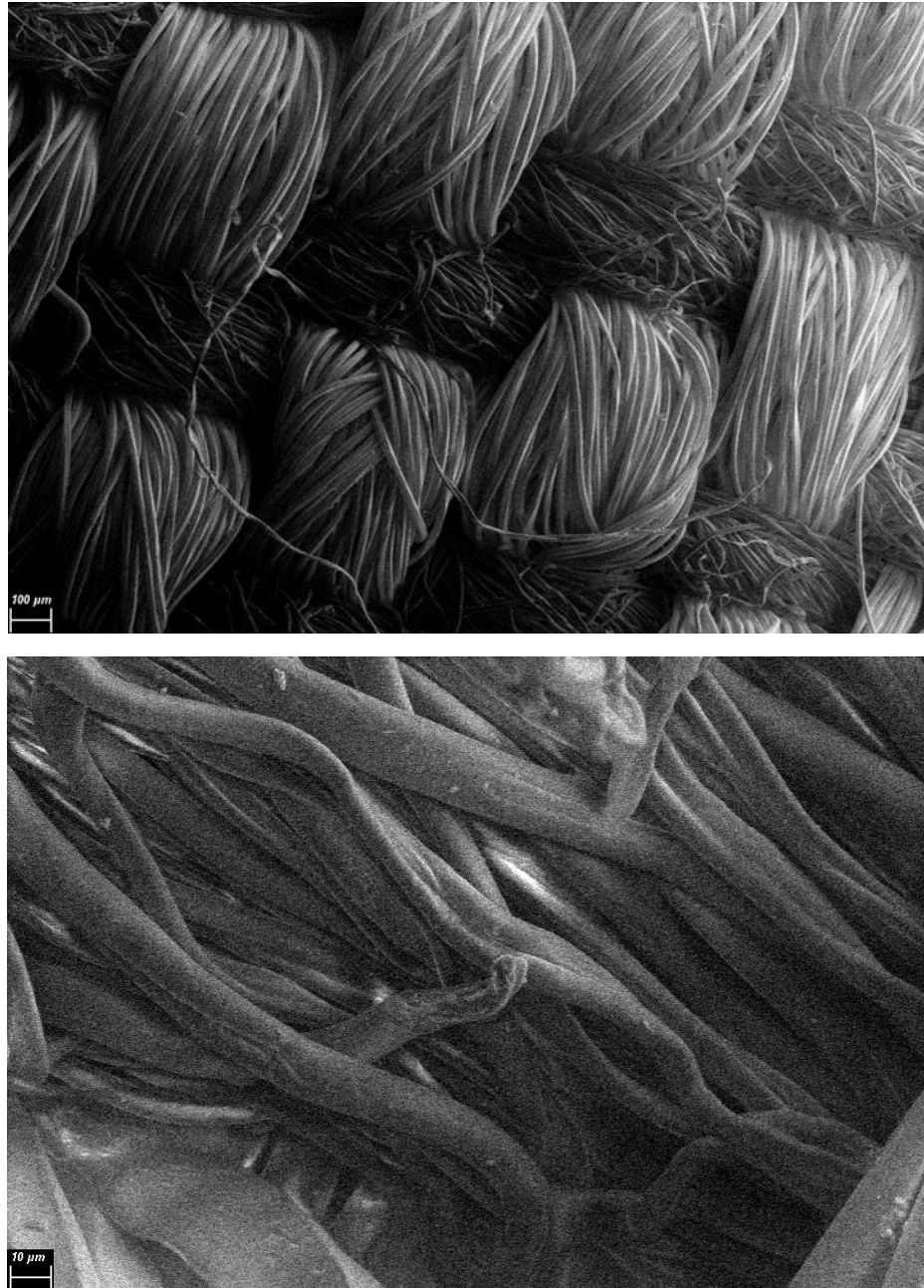
for cell recruitment on an attachment material, was analysed for each fabric (Cui, Yuan & Cao 2014; Cao et al. 2009; Huang et al. 2018).

Coated blend fabric exhibited a regular tight weave, but the fibre integrity was lacking (**Figure 2.7**). This could potentially decrease the fabric durability, which is an important parameter that ensures that the material is capable of withstanding multiple mechanical biomass harvestings in wet conditions (Gross, Jarboe & Wen 2015). The torn fibres were an indication of low-quality fabric, as opposed to damage during the coating application process, because the same fabric with no coating (uncoated blend) exhibited a similar level of fibre destruction. The plastic polymer coating was inhomogeneous but plentiful, providing substantial coverage of the fabric surface. Either the direction of the coating application, or the gravitational flow of the plastic polymer before settling resulted in more plentiful coverage of the vertical fibre clusters as compared to the horizontal clusters. The coating had a web-like appearance with a porous surface. The spatial distribution of the coating revealed better coverage of the inter-fibre spaces when compared to the actual fibres, linking them together into clusters. This could theoretically increase the area available for cell adsorption due to filling up the spaces between the fibres, while still allowing for gas transfer because of the porous nature of the coating. At the micrometre scale, it was observed that the coating was rather patchy, granulated and less than 1  $\mu\text{m}$  in thickness. The microscopic features created on the fabric surface due to the coating application significantly increased the material roughness compared to the bare fibres of the other fabrics. The coating concavities could entrap microalgal cells and shelter them from washing off, providing a favourable environment for biofilm formation (Schnurr & Allen 2015).



**Figure 2.7** Coated blend structure imaged with SEM at different magnifications.

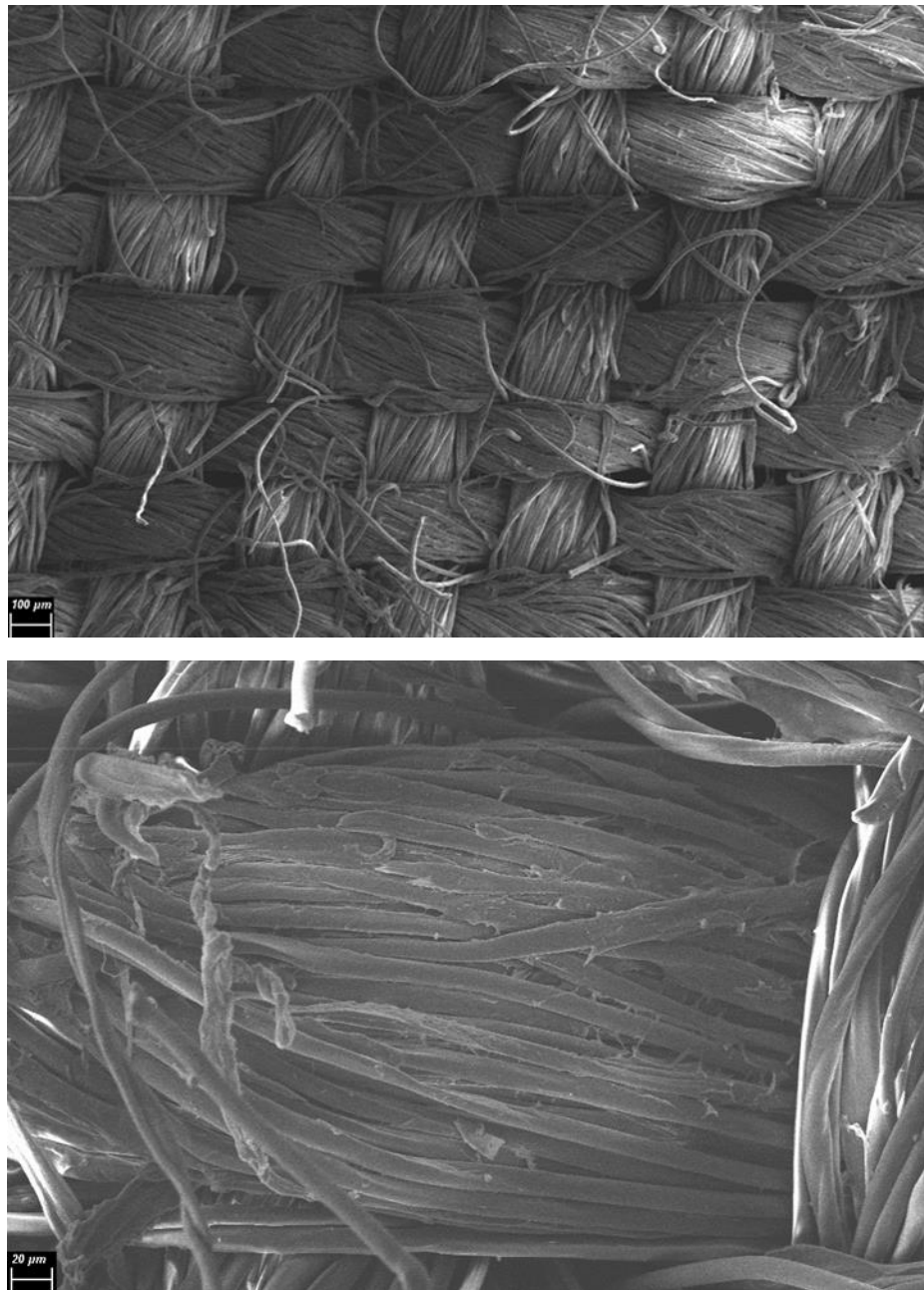
Cotton fabric also demonstrated regular weave, with larger fibre clusters and thicker individual fibres (**Figure 2.8**).



**Figure 2.8** Cotton structure imaged with SEM at different magnifications.

The weave of cotton was rather tight, with no clearly defined pores between fibre clusters. Using fabric with higher porosity could potentially improve gas transfer and consequently enhance attached biomass productivity (Christenson & Sims 2011; Podola, Li & Melkonian 2017). The fibre integrity was superior to coated blend. The fabric surface appeared quite smooth, suggesting that once in contact with a suspended culture, the microalgal cells would hypothetically settle between the fibres, rather than being entrapped and sheltered within surface crevices.

SEM imaging of uncoated blend revealed the presence of torn and damaged fibres with a plastic-like appearance at the micrometre scale (**Figure 2.9**), presumably due to the large polyester component of the fabric. Additionally, at higher magnifications, it was difficult to detect fully undamaged fibres, which indicated that the fabric quality could be improved. This surface roughness, however, could be advantageous in terms of microalgal cell entrapment during the inoculation stage. The observed material porosity was also higher compared to cotton. The fibre clusters and the individual fibres were smaller, explaining the beneficial lightweight nature of uncoated blend.



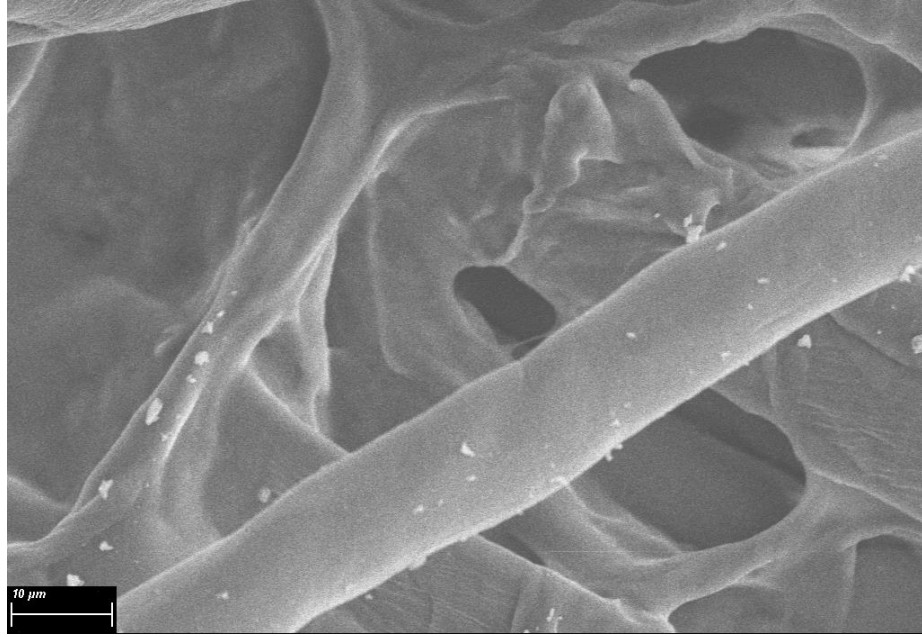
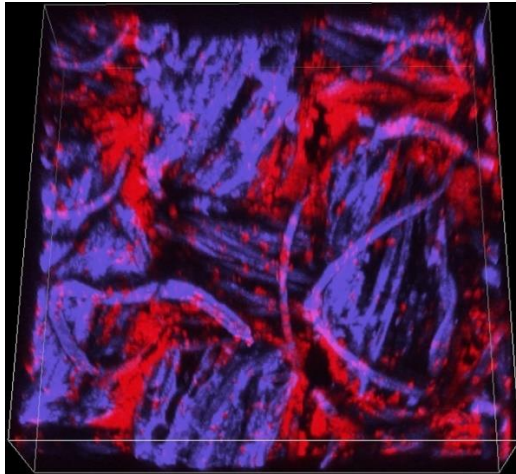


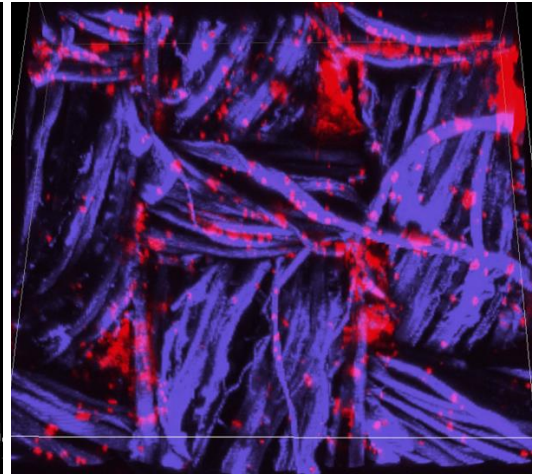
**Figure 2.9** Uncoated blend structure imaged with SEM at different magnifications.

Based on these results, coated blend was the preferred fabric to be used as a biofilm attachment material due to its surface roughness created by the coating, porous structure and lightweight nature.

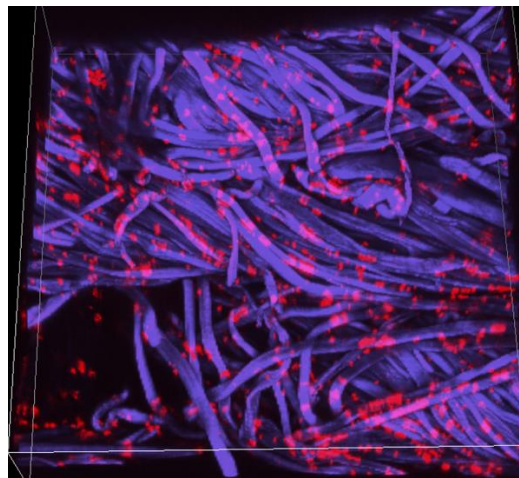
Once the surface structures were identified, the process of initial attachment of *C. vulgaris* cells to coated blend, uncoated blend and cotton, followed by the development of stable biofilms on these fabrics, was imaged with CLSM. The experiment was carried out for four weeks; each biofilm sample was imaged at two different locations across the fabric surface at liquid-air interface. Representative images of biofilms development over time are shown in **Figure 2.10**. In some areas on cotton fabric, stained fibre fluorescence was not clearly visible from the top view presented in **Figure 2.10**, presumably due to poor staining of the fibres within the thick fabric weave.



Coated blend

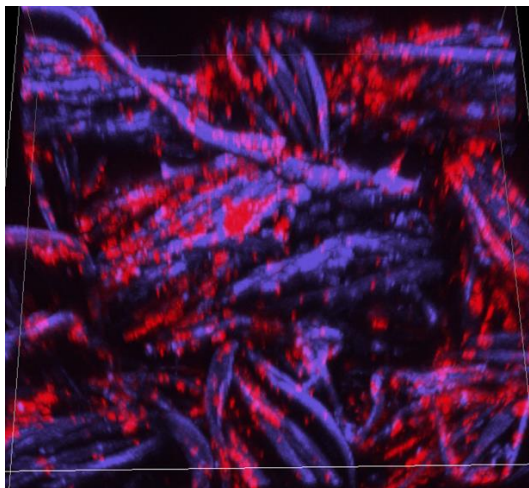


Uncoated blend

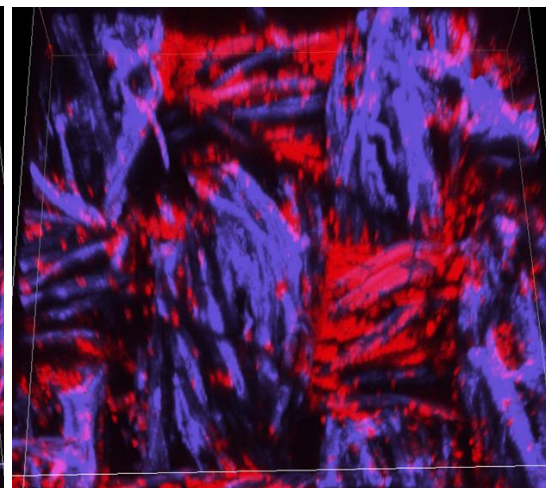


Cotton

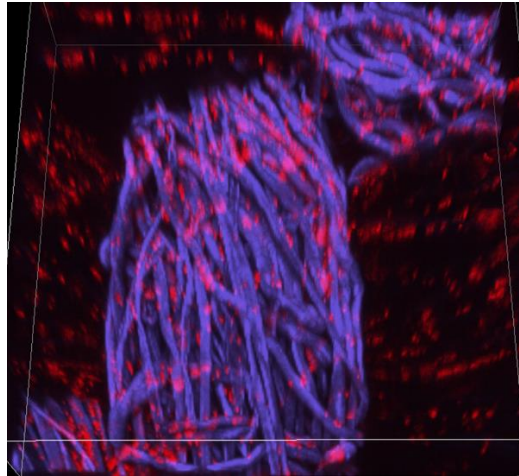
*A*



Coated blend

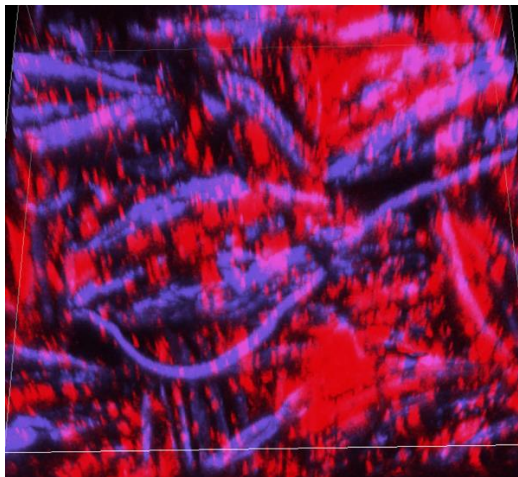


Uncoated blend

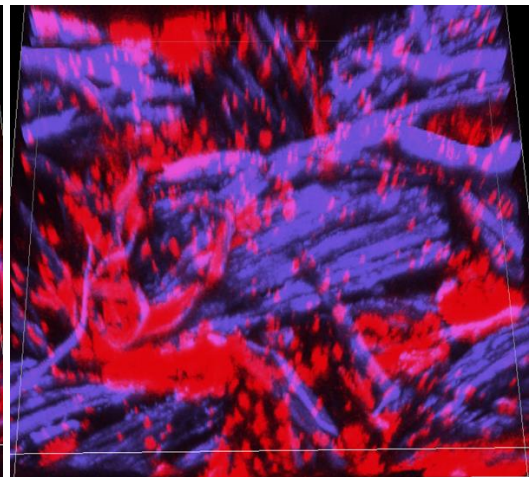


Cotton

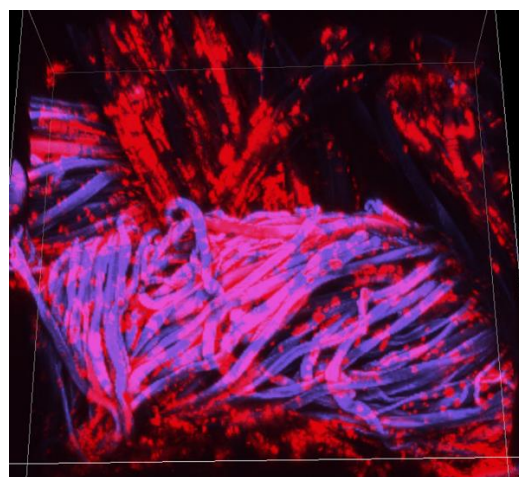
*B*



Coated blend

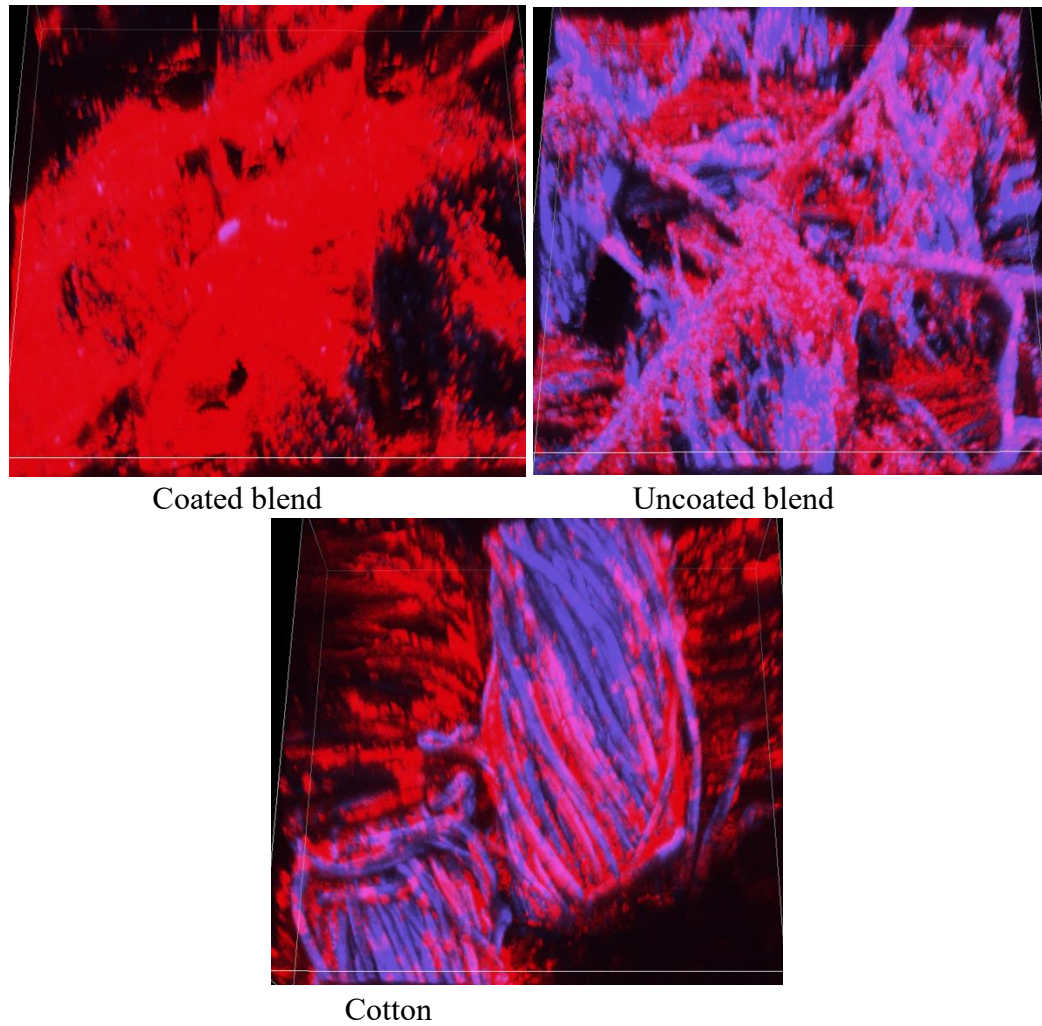


Uncoated blend



Cotton

*C*



**D**

**Figure 2.10** *C. vulgaris* biofilm development with time on coated blend, uncoated blend and cotton fabrics imaged by CLSM (red channel – microalgal chlorophyll autofluorescence, blue channel – Hoechst 33342 stained fabric fibres fluorescence; imaged square size 636  $\mu\text{m}$  x 636  $\mu\text{m}$ , variable depths): **A** – imaged biofilms after 7 days of attached growth; **B** - imaged biofilms after 14 days of attached growth; **C** - imaged biofilms after 21 days of attached growth; **D** - imaged biofilms after 28 days of attached growth.

More details about the process of biofilm development on the three fabrics were obtained after quantifying microalgal chlorophyll autofluorescence with ImageJ for each biofilm (**Figure 2.11**). The increase in autofluorescence was correlated with the increase in attached biomass density. Biofilm sections outside of the liquid-air interface (exposed to air and submerged in liquid) were also imaged and processed, and the lower biomass attachment compared to the interface was confirmed.

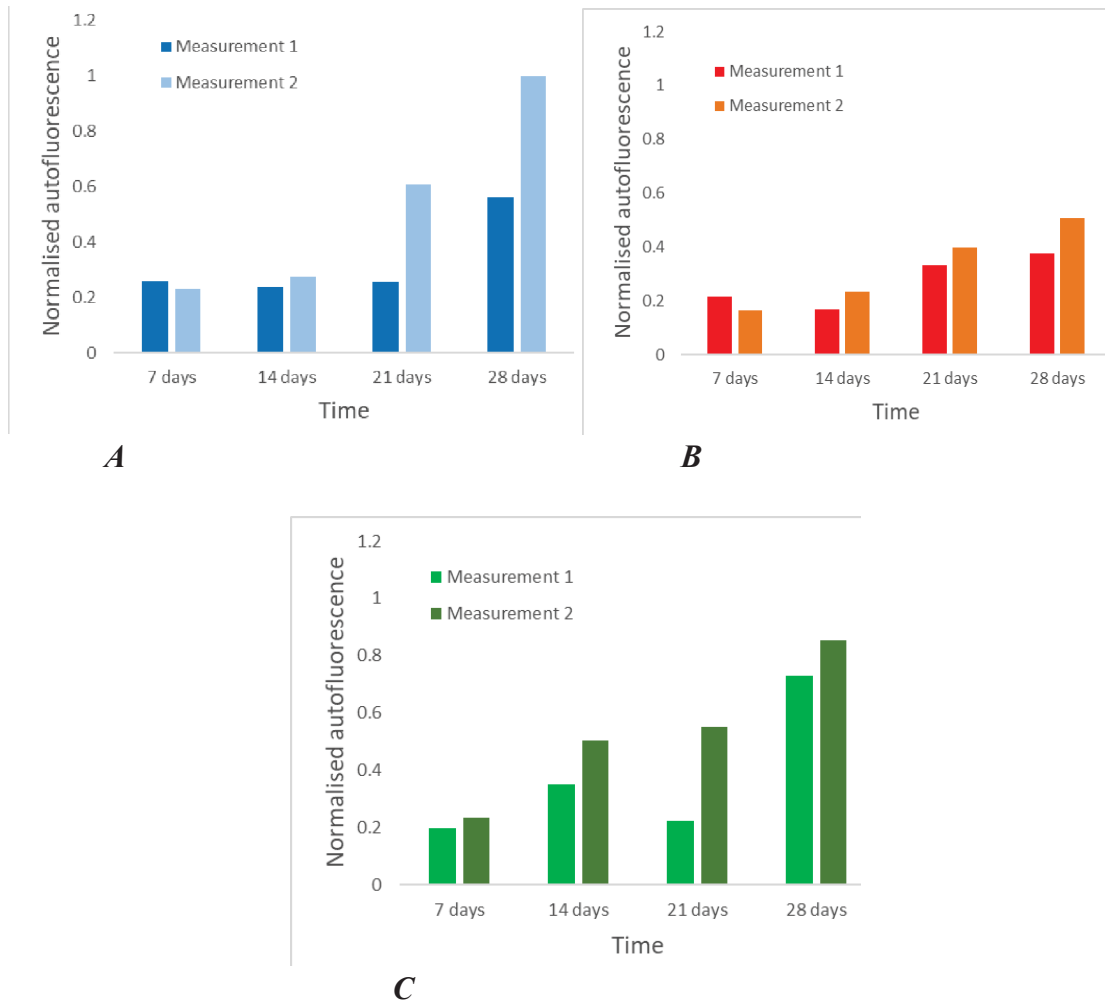


**Figure 2.11** Quantitative analysis of CLSM images: microalgal chlorophyll autofluorescence for two images (measurement 1 and measurement 2) at each datapoint: **A** – coated blend; **B** – cotton; **C** – uncoated blend.

The first seven days of the experiment (**Figure 2.10A**) corresponded to the initial attachment of the microalgal cells to the fabrics (Johnson & Wen 2010). The highest biomass attachment after the first week of biofilm cultivation was observed on the surface of coated blend. The cells settled predominantly in the spaces between the fibres spreading over individual fibres in the vicinity. This phenomenon might be linked to the spatial distribution of the plastic polymer coating, which exhibited better coverage of inter-fibre spaces than of separate fibres. The quantified autofluorescence for coated blend was approximately the same for the first two weeks of biofilm formation (**Figure 2.11A**). Both uncoated blend and cotton showed lower biomass attachment in the first seven days, with homogenous cell distribution on cotton fibres, and cell accumulation hotspots on uncoated blend surface (**Figure 2.10A**).

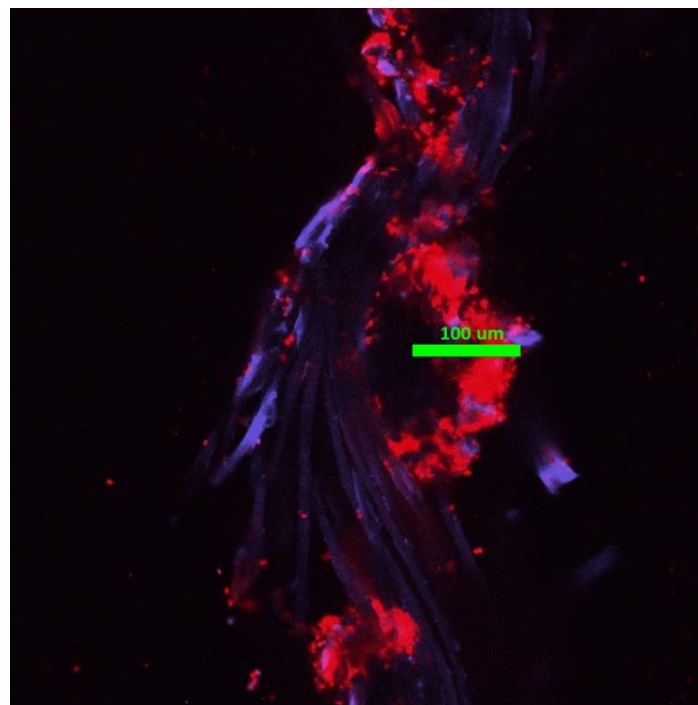
After fourteen days of *C. vulgaris* biofilm cultivation, uncoated blend demonstrated the thickest biofilm, which was unevenly spread on the fabric (**Figure 2.10B; 2.11C**). Elevated fibre clusters exhibited lower biomass accumulation. A possible explanation for this phenomenon is that the cells which attached to the fibres in the lower weave were better sheltered and less prone to shear stress and washing off (Cao et al. 2009; Gross, Jarboe & Wen 2015). For cotton, homogeneous cell attachment was observed in the first half of the experiment, and no significant differences in chlorophyll autofluorescence were detected for this fabric (**Figure 2.10A, B; 2.11B**). However, in the last two weeks (**Figure 2.10C, D**), the elevated fibre clusters of cotton fabric demonstrated decreased biomass attachment in comparison with the lower fibre clusters. It is hypothesised that as the biofilm matured, it became overly thick, and elevated parts of the biofilm were washed off from some areas of the fabric (Katarzyna, Sai & Singh 2015). The amount of autofluorescence predominantly detected on the more sheltered cotton fibre clusters nearly doubled for the third week (21 days) and slightly increased during the last week of the study (28 days) (**Figure 2.11B**).

Almost complete biofilm surface coverage was achieved with coated blend after 28 days of the biofilm growth (**Figure 2.10D**); however, the biofilm was inhomogeneous, with some fabric areas exhibiting higher coverage, which was also reflected on the amount of quantified chlorophyll autofluorescence (**Figure 2.11A**). For uncoated blend, high attached biomass density in the hotspots was measured in the end of the experiment (**Figure 2.11C**).

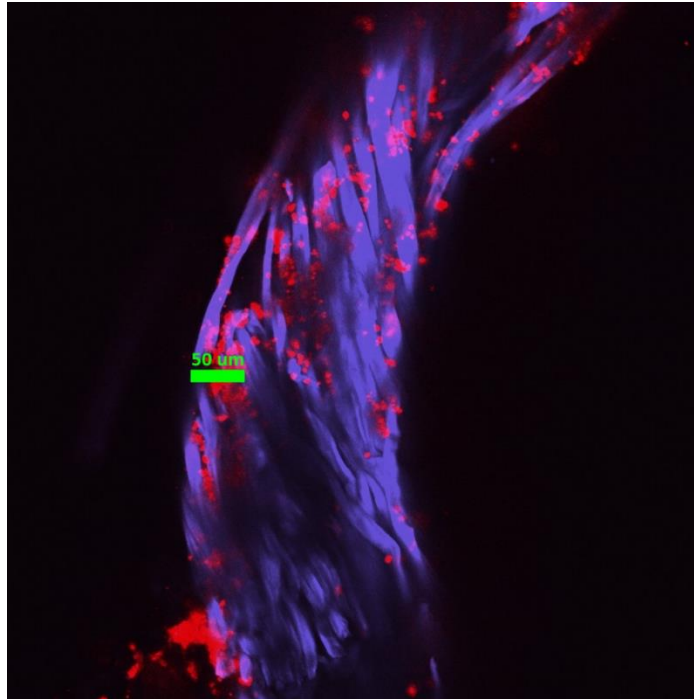
Overall, the three tested fabrics showed good performance as *C. vulgaris* biofilm attachment materials across four weeks of the experiment. Coated blend, cotton and uncoated blend demonstrated different patterns of biofilm formation on their surfaces at the liquid-air interface. Almost full surface coverage was achieved for coated blend. Biomass accumulation hotspots were spread out on the uncoated blend surface. Cotton showed the lowest attached cell density with decreased biomass coverage of the top layer of fibres that were exposed to the highest shear stress. Fabric-specific cell distribution on the three tested materials could be hypothetically explained by the differences in the surface topography. Both coated and uncoated blends had increased surface roughness compared to cotton. For coated blend, the additional crevices were created due to the application of the plastic polymer coating. The surface of uncoated blend was uneven because of the presence of torn and damaged fibres. Additionally, the

weave of these fabrics was looser, resulting in higher porosity. These factors hypothetically resulted in the more efficient initial entrapment of cells in the locations of the increased roughness (*i.e.* plentiful coating; torn fibres; surface topography created by porosity) and subsequent biofilm hotspots formation. On the contrary, cotton had tight weave made of smooth and thick fibres. Thus, cell settlement on this fabric was homogenous and evenly spread-out across the whole surface. The results of this experiment suggest that biofilms forming on coated blend fabric are less prone to sloughing, which makes this fabric beneficial for attached biomass cultivation.

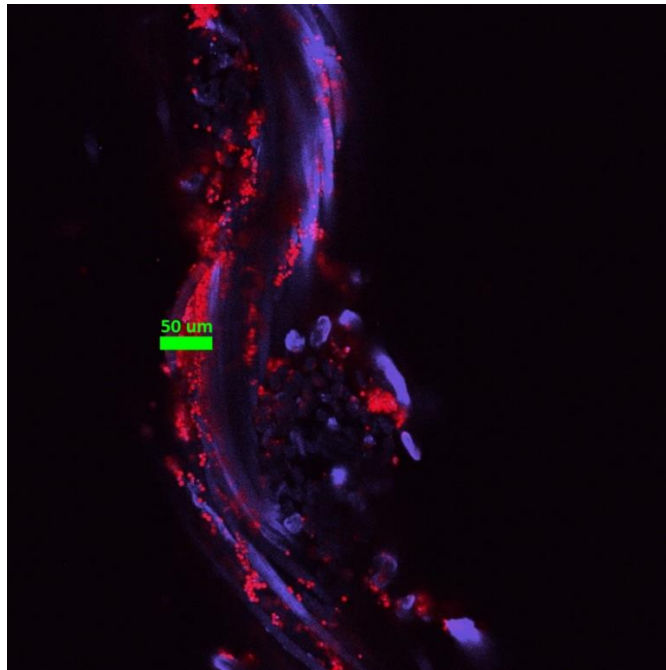
An easy and reliable method of biofilm thickness measurement by CLSM was also developed. Fabric samples with attached microalgal biofilms were imaged to visualise the arrangement of cell layers in a biofilm. The representative images of microalgal biofilm cross-sections with the measured thicknesses are shown in **Figure 2.12**:



Coated blend



Cotton



Uncoated blend

**Figure 2.12** Microalgal biofilm cross-sections on coated blend, cotton and uncoated blend for biofilm thickness measurements.

These images show that microalgal biofilms tend to form not only on the fabric surface, but also within the fabric weave. The described method for microalgal biofilm cross-section imaging with CLSM allowed fast and easy biofilm thickness estimation at any point of biofilm cultivation.

**Table 2.4** Summary of experimental procedure and main outputs of fabric attachment material selection.

	<b>Coated blend*</b>	<b>Polar fleece</b>	<b>Cotton</b>	<b>Hemp and linen blend</b>	<b>Linen</b>	<b>Hessian</b>	<b>Uncoated blend**</b>
<b>1. Preliminary screening</b>	Lightweight durable Polymer coating	Durable Heavy when wet	Durable Non UV-resistant	Durable UV-resistant	Durable Non-elastic	Durable Heavy	Lightweight Durable Flammable
<b>2. Initial cell attachment</b>	Very good	Very good	Good	Moderate	Moderate	None	-
<b>3. SEM imaging of surface structure</b>	Web-like coating	-	Smooth, tight weave	-	-	-	Damaged fibres
<b>4. Autofluorescence imaging and analysis (CLSM, ImageJ)</b>	Almost full surface coverage	-	Biofilm washes off under shear	-	-	-	Biomass accumulation hotspots
<b>6. CLSM measurement of biofilm thickness</b>	100 µm	-	50 µm	-	-	-	50 µm

\* Coated blend: 65% polyester and 35% **cotton** blend with plastic polymer coating.

\*\* Uncoated blend: 65% polyester and 35% **cotton** blend without coating.

The experimental procedure and the main results obtained in this chapter are summarised in **Table 2.4**.

## 2.5 Summary

Fabrics for microalgal biofilm cultivation were selected based on their structural properties and they were tested for initial cell attachment capacity. Polyester (65%) and cotton (35%) blend with plastic polymer coating (coated blend), cotton, and polar fleece showed the highest biomass attachment with different biofilm formation patterns. Polar fleece demonstrated high potential for filtering microalgal cells by entrapping them in its fibres, but stable biofilms did not form on its surface. Coated blend and cotton were selected for further experimentation. An intermediate fabric between these two materials, with exactly the same composition as coated blend, but with no coating (uncoated blend), was also tested.

Individual weave features of each fabric were studied with scanning electron microscopy. The surface roughness, which has a significant influence on microalgal cell adsorption and may also shelter attached cells from shear forces, was visualised and discussed. Coated blend fabric exhibited a microporous structure created by the coating layer on its surface. Uncoated blend fabric was characterised by a large number of torn and damaged fibres within its weave that increased the fabric roughness. Cotton fabric had a smooth, tight weave with large fibre clusters.

The process of microalgal biofilm formation and development on the fabrics was imaged by confocal laser scanning microscopy over a four-week experiment. Different patterns of biofilm formation for the coated blend, uncoated blend and cotton fibres were identified. Coated blend had the highest surface coverage with algal biomass. Hotspots of attached microalgal clusters were identified and imaged on the uncoated blend. The algal biofilm could be washed off from the cotton fabric surface. The attached microalgal cell density on the fabrics was estimated by quantifying microalgal chlorophyll autofluorescence in confocal microscopy images. Coated blend had the highest attached cell density out of the three fabrics tested here, although the biofilm surface attachment was inhomogeneous. A novel imaging method was developed to measure biofilm thickness along the fabric cross-section. The thickest biofilm developed on the coated blend fabric. Additionally, it was discovered that microalgal biofilms could form not only on top of the fabric surfaces, but also within the weave. Overall, coated blend showed to be the preferred fabric for microalgal biofilm formation

due to the optimal web-like coating structure, high cell attachment, lightweight nature and low cost.

## 2.6 References

- Berner, F., Heimann, K. & Sheehan, M. 2015, 'Microalgal biofilms for biomass production', *Journal of Applied Phycology*, vol. 27, no. 5, pp. 1793–804.
- Bernstein, H.C., Kesaano, M., Moll, K., Smith, T., Gerlach, R., Carlson, R.P., Miller, C.D., Peyton, B.M., Cooksey, K.E., Gardner, R.D. & Sims, R.C. 2014, 'Direct measurement and characterization of active photosynthesis zones inside wastewater remediating and biofuel producing microalgal biofilms', *Bioresource Technology*, vol. 156, pp. 206–15.
- Blanken, W., Janssen, M., Cuaresma, M., Libor, Z., Bhajji, T. & Wijffels, R.H. 2014, 'Biofilm growth of *Chlorella sorokiniana* in a rotating biological contactor based photobioreactor', *Biotechnology and Bioengineering*, vol. 111, no. 12, pp. 2436–45.
- Blersch, D.M., Kardel, K., Carrano, A.L. & Kaur, M. 2017, 'Customized 3D-printed surface topography governs species attachment preferences in a fresh water periphyton community', *Algal Research*, vol. 21, pp. 52–7.
- Bos, R., Van Der Mei, H.C. & Busscher, H.J. 1999, 'Physico-chemistry of initial microbial adhesive interactions - Its mechanisms and methods for study', *FEMS Microbiology Reviews*, vol. 23, no. 2, pp. 179–229.
- Cao, J., Yuan, W., Pei, Z.J., Davis, T., Cui, Y. & Beltran, M. 2009, 'A preliminary study of the effect of surface texture on algae cell attachment for a mechanical-biological energy manufacturing system', *Journal of Manufacturing Science and Engineering*, vol. 131, no. 6, p. 064505.
- Christenson, L. B. & Sims, R.C. 2011, 'Production and harvesting of microalgae for wastewater treatment, biofuels, and bioproducts', *Biotechnology Advances*, vol. 29, no. 6, pp. 686–702.
- Christenson, L.B. & Sims, R.C. 2012, 'Rotating algal biofilm reactor and spool harvester for wastewater treatment with biofuels by-products', *Biotechnology and Bioengineering*, vol. 109, no. 7, pp. 1674–84.
- Cui, Y. & Yuan, W. 2013, 'Thermodynamic modeling of algal cell-solid substrate interactions', *Applied Energy*, vol. 112, pp. 485–92.
- Cui, Y., Yuan, W.Q. & Cao, J. 2014, 'Effect of surface texturing on microalgal cell attachment to solid carriers', *International Journal of Agricultural and Biological Engineering*, vol. 7, no. 2, pp. 82–91.

- Dunne, W.M. 2002, 'Bacterial adhesion: seen any good biofilms lately?', *Clinical Microbiology Reviews*, vol. 15, no. 2, pp. 155–66.
- Flemming, H. & Wingender, J. 2010, 'The biofilm matrix.', *Nature reviews. Microbiology*, vol. 8, no. 9, pp. 623–33.
- Genin, S.N., Aitchison, S.J. & Allen, G.D. 2014, 'Design of algal film photobioreactors: Material surface energy effects on algal film productivity, colonization and lipid content', *Bioresource Technology*, vol. 155, pp. 136–43.
- Gross, M., Henry, W., Michael, C. & Wen, Z. 2013, 'Development of a rotating algal biofilm growth system for attached microalgae growth with in situ biomass harvest', *Bioresource Technology*, vol. 150, pp. 195–201.
- Gross, M., Jarboe, D. & Wen, Z. 2015, 'Biofilm-based algal cultivation systems', *Applied Microbiology and Biotechnology*, vol. 99, no. 14, pp. 5781–9.
- Gross, M. & Wen, Z. 2014, 'Yearlong evaluation of performance and durability of a pilot-scale Revolving Algal Biofilm (RAB) cultivation system', *Bioresource Technology*, vol. 171, pp. 50–8.
- Gross, M., Zhao, X., Mascarenhas, V. & Wen, Z. 2016, 'Effects of the surface physico-chemical properties and the surface textures on the initial colonization and the attached growth in algal biofilm', *Biotechnology for Biofuels*, vol. 9, no. 1, p. 38.
- Guillard, R.R.L. & Ryther, J.H. 1962, 'Studies of marine planktonic diatoms: I. *Cyclotella nana* Hustedt, and *Detonula confervacea* (Cleve) Gran', *Canadian Journal of Microbiology*, vol. 8, no. 2, pp.229–39.
- Huang, Y., Zheng, Y., Li, J., Liao, Q., Fu, Q., Xia, A., Fu, J. & Sun, Y. 2018, 'Enhancing microalgae biofilm formation and growth by fabricating microgrooves onto the substrate surface', *Bioresource Technology*, vol. 261, pp. 36–43.
- Irving, A.D., Tanner, J.E. & Collings, G.J. 2014, 'Rehabilitating seagrass by facilitating recruitment: Improving chances for success', *Restoration Ecology*, vol. 22, no. 2, pp. 134–41.
- Irving, T.E. & Allen, D.G. 2011, 'Species and material considerations in the formation and development of microalgal biofilms', *Applied Microbiology and Biotechnology*, vol. 92, no. 2, pp. 283–94
- Jechalke, S., Vogt, C., Reiche, N., Franchini, A.G., Borsdorf, H., Neu, T.R. & Richnow, H.H. 2010, 'Aerated treatment pond technology with biofilm promoting mats for the bioremediation of benzene, MTBE and ammonium contaminated

- groundwater’, *Water Research*, vol. 44, no. 6, pp. 1785–96.
- Johnson, M.B. & Wen, Z. 2010, ‘Development of an attached microalgal growth system for biofuel production’, *Applied Microbiology and Biotechnology*, vol. 85, no. 3, pp. 525–34.
- Katarzyna, L., Sai, G. & Singh, O.A. 2015, ‘Non-enclosure methods for non-suspended microalgae cultivation: literature review and research needs’, *Renewable and Sustainable Energy Reviews*, vol. 42, pp. 1418–27.
- Kesaano, M., Gardner, R.D., Moll, K., Lauchnor, E., Gerlach, R., Peyton, B.M. & Sims, R.C. 2015, ‘Dissolved inorganic carbon enhanced growth, nutrient uptake, and lipid accumulation in wastewater grown microalgal biofilms’, *Bioresource Technology*, vol. 180, pp. 7–15.
- Kesaano, M. & Sims, R.C. 2014, ‘Algal biofilm based technology for wastewater treatment’, *Algal Research*, vol. 5, no. 1, pp. 231–40.
- Melo, M., Fernandes, S., Caetano, N. & Borges, M.T. 2018, ‘Chlorella vulgaris (SAG 211-12) biofilm formation capacity and proposal of a rotating flat plate photobioreactor for more sustainable biomass production’, *Journal of Applied Phycology*, pp.1–13.
- Ozkan, A. & Berberoglu, H. 2013, ‘Cell to substratum and cell to cell interactions of microalgae’, *Colloids and Surfaces B: Biointerfaces*, vol. 112, pp. 302–9.
- Podola, B., Li, T. & Melkonian, M. 2017, ‘Porous substrate bioreactors: A paradigm shift in microalgal biotechnology?’, *Trends in Biotechnology*, pp. 121–32.
- Sathananthan, S., Genin, S.N., Aitchison, J.S. & Allen, D.G. 2013, ‘Micro-structured surfaces for algal biofilm growth’, *SPIE Micro/Nano Materials, Devices, and Systems*, SPIE, Melbourne, Victoria, Australia, vol. 8923, p. 892350.
- Schnurr, P.J. & Allen, D.G. 2015, ‘Factors affecting algae biofilm growth and lipid production: a review’, *Renewable and Sustainable Energy Reviews*, vol. 52, pp. 418–429.
- Sekar, R., Venugopalan, V.P., Satpathy, K.K., Nair, K.V.K. & Rao, V.N.R. 2004, ‘Laboratory studies on adhesion of microalgae to hard substrates’, *Hydrobiologia*, vol. 512, pp. 109–16.
- Shen, Y., Zhu, W., Chen, C., Nie, Y. & Lin, X. 2016, ‘Biofilm formation in attached microalgal reactors’, *Bioprocess and Biosystems Engineering*, vol. 39, no. 8, pp. 1281–8.

- Tao, Q., Gao, F., Qian, C.Y., Guo, X.Z., Zheng, Z. & Yang, Z.H. 2017, 'Enhanced biomass/biofuel production and nutrient removal in an algal biofilm airlift photobioreactor', *Algal Research*, vol. 21, pp. 9–15.
- Taylor, A.P.A., Holden, P.J., Finnie, K.S. & Bartlett, J. 2005, *Membrane bioreactor*, Patent 2005243606, Australian Intellectual Property Trademark Database.
- Taylor, A.P.A. 2006, *Sewage Treatment*, Patent 2006315091, Australian Intellectual Property Trademark Database.
- Zhang, Q., Liu, C., Li, Y., Yu, Z., Chen, Z., Ye, T., Wang, X., Hu, Z., Liu, S., Xiao, B. & Jin, S. 2017, 'Cultivation of algal biofilm using different lignocellulosic materials as carriers', *Biotechnology for Biofuels*, vol. 10, no. 1, p. 115.
- Zhao, X., Kumar, K., Gross, M.A., Kuntz, T.E. & Wen, Z. 2018, 'Evaluation of revolving algae biofilm reactors for nutrients and metals removal from sludge thickening supernatant in a municipal wastewater treatment facility', *Water Research*, vol. 143, pp. 467–78.
- Zheng, Y., Huang, Y., Liao, Q., Zhu, X., Fu, Q. & Xia, A. 2016, 'Effects of wettability on the growth of *Scenedesmus obliquus* biofilm attached on glass surface coated with polytetrafluoroethylene emulsion', *International Journal of Hydrogen Energy*, vol. 41, no. 46, pp. 21728–35.

## **CHAPTER 3. DEVELOPMENT OF A BIOFILM SYSTEM TO BE INSTALLED IN RACEWAY PONDS**

### **3.1 Introduction**

Laboratory-scale and pilot-scale raceway ponds are widely used to perform experimental studies and to test research hypotheses that are relevant to commercial raceway pond infrastructure. For example, He, Yang & Hu (2016) studied environmental adaptability, biomass and lipid productivities of five microalgal strains, and performed economical evaluation of various culturing modes in a 1,000 L (5 m<sup>2</sup>), as well as a 40,000 L (200 m<sup>2</sup>) open raceway ponds. Eustance et al. (2016) used three raceway ponds (2,300 L, 30 m<sup>2</sup> each) and flat-panel photobioreactors to compare microalgal biomass productivities and nitrogen assimilation potential under semi-continuous cultivation.

The factors that limit microalgal culture productivity in a raceway pond include temperature fluctuations, insufficient CO<sub>2</sub> mass transfer, low light availability and biological contamination (Hoh, Watson & Kan 2016). Microalgal biomass produced in a raceway pond needs to be harvested, *i.e.* separated from the liquid medium for further processing; however, all existing biomass harvesting methods are uneconomical (Laamanen, Ross & Scott 2016). Cultivation of microalgal biofilms and subsequent biomass harvesting by scraping is a promising method of decreasing algal bioproduct production costs by reducing the energy requirement for dewatering (Johnson & Wen 2010). In this chapter, a pilot-scale rooftop raceway pond was used to study the environmental variables that limit microalgal culture growth. Based on this knowledge, a biofilm-based microalgal growth and harvesting system was designed, installed and tested in the raceway pond.

## 3.2 Aim and objectives

**Aim:** Develop a biofilm-based harvesting system for microalgal raceway ponds.

**Objective 1:** Identify microalgal growth conditions and limitations in a pilot-scale raceway pond.

**Objective 2:** Design and install a biofilm-based harvesting system.

**Objective 3:** Operate and test this system at pilot-scale.

## 3.3 Research methodology

A number of experimental studies were carried out in a pilot-scale raceway pond. These preliminary experiments were used to select the most favourable raceway operating conditions, such as the inoculum volume and the paddlewheel rotation speed, as well as to obtain an in-depth understanding of all the processes that take place during microalgal culture growth. The representative dataset collected in Sydney, Australia, in summer 2016 is presented in this chapter.

### 3.3.1 Growth conditions and limitations in a raceway pond. Stock culture of *Nannochloropsis oceanica*

The unicellular green microalga *Nannochloropsis oceanica* (CS-179, Australian National Algae Culture Collection, CSIRO) was grown as a suspended culture in F/2 medium (Guillard & Ryther 1962) with regular re-inoculations to maintain the culture's health. Glass conical flasks (50 mL) containing *N. oceanica* were stored at 21.5°C in an incubator (Labec Pty Ltd, Australia) with fluorescent illumination at a 12/12 h light/dark cycle and a photon flux density of 40  $\mu\text{mol photon m}^{-2} \text{s}^{-1}$ .

### 3.3.2 Experimental culture of *Nannochloropsis oceanica*

*N. oceanica* culture (8 L) was grown in a 10 L transparent tank at 22°C in a temperature-controlled laboratory under LED illumination (Aqua Illumination Hydra 52 HD) in F/2 medium prepared with dry concentrate salts (Varicon Aqua Solutions, Cell-hi F2P). The microalgal cells were exposed to 12/12 h light/dark cycles and were subjected to an irradiance of 100–200  $\mu\text{mol photon m}^{-2} \text{s}^{-1}$ . Filtered ambient air with 400 ppm CO<sub>2</sub> was constantly supplied to the tank by means of an air diffuser.

Stationary phase microalgal cells (8 L), with an optical density (OD) of 1.20 measured at a wavelength of 750 nm (SPECTRONIC 200 spectrophotometer), were inoculated into a rooftop raceway pond on Day 0. The OD of the culture in the pond after inoculation was 0.06. The growth medium was prepared with dry F/2 concentrate dissolved in seawater.

### 3.3.3 Design and equipment of the rooftop raceway pond

The rooftop raceway pond with 660 L working volume and 220 mm depth (**Figure 3.1A,B**) was used for microalgae cultivation.



**A**



***B***

**Figure 3.1** Rooftop raceway pond: ***A*** – raceway pond; ***B*** – microalgal culture in the raceway pond.

The aeration was performed by delivering compressed air to the culture via two air diffusers fixed with metal loads at the bottom of the pond (**Figure 3.2**).



**Figure 3.2** Air diffusers with metal loads.

A paddlewheel was used to mix the culture; it was set at a frequency of 6 rpm for 4 days. On Day 4 of the raceway pond operation, the paddlewheel broke down, presumably due to salt accumulation and rapid corrosion of the motor structural elements. This problem was rectified by placing four air pumps (Quiet One® Aquarium

Pump 5000) into the pond to maintain microalgal cell suspension and the circulation of culture medium. One of the pumps was removed from the pond on Day 8 in order to reduce volumetric oxygen mass transfer coefficient.

### 3.3.4 Volumetric oxygen mass transfer

The volumetric oxygen mass transfer coefficient in the raceway pond was determined with a fibre-optic oxygen sensor (FireSting O<sub>2</sub>) by measuring the rate of increase in dissolved oxygen concentration from zero to equilibrium with air. An oxygen probe was placed in the pond while nitrogen gas was bubbled through the air diffusers. When the oxygen concentration in the pond approached zero, the air diffusers were switched to bubbling air until an oxygen-saturated equilibrium was attained. At a paddlewheel rotation speed of 6 rpm, a volumetric oxygen mass transfer coefficient of 6.52 h<sup>-1</sup> was calculated according to the equation below (Mendoza et al. 2013):

$$k_{La} t = \ln\left(\frac{[O_2^*] - [O_{2,0}]}{[O_2^*] - [O_{2,t}]}\right), \text{ where}$$

$k_{La}$  – volumetric oxygen mass transfer coefficient, s<sup>-1</sup>;

$t$  – time, s;

$O_2^*$  – equilibrium dissolved oxygen concentration, μmol L<sup>-1</sup>;

$O_{2,0}$  – dissolved oxygen concentration at the end of nitrogen bubbling, μmol L<sup>-1</sup>;

$O_{2,t}$  – dissolved oxygen concentration at time  $t$ , μmol L<sup>-1</sup>.

The same methodology was used to measure the oxygen evolution rate with 4 or 3 air pumps circulating the water instead of the paddlewheel. The volumetric mass transfer coefficients were equal to 8.96 h<sup>-1</sup> and 7.36 h<sup>-1</sup> respectively, indicating that 3 pumps induce similar mass transfer to a paddlewheel at 6 rpm.

### 3.3.5 Evaporative loss in the raceway pond

The liquid volume loss due to evaporation was calculated daily from the difference in the initial culture medium depth (220 mm) and depth measured at 11:00 h (sampling time).

### 3.3.6 Monitoring of microalgal growth conditions

Light intensity and temperature in the raceway pond were measured continuously with three HOBO Data Loggers (HOBO Pendant® Temperature/Light 64K Data Logger) placed at three positions in the pond as shown in **Figure 3.3**.

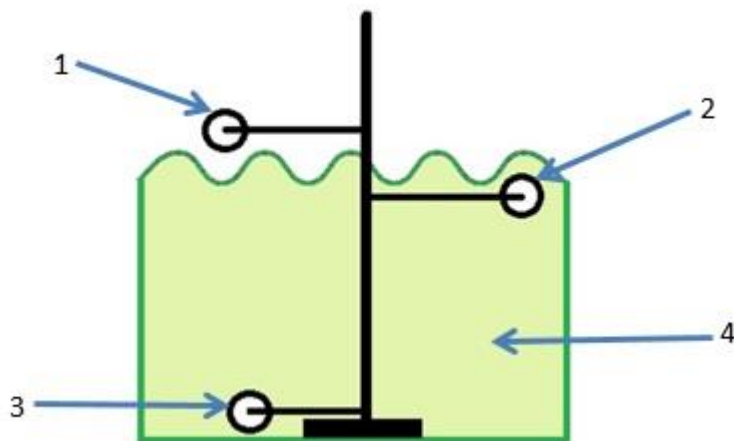


**Figure 3.3** HOBO Data Loggers positions in the raceway pond: (1) above the microalgal culture surface; (2) in the top layer of the culture; (3) close to the bottom of the pond; (4) microalgal suspension in the pond.

Continuous pH measurement was carried out using a pH probe (BlueBox-pH, Instrument Works Pty Ltd, Australia) placed in the raceway pond and wirelessly connected to a recording device. The pH probe was calibrated once per week.

Salinity was measured daily with a hydrometer (CORALIFE Deep Six®) and maintained at 33 g L<sup>-1</sup>. Changes in salinity and water depth in the pond due to rainfall were corrected by draining the excess culture volume and adding sea salt to maintain salinity of 33 g L<sup>-1</sup>. Evaporative liquid loss was replaced with seawater or a mixture of seawater and freshwater, depending on salinity.

### 3.3.7 Sampling protocol

Sampling of *N. oceanica* from the raceway pond was carried out daily at 11:00 h for 26 days. Samples were taken from three different locations within the pond. OD and dry weight (DW) measurements were conducted immediately after sampling, whereas cell density determination, chlorophyll *a* extraction and nitrate quantification were carried out at the end of the pilot study. Dilutions were applied whenever the OD measurement exceeded an OD of 0.5.

### 3.3.8 Dry weight

Biomass concentration in the raceway pond was determined by measuring the DW daily starting on Day 6 according to a protocol adapted from Borowitzka & Moheimani (2013). Briefly, a 47 mm GF/C filter was dried at 100°C in an oven (Labec Pty Ltd, Australia), cooled in a desiccator for 2 hours and weighted. A sample of a known volume (100 mL for low cell density; 50 mL for high cell density, determined by filter clogging if 100 mL sample volume used) was filtered and washed with 10–20 mL of 0.65 M ammonium formate solution to remove salts. The algae filter was stored at 100°C overnight, cooled in a desiccator and weighted. The weight of the dry biomass per litre was expressed using the equation below:

$$DW = ((\text{weight of filter with microalgae}) - (\text{weight of filter})) \times 10^*$$

\*multiply by 20 if 50 mL sample used.

### 3.3.9 Automated cell density determination

A 1 mL sample of *N. oceanica* was removed from the raceway pond, fixed with 1% glutaraldehyde and stored at 4°C until analysis. A 10 µL aliquot of the stored sample was placed on a haemocytometer under a microscope (Nikon Upright Automated Fluorescence Microscope), and 9 pictures were taken with a digital camera (Nikon DS-Qi2 monochrome microscope camera). The number of cells in 1 mL was determined by counting the cells in the pictures using ImageJ (Fiji) software.

### 3.3.10 Chlorophyll *a* extraction

Chlorophyll *a* concentration was measured by adapting the protocol from Borowitzka & Moheimani (2013). Briefly, a 1.5 mL *N. oceanica* sample was removed from the raceway pond, vacuum-filtered (GF/C filter) and stored at -80°C until extraction. Pure methanol (5 mL) was added to a 15 mL falcon tube containing the GF/C filter and stored in the dark at 4°C for 20 min. The sample was disrupted by sonication for 15 min and centrifuged for 10 min at 4,000 rpm (Rotanta 460R centrifuge). The absorbance at 666 nm ( $A_{666}$ ) was measured, and the chlorophyll *a* concentration in µg per mL was calculated using the equation below (Henriques, Silva & Rocha 2007):

$$Chl\ a = 15.65 \times A_{666}$$

### 3.3.11 Nitrate concentration

Nitrate concentration in the growth medium was determined according to the protocol adapted from Schnetger & Lehnert (2014). In brief, NO<sub>x</sub> reagent was prepared by mixing 5 parts of saturated vanadium chloride reduction solution, 1 part of 0.2% NEDD solution and 1 part of 2% sulphanilamide solution. 500 µL of the reagent were added to a 2 mL microtube containing 40 µL of sample, followed by incubation for 1 hour at 45°C and measuring the absorbance at 540 nm. The colour of the samples with the NO<sub>x</sub> reagent after the incubation changed from bright pink (the highest nitrite content) to blue (nitrite content close to zero).

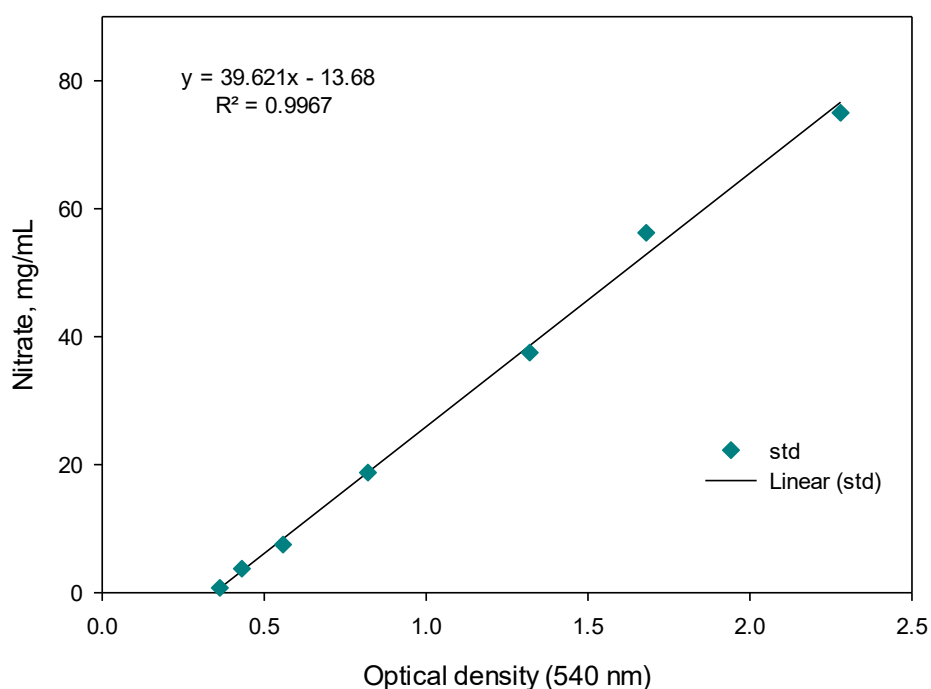


**Figure 3.4** Nitrate analysis standard.

The developed standard curve for nitrate concentration determination is shown in **Figure 3.4**.

### 3.3.12 Light attenuation in the raceway pond

Light attenuation coefficient was calculated using the ratio between the photon flux density at the top/bottom of the raceway pond using the equation below:

$$a = \frac{\ln(I_{top}/I_{bot})}{z}, \text{ where}$$

$\alpha$  – attenuation coefficient,  $\text{m}^{-1}$ ;

$I_{top}$  – light intensity at the surface of the microalgal culture,  $\mu\text{mol photons m}^{-2} \text{ s}^{-1}$ ;

$I_{bot}$  – light intensity at the bottom of the microalgal culture,  $\mu\text{mol photons m}^{-2} \text{ s}^{-1}$ ;

$z$  – light path length, m.

The length of the light path  $z$  is the distance between the middle and the lower HOBO Data Loggers, which was equal to 14 cm.

### 3.3.13 Biofilm system design

The schematic layout of a biofilm device designed for microalgal growth and harvesting in a raceway pond is shown in **Figure 3.5**. The assembly comprised a rotating paddlewheel driven by an electric motor. The paddlewheel consisted of a supporting rod that held 4 rectangular vanes.

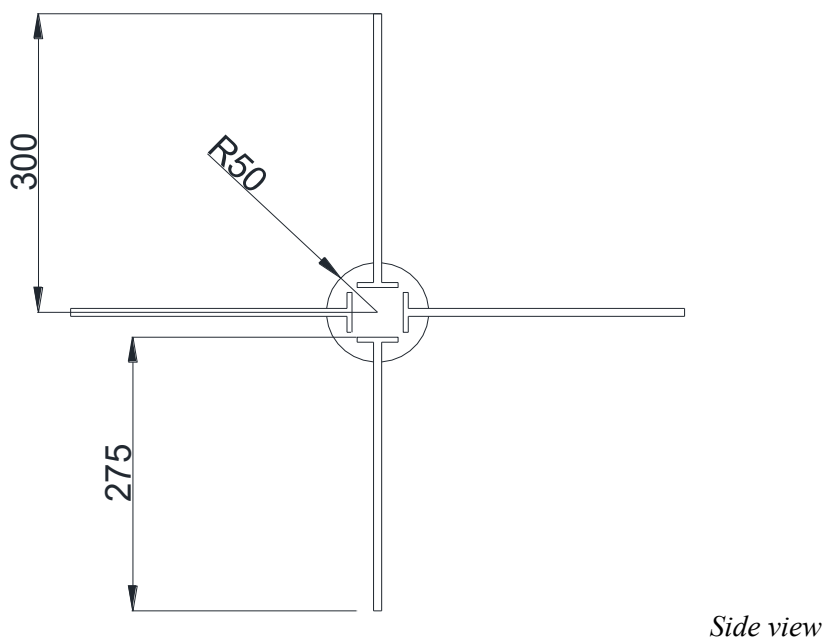


**Figure 3.5** Schematic design of a biofilm device in the form of a paddlewheel (dimensions in mm).

A different fabric (see **Chapter 2**) was wrapped around each vane of the paddlewheel. These fabrics acted as microalgal biofilm attachment materials to which the cells were

attaching. The rotation of the paddlewheel partially submerged in the suspended microalgal culture growing in the raceway pond allowed the cells to settle onto the fabric surfaces, and provided mixing of the suspended culture. The microalgal cells on the fabrics formed biofilms, and the attached biomass was naturally concentrated providing a beneficial way of simple harvesting by scraping the vanes. There were 4 paddlewheels installed in the raceway pond, and 16 vanes were available in total, which gave opportunities for replication and allowed testing of different attachment materials fixed on different vanes at precisely the same conditions.

### **3.3.14 Biofilm system operation. Stock culture of *Chlorella vulgaris***

The unicellular green microalga *Chlorella vulgaris* (CS-42, Australian National Algae Culture Collection, CSIRO) was cultured under a similar protocol as *N. oceanica* (see 3.3.1 Growth conditions and limitations in a raceway pond. Stock culture of *Nannochloropsis oceanica*) with the following modifications:

- The culture was grown in MLA medium prepared using an MLA 4-part concentrate (Algaboost™, AusAqua Pty Ltd, Australia).
- The glass conical flasks with the microalgal culture were stored in an incubator at 20°C.
- A 10 L modified transparent carboy containing MLA medium was inoculated with 100 mL of *C. vulgaris* stock culture, and was kept at 23.5°C in a temperature-controlled laboratory under LED illumination for 8 days before it was used to inoculate a 500 L transparent bag.

### **3.3.15 Experimental culture of *Chlorella vulgaris***

The *C. vulgaris* culture grown in the carboy was used to inoculate a 500 L transparent bag containing MLA medium aerated with an air pump (Quiet One® Aquarium Pump 5000). The bag with *C. vulgaris* was placed in a temperature-controlled laboratory at 20°C. Illumination was provided with 6 LED lights fixed at the sides of the bag; the average light intensity in the bag was 350  $\mu\text{mol photon m}^{-2} \text{s}^{-1}$ .

The OD of *C. vulgaris* culture in the bag measured as absorbance at 750 nm (SPECTRONIC 200 spectrophotometer) was 0.84, and the turbidity was 53.7 NTU (WP-88 Turbidity Meter, TPS Australia) on the day of the raceway pond inoculation (Day 0).

### 3.3.16 Raceway pond inoculation

A number of experiments were carried out with the retrofitted raceway pond to test the performance of the paddlewheel biofilm system at pilot scale. However, all of them had to be terminated due to contamination of the suspended cultures caused by heavy building works in close proximity (**Supplement 3.1**).

The inoculation of the rooftop raceway pond was carried out by addition of 40 L of *C. vulgaris* culture grown in the bag to 660 L of Jaworski's medium in the raceway pond. The medium was prepared from dry nutrients (Cell-Hi JW, Varicon Aqua Solutions Ltd, UK) by making a concentrated solution and adding 3 mL of the solution per litre of water in the pond. The concentrated solution was prepared by dissolving 67 g of dry nutrients in 1 L of ultrapure water (Arium®pro Ultrapure Water Systems, Sartorius, Germany). The average OD in the raceway pond after the inoculation on Day 0 was 0.04, and the average turbidity was 5.1 NTU.

Sampling of the suspended *C. vulgaris* culture in the raceway pond took place daily from 10:00 to 11:00 h for 18 days. Turbidity was measured at three different locations within the pond.

### 3.3.17 Raceway pond dilutions

Regular dilutions of the suspended *C. vulgaris* in the raceway pond were used to maintain OD at approximately 0.08 from Day 6. The dilutions were carried out on the days when the OD in the pond reached or exceeded 0.09. The process involved draining a certain volume of the suspension depending on the culture density on a given day, and replacing it with fresh Jaworski's medium.

### 3.3.18 Mounting of fabrics on paddlewheels

Three fabrics were used: cotton, 65% polyester and 35% cotton blend with plastic polymer coating (coated blend), and the same blend without the coating (uncoated blend). On Day 13, each fabric was attached to one specific vane of three of the paddlewheels; one paddlewheel (control) remained uncovered (**Figure 3.6**).

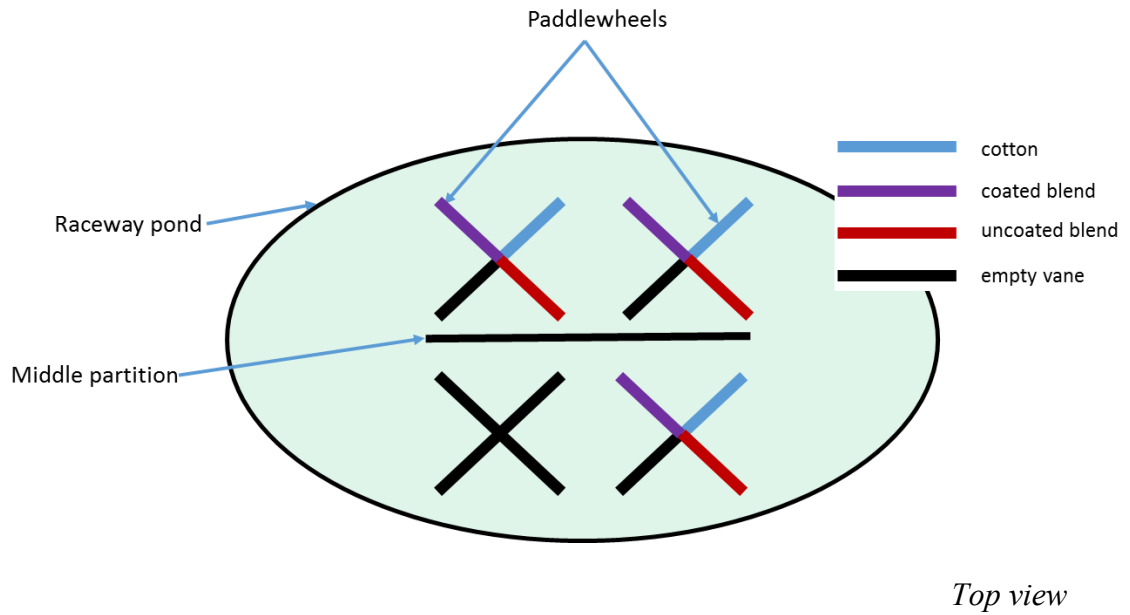


**Figure 3.6** Schematic diagram of the paddlewheels with the fabrics in the raceway pond.

The mounting of the fabrics was performed by drilling small holes around the perimeter of each vane and then sewing the fabrics on the vane with a plastic thread.

### 3.4 Results and discussion

The *N. oceanica* culture in the rooftop raceway pond was subject to solar irradiance and ambient temperature. The light intensity experienced by the microalgal culture during the entire growth period is shown in **Figure 3.7**. The photon flux density measured in the air above the culture was high, reaching  $3,300 \mu\text{mol photons m}^{-2} \text{s}^{-1}$ . This may be attributed to light reflection from the white walls of the raceway pond, as well as from neighbouring buildings. In fact, the average maximum solar irradiance measured in a study conducted in an outdoor tubular photobioreactor was  $2,100 \mu\text{mol photons m}^{-2} \text{s}^{-1}$  (Vonshak et al. 2001).

The highest daily incident PAR experienced by the cells at the surface of the raceway pond was approximately  $1,500 \mu\text{mol photons m}^{-2} \text{s}^{-1}$ , and the brief maximum of  $2,300 \mu\text{mol photons m}^{-2} \text{s}^{-1}$  occurred on Day 2 under direct sunlight.

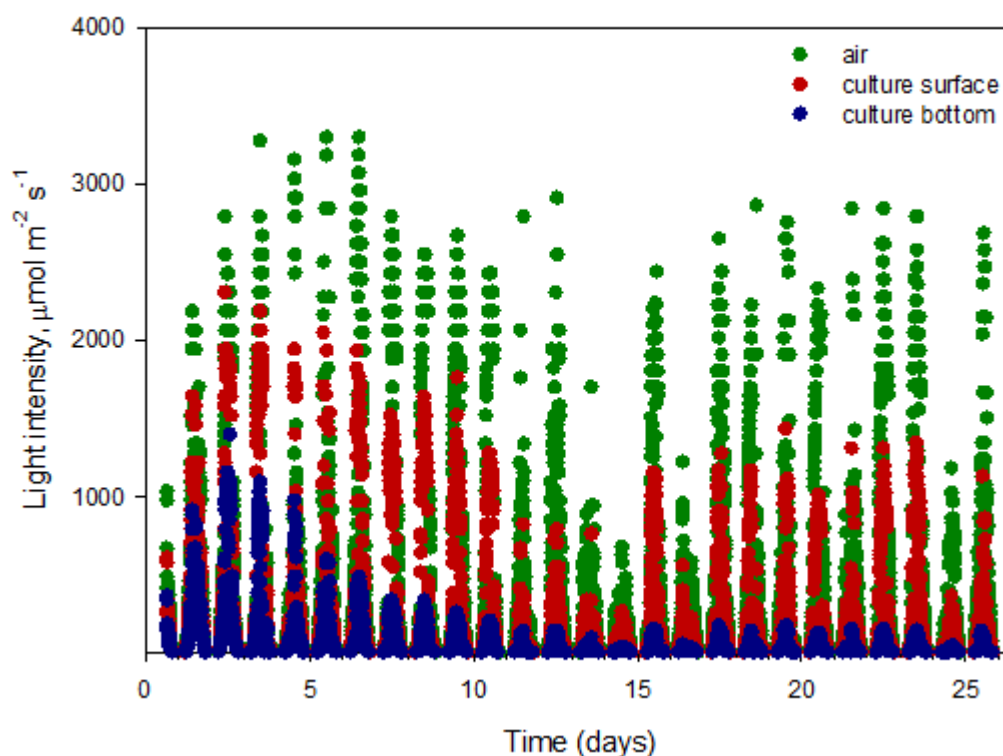


**Figure 3.7** Light intensity measured in the rooftop raceway pond.

The measured temperature variations are shown in **Figure 3.8**. The daily ambient temperature was high, with a maximum of  $55^{\circ}\text{C}$  on Day 3. Interestingly, the minimal

temperature of 15°C was measured on Day 4, indicating that a 40°C ambient temperature decrease happened in less than 24 hours. Similarly, a temperature decrease from a midday peak of 33°C to a night minimum of approximately 10°C has previously been measured in a 1 cm<sup>2</sup>, 16 cm deep, outdoor raceway pond (Moheimani & Borowitzka 2006).

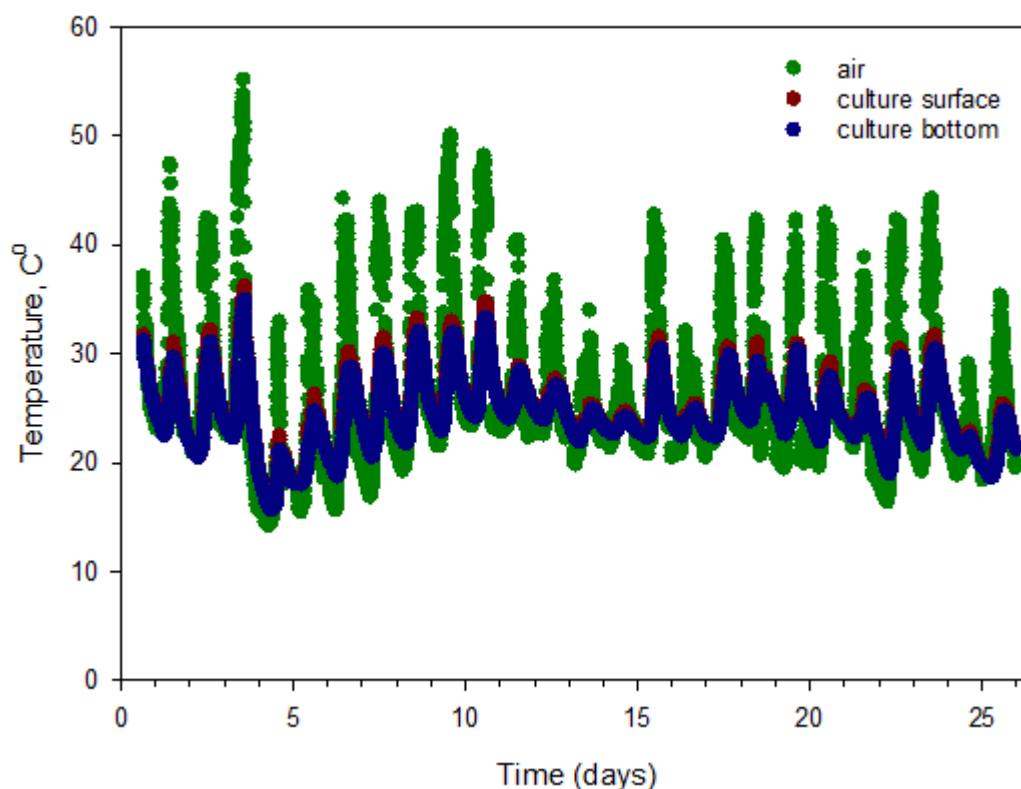
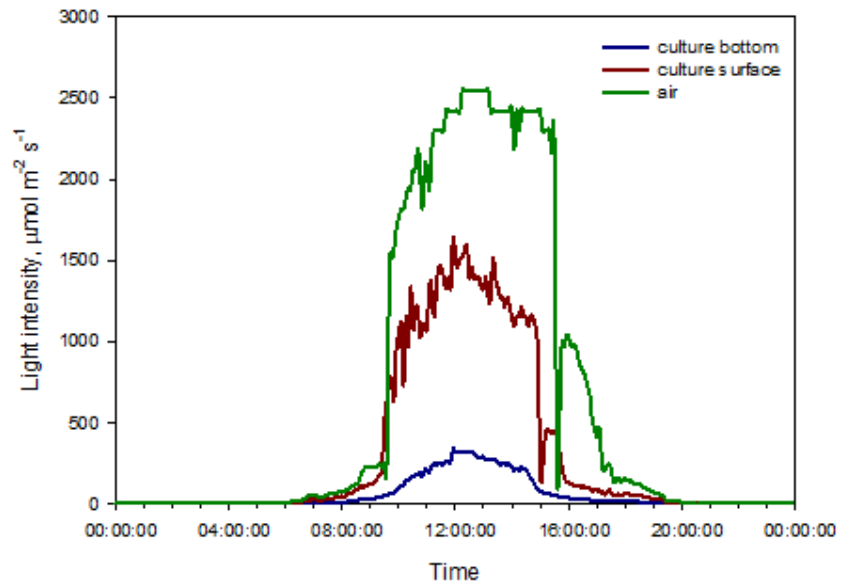


**Figure 3.8** Temperature measured in the rooftop raceway pond.

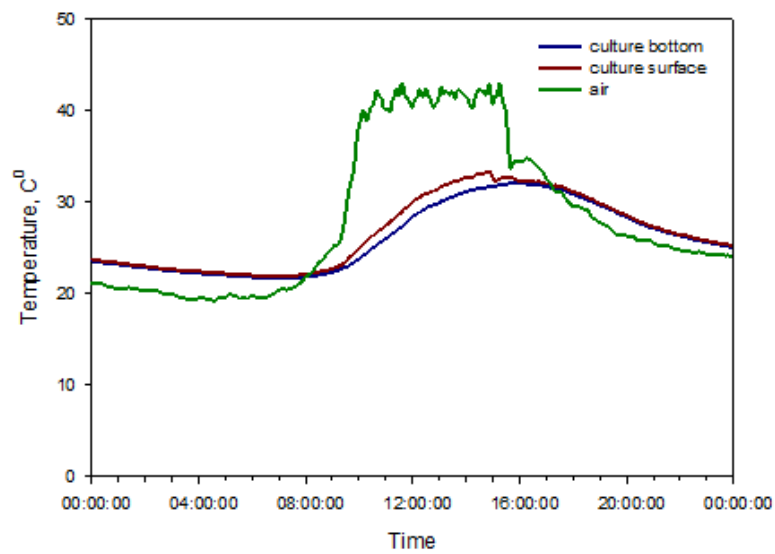
The diel cycle temperature variations in the microalgal culture were less abrupt than in the air. The maximum daily temperature in the pond was approximately 30°C, and the night time minimum was close to 22°C. Extreme temperature events in microalgal suspension were prevented by good culture mixing (Carvalho, Meireles & Malcata 2006) and evaporation (Ghasemi et al. 2012). The evaporative loss on a sunny day was equal to approximately 70 L, or 10% of the raceway working volume.

Daily light intensity and temperature variations are shown in **Figure 3.9A** and **B**. The microalgal cells experienced peak incident irradiance for approximately four hours on any given day. The 5-fold difference between photon flux density at the culture surface

and at the bottom of the pond emphasises the importance of adequate mixing in the raceway pond. Mixing is essential not only to eliminate gradients of light, temperature, nutrients and gas concentrations, but also to ensure rapid cell circulation between light and dark zones, thus maintaining elevated biomass productivity (Carvalho, Meireles & Malcata 2006).



**A**



**B**

**Figure 3.9** Daily variations in environmental conditions in the rooftop raceway pond: *A* – daily light intensity; *B* – daily temperature.

The abrupt decrease in the incident irradiance and temperature starting at 15:00 h, which occurred every day, happened as a result of solar shading behind the walls of the raceway pond. A 4-hour time lag existed between the maximum ambient temperature and the peak temperature in the microalgal culture (**Figure 3.9B**), such that the microalgal culture was approximately 10°C warmer in the afternoon. The peak ambient temperature was recorded daily at approximately 10.30 h, whereas the maximum temperature at the surface of the microalgal culture was measured at around 14.30 h. This observation may be useful for laboratory simulation of natural environmental conditions in photobioreactors.

The growth of the *N. oceanica* culture in the raceway pond was monitored by OD, DW and automated cell density measurements. The cell density was the most reliable measurement because it had the highest precision.

The microalgal growth curve, measured in terms of OD, is shown in **Figure 3.10**. The growth curve consisted of a distinct lag phase, which lasted for 3 days after inoculation (Day 0—2), presumably due to the difference between the growth conditions in the laboratory and on the rooftop. A brief exponential phase occurred on Days 3–5 and it was followed by linear growth until Day 22. Cells entered the stationary phase from Day 23, which resulted in a gradual decrease in OD. Periodic rainfall reduced the OD by dilution.

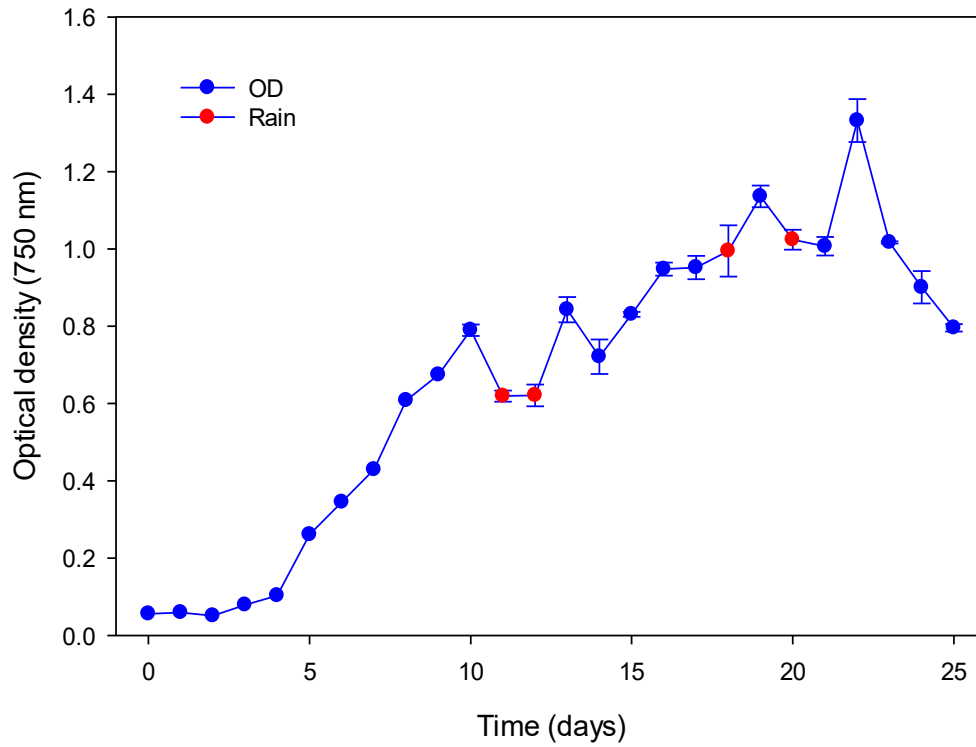


**Figure 3.10** OD of *N. oceanica* in the rooftop raceway pond.

The automated cell density (**Figure 3.11**) followed a similar trend to OD. Although cell density is a more reliable measurement, OD measurements are quick and easy, and they were used with confidence for subsequent experiments.

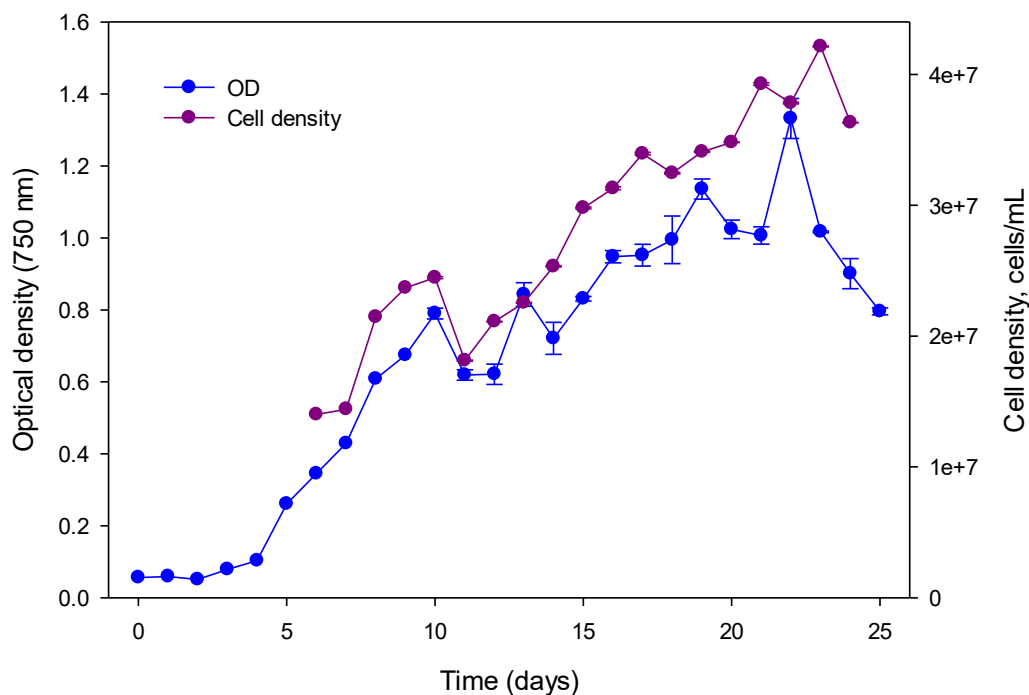


**Figure 3.11** Comparison between OD and automated cell density of *N. oceanica* in the rooftop raceway pond.

The final cell density of *N. oceanica* was  $43 \times 10^6$  cells  $\text{mL}^{-1}$ . However, this is likely to be an underestimate, since a green layer of flocculated microalgal cells was observed at the bottom of the raceway pond at the end of the experiment.

DW and OD shared a common trend (correlation coefficient 0.88), while DW and automated cell density exhibited positively correlated increasing trends (correlation coefficient 0.86), but at different rates.

The *N. oceanica* culture grew to a final DW of  $0.23 \text{ g L}^{-1}$ . Volumetric and areal productivities were calculated using the equations below (De Vree et al. 2016):

#### Areal productivity

$$P_{areal} = \left( \frac{V \times Y}{A} \right) / d,$$

where  $P_{areal}$  – areal biomass productivity ( $\text{g m}^{-2} \text{ d}^{-1}$ );  $V$  – culture volume (L);  $Y$  – DW ( $\text{g L}^{-1}$ );  $A$  – raceway pond area ( $\text{m}^2$ );  $d$  – number of days of culture growth.

$$P_{areal} = \left( \frac{660 \times 0.23}{2.98} \right) / 20 = 2.55 \text{ g m}^{-2} \text{ d}^{-1}.$$

### Volumetric productivity

$$P_{vol} = P_{areal} \times \frac{A}{V},$$

where  $P_{vol}$  – volumetric biomass productivity ( $\text{g L}^{-1} \text{ d}^{-1}$ ).

$$P_{vol} = 2.55 \times \frac{2.98}{660} = 0.01 \text{ g L}^{-1} \text{ d}^{-1}.$$

The DW per cell at any given time was compared to the average DW per cell over the whole growth cycle, and the percentage difference from the mean is shown in **Figure 3.12**. A distinct upward trend was observed, indicating that the microalgal cells were becoming heavier, either larger or denser, over time. A possible explanation is a reduction in nitrogen bioavailability over time, which is known to reduce cell division rate and trigger lipid accumulation (Praveenkumar et al. 2012; Van Vooren et al. 2012).

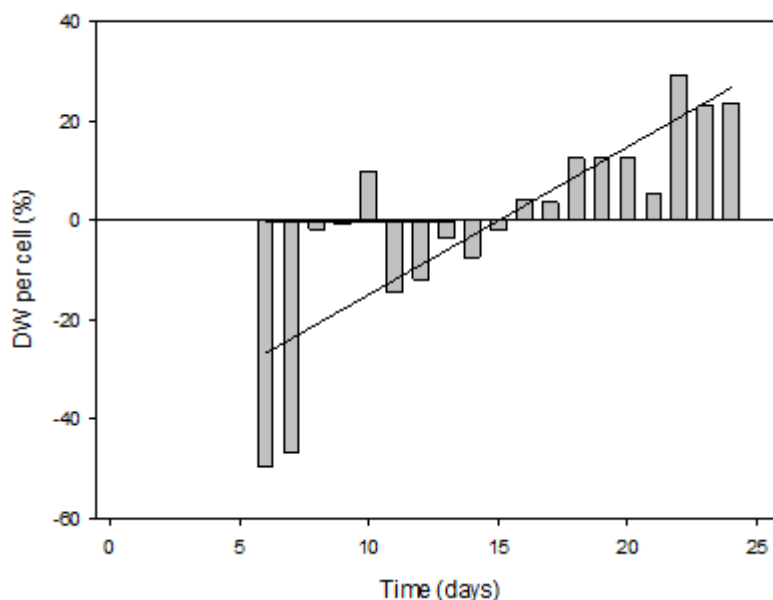


**Figure 3.12** DW per cell of the microalgal culture in the rooftop raceway pond.

Recently, Tran et al. (2016) grew *N. oceanica* under both nitrogen-replete and nitrogen-deplete conditions. The study reported that DW was higher for the nitrogen-deplete environment, although the cell number was lower when compared with the nitrogen-replete culture. The authors stated that the microalgal cells in the nutrient-deplete

conditions grew larger or denser, and visually confirmed this conclusion by fluorescence microscopy.

In any dense microalgal culture growing in a raceway pond, there is a light-saturated upper layer with low photon energy conversion efficiency, and a deeper light attenuated layer in which photosynthesis is too low to compensate for respiration due to insufficient photon flux (Ritchie & Larkum 2012). Between these two layers, light decreases exponentially and reaches a layer with optimum light intensity that ensures maximum photosynthesis (Ritchie & Larkum 2012). Mixing with a paddlewheel must be maintained in order to cycle microalgal cells between these different layers in the raceway pond (Ritchie & Larkum 2012).

Optical quantification of irradiance distribution within a photosynthetic culture is complex because of the complicated nature of light scattering, as well as absorption by the microalgal cells. Light intensity in the culture medium is generally measured according to Beer-Lambert law (Lee 1999), which states that the quantity of light absorbed by a solution is proportional to the solution concentration and the depth that the light beam travels. OD of a microalgal suspension measured at 750 nm provides an estimate of cell density in the suspension. It measures light scattering, as there is no light absorption by pigments at the given wavelength. Attenuation coefficient  $a$  (**Figure 3.13**) is an estimate of photon flux that measures attenuation as absorption and scattering across all wavelengths. The coefficient was calculated from changes of the ratio between the light intensity at the surface and at the bottom over time (**Figure 3.3**). The light limitation in the suspended culture was observed after Day 10 of the raceway pond operation when the attenuation coefficient graph became considerably more linear, which resulted in the decrease of the *N. oceanica* growth rate (**Figure 3.13**).

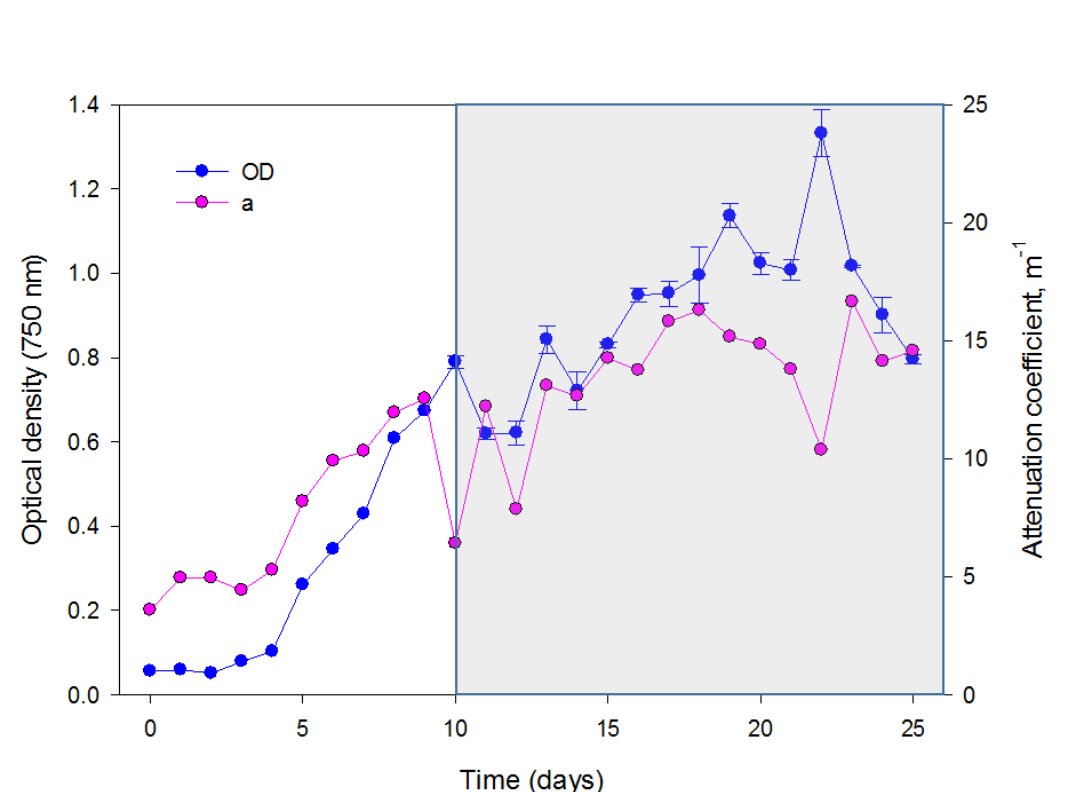


**Figure 3.13** Relationship between attenuation coefficient ( $a$ ) and OD of the microalgal culture in the rooftop raceway pond; shaded section marks light limitation.

Photosynthetic  $\text{CO}_2$  consumption of the culture in the raceway pond is shown in **Figure 3.14**. Saturation of seawater with dissolved  $\text{CO}_2$  reduces the concentration of  $\text{CO}_3^{2-}$  ions, and increases the concentration of  $\text{HCO}_3^-$  ions. Marine microalgal cells incorporate bicarbonate and convert it to  $\text{CO}_2$  at the active site of RuBisCO; bicarbonate consumption triggers the increase in pH of the medium (Tamburic et al. 2015). The diurnal changes in pH reflected in **Figure 3.14** are the result of active photosynthesis during the day and mass transfer of atmospheric  $\text{CO}_2$  into dissolved bicarbonate at night. While the cells are in the exponential growth phase, the rate of photosynthesis exceeds the rate of the mass transfer, shifting the pH baseline upwards (Tamburic et al. 2015). Once the microalgal culture becomes bicarbonate-limited, it enters the linear growth phase. Thus, the increase of pH above 9.5 on Day 5 shows the beginning of bicarbonate limitation in the raceway pond (Tamburic et al. 2015).

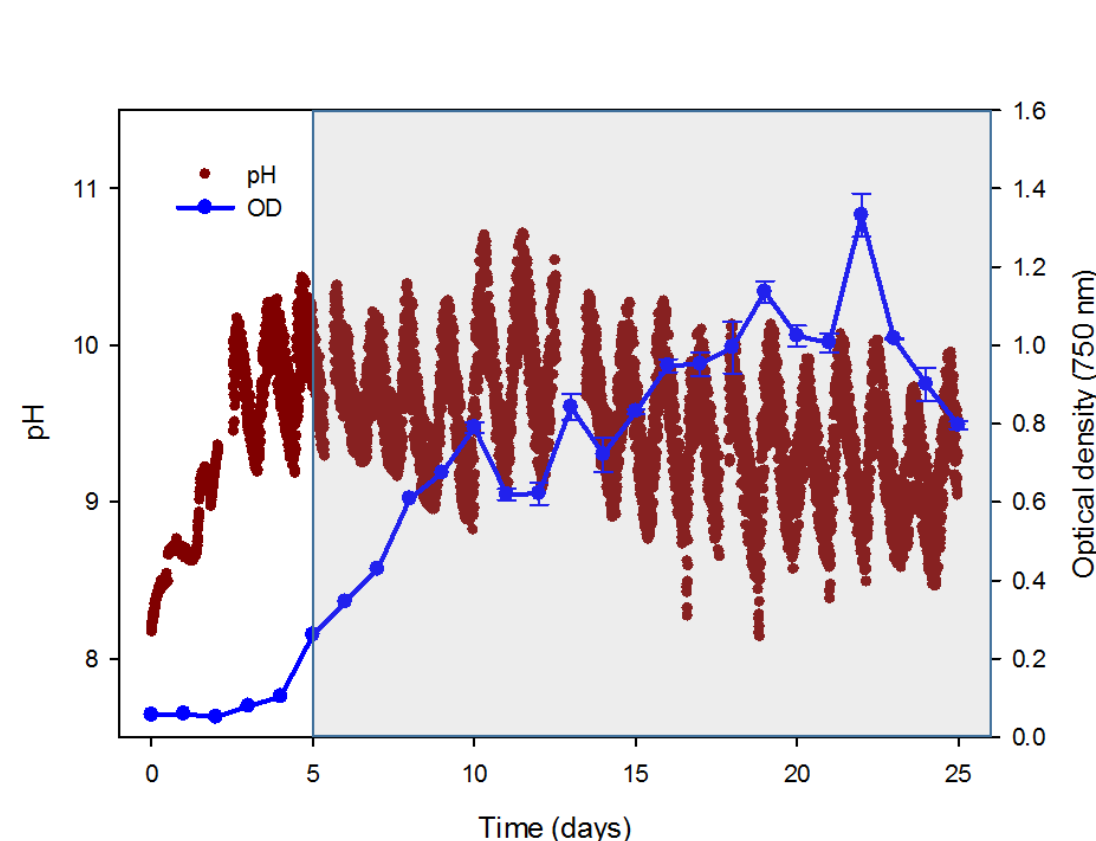


**Figure 3.14** Relationship between pH and OD measured in the rooftop raceway pond; shaded section marks CO<sub>2</sub> limitation.

Daily alkaline conditions caused biomass autoflocculation in the pond that generally happens due to calcium or magnesium precipitation when the pH of the culture medium exceeds 10 (Vandamme, Foubert & Muylaert 2013). The inorganic precipitate formation, not the alkaline conditions as such, is the reason for microalgal autoflocculation (Vandamme et al. 2015; Vandamme, Foubert & Muylaert 2013).

The nitrate limitation in the culture growth medium was observed starting from Day 20, when the nitrate concentration decreased below 1%. The average rate of nitrate consumption from Day 6 to Day 11 was 39.1 mg mL<sup>-2</sup> d<sup>-1</sup>, and it decreased to 2.3 mg mL<sup>-2</sup> d<sup>-1</sup> during the period from Day 12 to Day 15. The decline in the nitrate uptake after Day 11 showed a strong correlation with the trend of OD increase (**Figure 3.15**), suggesting that dense cultures become nutrient limited.

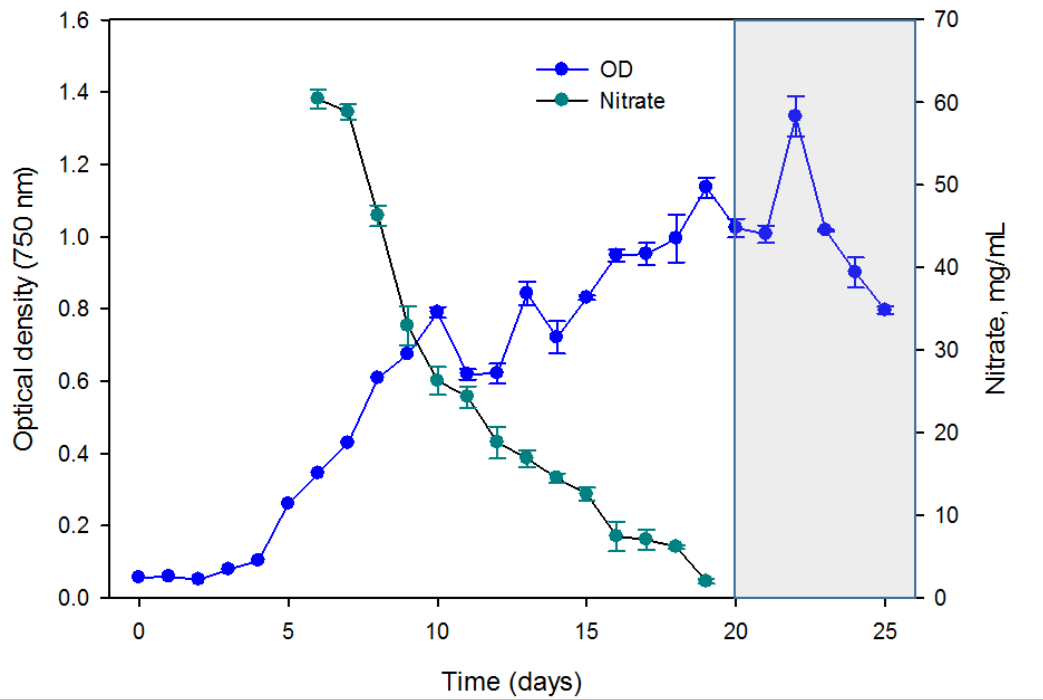


**Figure 3.15** Relationship between nitrate concentration and OD measured in the rooftop raceway pond; shaded section marks nitrate limitation.

Insufficient nitrate concentration presumably resulted in the subsequent cell death phase after the microalgal cells used all nitrate resources (Jin, Lim & Lee 2006).

The primary microalgal culture growth limitations in the rooftop raceway pond are summarised in **Figure 3.16**.

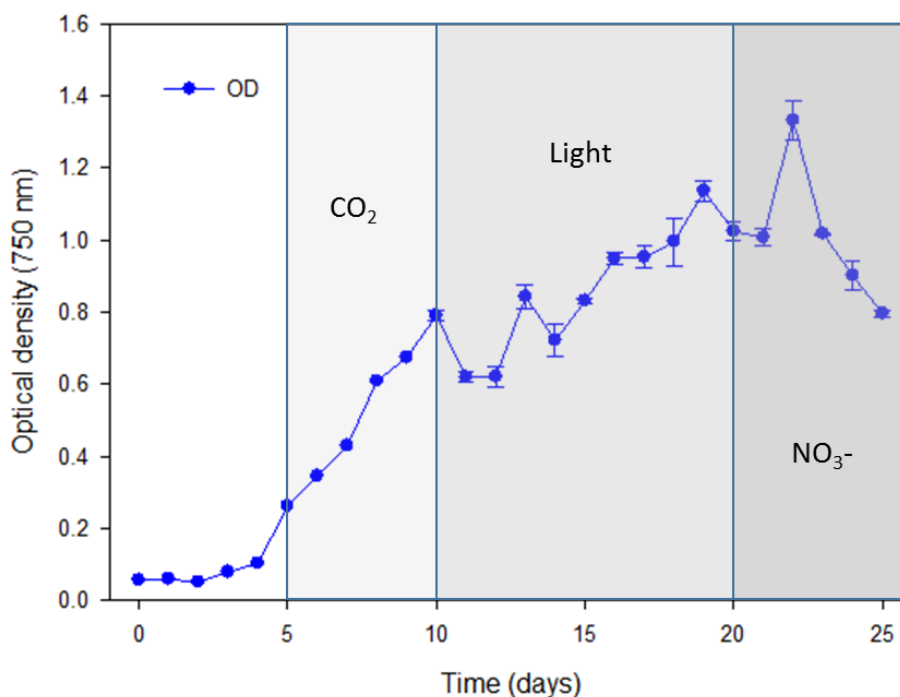


**Figure 3.16** Microalgal culture growth limitations identified in the raceway pond.

The *N. oceanica* culture in the pond experienced carbon dioxide limitation starting from Day 5 of the culture growth, followed by light limitation from Day 10 and nitrate limitation from Day 20.

Considering these environmental limitations that adversely impact a microalgal culture productivity in the raceway pond, a favourable biofilm-based harvesting system was designed and installed in the rooftop raceway pond. The installation of this system in the pond was aimed at facilitating easy and economical attached biomass harvesting by scraping, together with decreasing the negative influence of the environmental variables on the microalgal culture growth.

The biofilm system, which consisted of four identical paddlewheels installed in the rooftop raceway pond, is shown in **Figure 3.17**. Two paddlewheels were mounted in each bend of the pond and rotated in opposite directions to ensure circular motion of the suspended culture medium. They were partially submerged into the raceway pond and rotated, which allowed the attached cells to access alternatively the nutrients in the raceway pond as well as atmospheric CO<sub>2</sub> and sunlight when out of the water.



**Figure 3.17** The 4 paddlewheels in the rooftop raceway pond.

The installation of additional paddlewheels in the raceway pond not only offered an easy attached biomass harvesting method, but also provided the benefit of enhanced agitation of the suspended culture. However, additional energy could be required to rotate four paddlewheels, as opposed to one conventional paddlewheel in the raceway pond. In order to decrease the power consumption of the system, the paddlewheels could be rotated with lower frequency than a conventional paddlewheel (Kadu & Rao 2012).

The paddlewheel configuration of the designed system allowed separate assembling and disassembling of the rotating vanes whenever necessary, thus maintaining the important feature of testing different attachment materials simultaneously at the same conditions. Additionally, it provided the benefit of easy vane replacement decreasing downtime in case of failure during prolonged operation.

The pilot-scale testing of the designed paddlewheel system for biofilm cultivation and biomass harvesting is presented based on the experiment carried out in winter 2017 in Sydney, Australia.

The experiment in the raceway pond with *C. vulgaris* culture lasted for 24 days (Day 0 – Day 23) and had to be terminated due to contamination (**Supplement 3.1**). The microalgal culture growth is shown in **Figure 3.18**; it was monitored by both OD and turbidity measurements in order to verify the reliability of the turbidity measurements for future experiments. The turbidity measurements with the portable turbidity meter WP-88, TPS Australia, could be performed directly in the raceway pond without the need in transporting the sample to the laboratory.

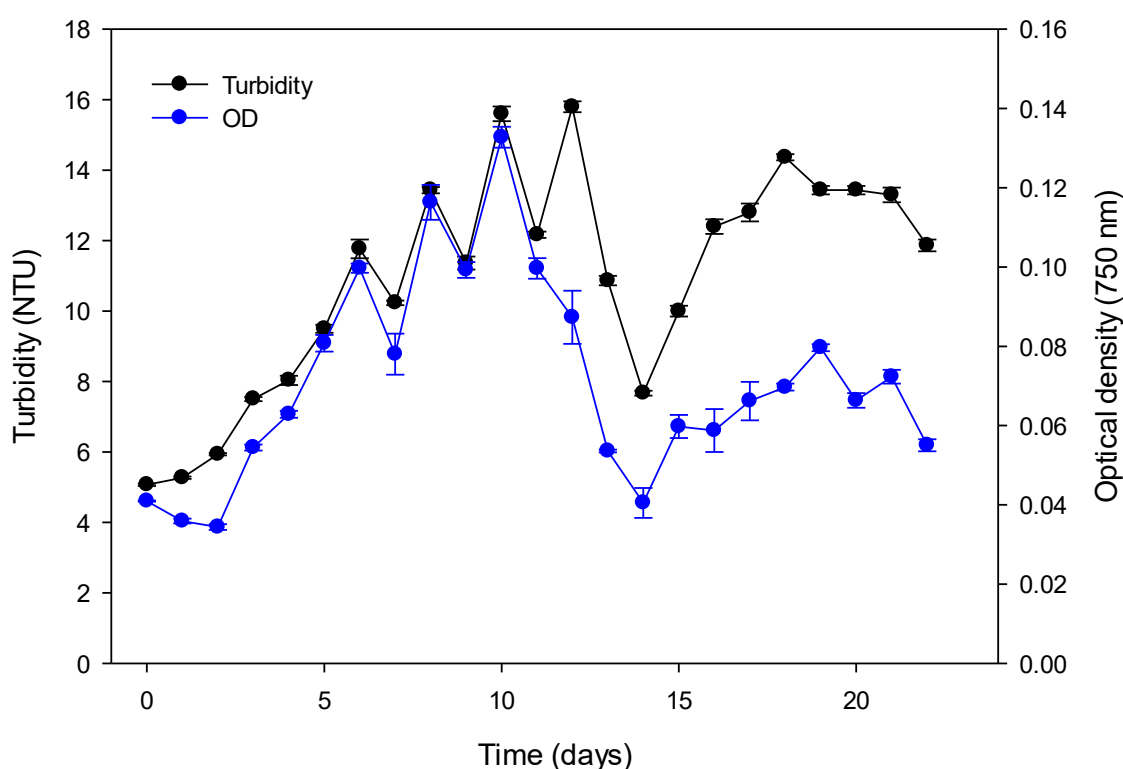


**Figure 3.18** Microalgal culture growth determined by OD and turbidity measurements in the raceway pond.

The suspended culture growth was characterised by a brief exponential phase from Day 3 until Day 6, when daily culture dilutions with fresh Jaworski's medium were started. The dilutions to OD 0.08 were performed to maintain *C. vulgaris* at a constant OD and to keep the culture in the exponential phase. On Day 12, the microalgal attachment materials were introduced, *i.e.* the vanes of three paddlewheels were wrapped with cotton, coated blend and uncoated blend. After the introduction of the attachment materials, the OD and turbidity in the raceway pond decreased, presumably due to the

rapid attachment of the cells to the fabrics. The fast settlement of the microalgal cells on the vanes is favourable as the primary function of the biofilm system is to facilitate easy biomass harvesting. Subsequent cell density increase was observed until Day 19, at which point the culture became heavily contaminated and the experiment was terminated.

An interesting feature of microalgal biofilm formation was observed for all attachment materials on all three paddlewheels. **Figure 3.19** shows *C. vulgaris* biofilm formation on an attachment material covering one of the vanes. The interface between the part of the vane that was submerged in the liquid medium during rotation and the part that was exposed only to the air is characterised by considerably higher cell attachment.

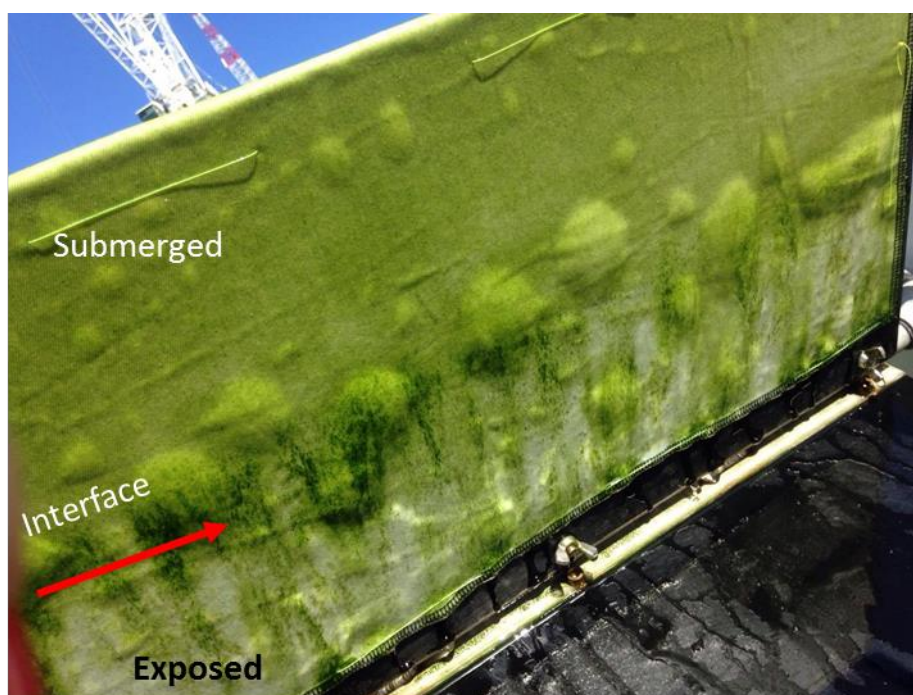


**Figure 3.19** Higher microalgal cell accumulation at the liquid-air interface on an attachment material mounted on a vane of a paddlewheel.

The same phenomenon was observed during the formation and development of microalgal biofilms in the laboratory, where the biofilms were grown on fabrics submerged in a microalgal suspension and stirred (**Figure 3.20**). The biofilm shown in **Figure 3.20** was cultivated according to the methodology described in 2.3.7 Experimental setup and conditions.



**Figure 3.20** Dense microalgal biofilm at the liquid-air interface grown in the laboratory.

The phenomenon of denser biofilms development at the liquid-air interface in laboratory conditions could be attributed to higher carbon availability in the upper part of the fabric when it is submerged in the suspended culture medium. However, for the biofilms forming on the paddlewheel vanes, this phenomenon needs to be further studied; it can be useful for designing biofilm systems and enhancing existing system layouts.

Additionally, both in conical flasks at laboratory scale and in the raceway pond at pilot scale, a decrease in suspended cell density was measured immediately after the introduction of growth substrates. Subsequently, the suspended cell density increased slightly and stabilised. No exponential growth of the cultures in suspension was observed. The biofilms, however, were growing throughout the entire experiment. The absence of considerable suspended culture growth in the systems could be explained by constant cell entrapment in the substrate weave and subsequent biofilm development, which is important for biomass harvesting purposes.

### 3.5 Summary

The environmental conditions and the primary limitations that influence a microalgal culture growth in the rooftop raceway pond were identified. This pilot-scale raceway pond with a 660 L working volume and 220 mm depth was equipped with two compressed air diffusers, three data loggers for continuous light intensity and temperature measurement, and a pH probe; salinity was measured and adjusted daily. In order to monitor the suspended culture growth, a number of variables were measured on a daily basis, including OD, DW, cell density, chlorophyll *a* and nitrate concentrations. The growth limitations on the suspended culture included carbon dioxide limitation from Day 5 of the culture growth, light limitation from Day 10, and nitrate limitation from Day 20.

In order to facilitate biomass harvesting and to address the factors limiting growth of a microalgal culture in the raceway pond, a microalgal biofilm system in the form of four paddlewheels was designed and retrofitted to the raceway pond. Two paddlewheels were rotated in opposite directions in each channel of the raceway pond to create a circular motion of the suspended culture. Their vanes were covered in fabrics for biofilm attachment, and they were partially immersed in the growth medium. The rotation of the paddlewheels created an advantageous growth environment for microalgal cells attached to the fabrics, as they could access nutrients while immersed under water, followed by periodic exposure to atmospheric CO<sub>2</sub> and sunlight.

Pilot studies of the designed biofilm system, although short due to contamination issues, revealed a pattern of biofilm development, where the liquid-air interface of an attachment material is characterised by the highest cell attachment. The same phenomenon was also observed at laboratory scale, suggesting that this feature of biofilm formation could be taken into consideration for future biofilm system design.

### 3.6 References

- Borowitzka, M.A. & Moheimani, N.R. (eds) 2013, *Algae for Biofuels and Energy*, vol. 5, Springer Netherlands, Dordrecht.
- Carvalho, A.P., Meireles, L.A. & Malcata, F.X. 2006, 'Microalgal reactors: A review of enclosed system designs and performances', *Biotechnology Progress*, vol. 22, no. 6, pp. 1490–506.
- Eustance, E., Badvipour, S., Wray, J.T. & Sommerfeld, M.R. 2016, 'Biomass productivity of two *Scenedesmus* strains cultivated semi-continuously in outdoor raceway ponds and flat-panel photobioreactors', *Journal of Applied Phycology*, vol. 28, no. 3, pp. 1471–83.
- Ghasemi, Y., Rasoul-Amini, S., Naseri, A.T., Montazeri-Najafabady, N., Mobasher, M.A. & Dabbagh, F. 2012, 'Microalgae biofuel potentials', *Applied Biochemistry and Microbiology*, vol. 48, no. 2, pp. 126–144.
- Guillard, R.R.L. & Ryther, J.H. 1962, 'Studies of marine planktonic diatoms: I. *Cyclotella nana* Hustedt, and *Detonula confervacea* (Cleve) Gran', *Canadian journal of microbiology*, vol. 8, no. 2, pp. 229–39.
- He, Q., Yang, H. & Hu, C. 2016, 'Culture modes and financial evaluation of two oleaginous microalgae for biodiesel production in desert area with open raceway pond', *Bioresource Technology*, vol. 218, pp. 571–579.
- Henriques, M., Silva, A. & Rocha, J. 2007, 'Extraction and quantification of pigments from a marine microalga: a simple and reproducible method', *Communicating Current Research and Educational Topics and Trends in Applied Microbiology*, vol. 2, pp. 586–93.
- Hoh, D., Watson, S. & Kan, E. 2016, 'Algal biofilm reactors for integrated wastewater treatment and biofuel production: A review', *Chemical Engineering Journal*, vol. 287, pp. 466–73.
- Jin, H.F., Lim, B.R. & Lee, K. 2006, 'Influence of nitrate feeding on carbon dioxide fixation by microalgae', *Journal of Environmental Science and Health - Part A Toxic/Hazardous Substances and Environmental Engineering*, vol. 41, no. 12, pp. 2813–24.
- Johnson, M.B. & Wen, Z. 2010, 'Development of an attached microalgal growth system for biofuel production', *Applied Microbiology and Biotechnology*, vol. 85, no. 3, pp. 525–34.

- Kadu, P.A. & Rao, Y.R.M. 2012, 'Rotating biological contactors: A critical review', *Journal of Scientific and Engineering Research*, vol. 3, no. 9, pp. 1–6.
- Laamanen, C.A., Ross, G.M. & Scott, J.A. 2016, 'Flotation harvesting of microalgae', *Renewable and Sustainable Energy Reviews*, vol. 58, pp. 75–86.
- Lee, C.G. 1999, 'Calculation of light penetration depth in photobioreactors', *Biotechnology and Bioprocess Engineering*, vol. 4, no. 1, pp. 78–81.
- Mendoza, J.L., Granados, M.R., de Godos, I., Ación, F.G., Molina, E., Heaven, S. & Banks, C.J. 2013, 'Oxygen transfer and evolution in microalgal culture in open raceways', *Bioresource Technology*, vol. 137, pp. 188–95.
- Moheimani, N.R. & Borowitzka, M.A. 2006, 'The long-term culture of the coccolithophore *Pleurochrysis carterae* (Haptophyta) in outdoor raceway ponds', *Journal of Applied Phycology*, vol. 18, pp. 703–12.
- Praveenkumar, R., Shameera, K., Mahalakshmi, G., Akbarsha, M.A. & Thajuddin, N. 2012, 'Influence of nutrient deprivations on lipid accumulation in a dominant indigenous microalga *Chlorella* sp., BUM11008: Evaluation for biodiesel production', *Biomass and Bioenergy*, vol. 37, pp. 60–6.
- Ritchie, R.J. & Larkum, A.W.D. 2012, 'Modelling photosynthesis in shallow algal production ponds', *Photosynthetica*, vol. 50, no. 4, pp. 481–500.
- Schnetger, B. & Lehnert, C. 2014, 'Determination of nitrate plus nitrite in small volume marine water samples using vanadium (III) chloride as a reduction agent', *Marine Chemistry*, vol. 160, pp.91–98.
- Tamburic, B., Evenhuis, C.R., Suggett, D.J., Larkum, A.W.D., Raven, J.A. & Ralph, P.J. 2015, 'Gas transfer controls carbon limitation during biomass production by marine microalgae', *ChemSusChem*, vol. 8, no. 16, pp. 2727–36.
- Tran, N.A.T., Padula, M.P., Evenhuis, C.R., Commault, A.S., Ralph, P.J. & Tamburic, B. 2016, 'Proteomic and biophysical analyses reveal a metabolic shift in nitrogen deprived *Nannochloropsis oculata*', *Algal Research*, vol. 19, pp. 1–11.
- Vandamme, D., Foubert, I. & Muylaert, K. 2013, 'Flocculation as a low-cost method for harvesting microalgae for bulk biomass production', *Trends in Biotechnology*, vol. 31, no. 4, pp. 233–9.
- Vandamme, D., Pohl, P.I., Beuckels, A., Foubert, I., Brady, P.V., Hewson, J.C. & Muylaert, K. 2015, 'Alkaline flocculation of *Phaeodactylum tricornutum* induced by brucite and calcite', *Bioresource Technology*, vol. 196, pp. 656–61.

- Vonshak, A., Torzillo, G., Masojidek, J. & Boussiba, S. 2001, 'Sub-optimal morning temperature induces photoinhibition in dense outdoor cultures of the alga *Monodus subterraneus* (Eustigmatophyta)', *Plant, Cell and Environment*, vol. 24, no. 10, pp. 1113–8.
- Van Vooren, G., Le Grand, F., Legrand, J., Cuiné, S., Peltier, G. & Pruvost, J. 2012, 'Investigation of fatty acids accumulation in *Nannochloropsis oculata* for biodiesel application', *Bioresource Technology*, vol. 124, pp. 421–32.
- De Vree, J.H., Bosma, R., Wieggers, R., Gegic, S., Janssen, M., Barbosa, M.J. & Wijffels, R.H. 2016, 'Turbidostat operation of outdoor pilot-scale photobioreactors', *Algal Research*, vol. 18, pp. 198–208.

### Supplement 3.1

Multiple attempts to perform a prolonged pilot study of the designed microalgal biofilm system were made during the period from May 2016, after the system was installed in the raceway pond, until August 2017 (**Table S3.1**). Unfortunately, those attempts coincided with heavy building works in surrounding areas. The microalgal cultures were severely affected by dust and pollution originating from the construction works, and in general, the cells died approximately 3 weeks after the raceway pond inoculation in every experiment.

**Table S3.1** Experimental run attempts in the rooftop raceway pond retrofitted with the microalgal biofilm system.

<b>Mar-May 2016 – Pond retrofitting</b>	
May 2016	<i>Dunaliella tertiolecta</i>
Jul 2016	<i>Nannochloropsis oceanica</i>
Aug 2016	<i>Chaetoceros muelleri</i>
Nov 2016	<i>Nannochloropsis oceanica</i>
Dec 2016	<i>Nannochloropsis oceanica</i>
<b>Summer-autumn 2017 – Heavy building works</b>	
Jul 2017	<i>Chlorella vulgaris</i>
Aug 2017	<i>Chlorella vulgaris</i>

Several approaches to fixing the contamination problem in the raceway pond were considered, including:

- purchasing or constructing a cover that would prevent the dust from polluting the microalgal suspension;
- moving the raceway pond into a glasshouse;

- manufacturing a new microalgal biofilm system and installing it in another raceway pond located in a glasshouse;
- designing and building a laboratory-scale raceway pond with the biofilm system and placing it on the rooftop under a cover.

Unfortunately, all of the approaches proved to be either economically or technically unfeasible.

## **CHAPTER 4. DEVELOPMENT OF A MODIFIED CASCADE SYSTEM FOR ATTACHED BIOMASS PRODUCTION**

### **4.1 Introduction**

Microalgal biomass is usually cultivated as a suspension in open raceway ponds, or in enclosed tubular or flat panel photobioreactors (PBRs) (Norsker et al. 2011). The closed nature of PBRs enables better control of growth parameters, reduced evaporation losses and protection against culture contamination or grazing (Borowitzka & Moheimani 2013). However, the low cost, simple design, and easy maintenance of raceway ponds (Brennan & Owende 2010) make them the system of choice for large-scale biomass production (Borowitzka & Moheimani 2013). Vree et al. (2015) carried out a comparison of suspended microalgal cultivation systems at a pilot scale under identical climatological conditions using the marine microalga *Nannochloropsis* sp. The highest average productivity was reported for closed PBRs, with the maximum aerial productivity of 24 g m<sup>-2</sup> d<sup>-1</sup> and volumetric productivity of 1.7 g L<sup>-1</sup> d<sup>-1</sup> reported for the flat panel PBR. The open raceway pond resulted in lower aerial productivity of 6-14 g m<sup>-2</sup> d<sup>-1</sup>. Similarly, Narala et al. (2016) recorded approximately 1.5 times lower biomass productivity of *Tetraselmis* sp. grown outdoors in a raceway pond compared to growth in a tubular PBR at pilot scale.

Microalgal biomass cultivation as a biofilm on a solid attachment material offers several advantages compared with suspended systems. The energy input is lower because no mixing is required and the microalgal biomass is more concentrated and therefore easier to harvest (Wang et al. 2018). In suspended cultures, microalgal cell concentrations are often as low as 0.05-0.60% dry weight, which means that up to 2,000 kg of water are required to obtain 1 kg of dry biomass (Lee 2001). Multiple time-consuming and expensive processes are required to concentrate the biomass to 20% dry weight (Davis, Aden & Pienkos 2011; Gross, Jarboe & Wen 2015). The solid biomass fraction of attached microalgal cultivation is between 10-20% dry weight, which reduces the need for uneconomical dewatering processes (Gross, Jarboe & Wen 2015; Christenson & Sims 2012). Indeed, Blanken et al. (2014) determined that no further dewatering was required when microalgae were grown attached to rotating disks in a bioreactor. A number of biofilm-based systems have been recently designed and tested both at

laboratory and pilot scales for microalgal biomass production and wastewater bioremediation. These systems used a wide variety of geometries and diverse microalgal cell attachment material. They have been broadly classified into stationary and rotating systems based on the motion of the biofilm with respect to the growth medium (Gross et al. 2015). The reported biomass productivity for attached systems ranges from below  $1 \text{ g m}^{-2} \text{ d}^{-1}$  (Ozkan et al. 2012; Gao et al. 2015) to  $30 \text{ g m}^{-2} \text{ d}^{-1}$  (Schultze et al. 2015; Christenson & Sims 2012), and even above  $50 \text{ g m}^{-2} \text{ d}^{-1}$  (Liu et al. 2013).

The selection of an attachment material for microalgal biofilm cultivation is an important factor that can have a crucial impact on biofilm productivity (Gross, Jarboe & Wen 2015). Attachment material selection is often carried out separately for each system and there is no universally accepted or recommended material to date. Different types of materials, including fabrics, plastics, ceramics, metals and composites, have been tested for attached biomass cultivation with variable performance. Performance differences have been explained in terms of the material's physicochemical properties (Ozkan & Berberoglu 2013; Gross et al. 2016) and surface structure (Cao et al. 2009; Cui, Yuan & Cao 2014; Huang et al. 2018). Johnson & Wen (2010) carried out an evaluation of six materials to induce *Chlorella vulgaris* cell settlement, with polystyrene foam showing the highest attachment. Genin, Aitchison & Allen (2014) tested five attachment materials in an airlift reactor for biofilm growth and found that cellulose acetate demonstrated the highest mixed microalgal community productivity. Cotton fabric was claimed to be an effective material in terms of cell attachment (Christenson & Sims 2012; Gross et al. 2013; Bernstein et al. 2014; Kesaano et al. 2015; Gross et al. 2016). The poor durability of cotton, however, may be limiting its use for long-term biofilm system operation, as this fabric was shown to deteriorate within six months of pilot-scale operation of a revolving algal biofilm reactor (Gross & Wen 2014).

Material durability is an important parameter, especially for prolonged biofilm system operation, as the attachment material has to withstand mechanical harvesting as well as moist environments, sometimes in the presence of saltwater (Gross, Jarboe & Wen 2015). Rigid materials with improved durability, such as titanium, stainless steel and glass, were also used to support microalgal biofilm cultivation (Sekar et al. 2004; Cao et al. 2009; Cui & Yuan 2013; Schnurr, Espie & Allen 2013; Blanken et al. 2014). However, these materials are inflexible and comparatively heavy, and therefore unsuitable for application in some biofilm system configurations. A material that is

lightweight, flexible, durable in moist environments and promotes microalgal cell attachment still needs to be identified.

Management of the liquid volume required for microalgal cultivation is a crucial task within the biomass production process. Considerable energy input is required for mixing, pumping, thermoregulation and harvesting (Pruvost, Cornet & Pilon 2016). Thus, enhancing volumetric productivity, while maintaining high aerial productivity, is an important task for microalgal production process. Aerial productivity is primarily a function of the incident irradiance. Volumetric productivity, on the other hand, increases when the culture depth is reduced and there is less self-shading from algal cells within the upper layer (Pruvost, Cornet & Pilon 2016). This upper layer is referred to as the photic zone and it is limited to a depth of approximately 20 cm for suspended algal cultivation. Cascade bioreactors use a thin layer of microalgal suspension that flows under gravity over an inclined surface (Šetlík, Šust & Málek 1970), which increases volumetric productivity together with sustaining high aerial productivity (Pruvost, Cornet & Pilon 2016; Apel et al. 2017). Cell concentration of 5% dry weight can be achieved in these systems (Doucha and Livansky 2009). Although cascade bioreactors have been reported to maintain high microalgal growth rates, the construction materials and other design features require further improvement (Borowitzka 1999; Apel et al. 2017). A comparison of *Arthrospira platensis* biomass productivity in a cascade system and in a circular open pond has been performed (Benavides et al. 2017). The aerial productivity in the thin-layer cascade was equal to  $20 \text{ g m}^{-2} \text{ day}^{-1}$ , which was approximately 30% higher than the productivity recorded for the open pond. Apel et al. (2017) conducted a pilot-scale evaluation of cascade reactor performance under favourable climatic conditions and reported the highest productivity as  $25 \text{ g m}^{-2} \text{ d}^{-1}$  (volumetric productivity  $4 \text{ g L}^{-1} \text{ d}^{-1}$ ). Generally, the productivity achieved in thin-layer cascades is between  $4.5$  and  $25 \text{ g m}^{-2} \text{ d}^{-1}$  (Torzillo et al. 2010; De Marchin, Erpicum & Franck 2015; Apel et al. 2017; Benavides et al. 2017).

In this study, the thin-layer cascades and microalgal biofilm-based cultivation were merged in order to combine their benefits and create an efficient microalgal biomass production system. The performance of this novel system was evaluated by measuring biomass productivity and the mass fraction of biomass to water.

The most common method of harvesting microalgal biofilms is mechanical scraping (Zhao et al. 2018; Ekelhof & Melkonian 2017; Shayan et al. 2016). Christenson and Sims (2012) developed a rotating microalgal biofilm reactor for wastewater treatment and biomass production. The authors used cotton cord as the microalgal attachment material and they designed a spool harvester to automatically scrape biomass off the cord. The biomass remaining on the growth material after scraping is usually used as an inoculum for the next microalgal growth cycle (Johnson & Wen 2010; Blanken et al. 2014; De Assis et al. 2017). In this study, the remaining biomass entrapped in the biofilm attachment material was imaged with a confocal laser scanning microscope and these images were analysed using ImageJ (Fiji) software. The images were used to identify the spatial distribution of the microalgal biofilm for every growth/harvesting cycle. Similarly, Wijihastuti et al. (2016) imaged *Botryococcus braunii* biofilms by confocal microscopy to visualise the biofilm structure and they performed quantitative analysis of microalgal and lipid distributions on the biofilm.

## 4.2 Aim and objectives

**Aim:** Assess microalgal biomass production on a fabric surface in a thin-layer cascade system.

**Objective 1:** Measure microalgal biomass productivity and cell concentration on the coated blend (65% polyester and 35% cotton with plastic polymer coating) fabric in a thin-layer cascade system.

**Objective 2:** Image and quantify the microalgal biomass that remains attached to the fabric after mechanical harvesting.

## 4.3 Research methodology

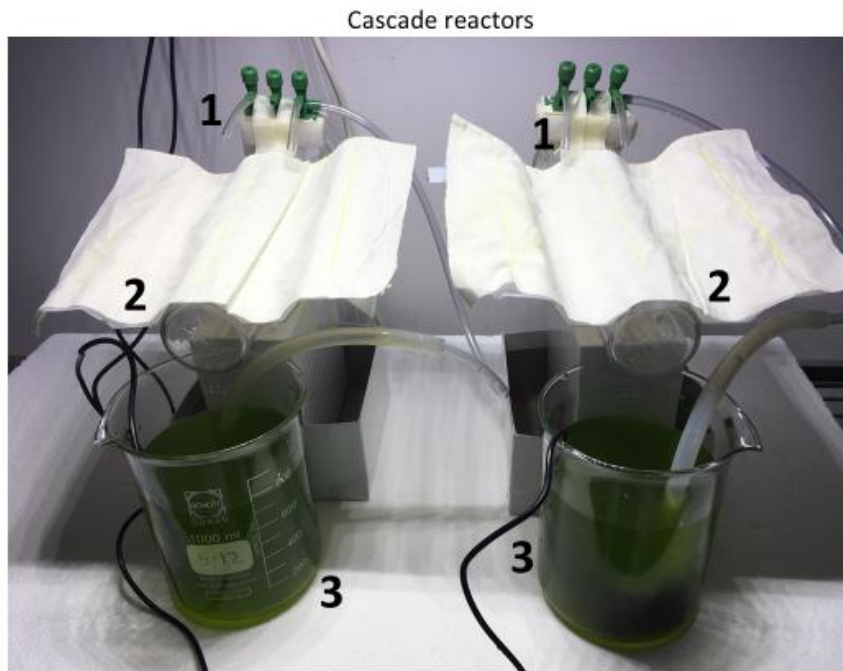
### 4.3.1 Stock and experimental cultures of *Nannochloropsis oceanica*

*Nannochloropsis oceanica* (CS-179, Australian National Algae Culture Collection, CSIRO) stock culture was grown under fluorescent illumination of  $40 \mu\text{mol photon m}^{-2} \text{s}^{-1}$  at a 12/12h light/dark cycle. The 50 mL stocks were stored in an incubator (Labec Pty Ltd, Australia) set to a temperature of  $21.5^\circ\text{C}$ . Re-inoculations of fresh F/2 medium (Guillard & Ryther 1962) took place every fortnight to maintain the culture health. The stock culture was used to inoculate 10 L of F/2 medium in an aerated transparent carboy. The carboy with the microalgal culture was kept at  $23.5^\circ\text{C}$  under LED illumination of  $100\text{--}200 \mu\text{mol photon m}^{-2} \text{s}^{-1}$  for 10 days before an aliquot was taken for experimentation in the cascade system. Optical density (OD) of the experimental culture measured at 750 nm (Spectronic 200 spectrophotometer) was 0.82 prior to cascade system inoculation.

### 4.3.2 Experimental setup – cascade system

The experimental setup comprised of a custom-built laboratory-scale thin-layer cascade system  $200 \text{ mm} \times 205 \text{ mm} \times 200 \text{ mm}$  (width x length x height) in dimension. The cascade system consisted of two cascade reactors, reactor A and reactor B. Each reactor contained a corrugated polycarbonate sheet with two channels holding *N. oceanica* biofilms (four biofilms in total in the system); the reactors were treated as biological replicates (**Figure 4.1A**). The corrugated polycarbonate sheets were fixed at a  $3^\circ$  inclination to horizontal. The wet surface area of each biofilm channel was  $0.004 \text{ m}^2$ . The corrugated polycarbonate sheets were covered with 65% polyester and 35% cotton blend with plastic polymer coating (coated blend) fabric (see **Chapter 2**), which was used as the algal cell attachment material. The coated blend fabric was selected because of its affordability, light weight and successful performance as a bacterial biofilm attachment material in trickle-feed bioreactors for industrial wastewater treatment (Taylor et al. 2005; Taylor 2006). Scanning electron microscopy (**Chapter 2**) revealed that the plastic polymer coating of the fabric had a web-like structure, which formed a favourable environment for enhanced cell entrapment (**Supplement 4.1**). The F/2 medium was pumped (Aquapro AP200LV Low Voltage Tabletop Feature Pump) above the fabric and then trickled from the top of each channel through media distribution

tubes (**Figure 4.1B**). The medium then flowed at  $0.42 \text{ L h}^{-1}$  through the channel under gravity and into 1 L glass collection flasks placed underneath the bottom end of each channel. The channels were illuminated by white light LEDs that produced a photosynthetic photon flux density of  $100 \mu\text{mol photon m}^{-2} \text{ s}^{-1}$  (Aqua Illumination Hydra 52 HD), and the system was maintained at  $21^\circ\text{C}$  in a temperature-controlled laboratory.



**A**



**B**

**Figure 4.1** Cascade reactors: *A* – reactor A (left) and reactor B (right) components, 1 – media distribution tubes, 2 – channels for biofilm formation, 3 – collection flasks with pumps; *B* – *N. oceanica* biofilm formation on coated blend fabric in the reactor channels.

Prior to mounting the fabric, which was kindly provided by BioGill Operations Pty Ltd, and inoculating the cascade system with microalgae, household bleach (Sodium Hypochlorite 42 g L<sup>-1</sup>; available Chlorine 4.0 % w/v; Sodium Hydroxide 4.0 g L<sup>-1</sup>) was pumped through the reactors for 2 days, followed by 1 day of running ultrapure water (Arium®pro Ultrapure Water Systems, Sartorius, Germany) through the system. Each cascade reactor was inoculated with 700 mL of *N. oceanica* suspension from the same stock culture on Day 0. The microalgal culture was circulated in the reactors for 7 days to allow initial cell attachment to the fabric. On Day 6, the *N. oceanica* cultures in the collection flasks were replaced with 700 mL of fresh F/2 medium. The daily evaporative loss from each reactor, which was approximately 200 mL (Apel et al. 2017), was replaced with fresh medium to prevent nutrient limitation and biofilm sloughing (Schnurr et al. 2013).

### 4.3.3 Optical density

OD of *N. oceanica* in the collection flasks was measured daily at 11.00 h as absorbance at 750 nm wavelength (Spectronic 200 spectrophotometer) for the first 7 days (Day 0 – Day 6) of cascade system operation to detect the decrease in suspended cell density due to cell settlement on the fabrics. OD was also measured during every subsequent growth/harvesting cycle to measure the re-suspended microalgal cells density in the F/2 medium. Dilutions were applied whenever the measurement exceeded an OD of 0.5.

### 4.3.4 Biomass sampling and harvesting

Biofilm was sampled weekly starting from week 2 (14 days) of cascade system operation for multiple measurements, including biomass productivity and attached cell density during growth and after harvesting, *i.e.* while the biofilms were growing on the substrate and following biomass harvesting by mechanical scraping. Biofilm imaging with a confocal laser scanning microscope commenced from week 1 (7 days) of cascade system operation. Each cascade reactor contained two microalgal biofilms. One whole biofilm from each reactor was harvested on a weekly basis to determine the biomass

productivity and mass fraction of biomass to water. The other biofilm in that reactor was used for weekly confocal microscope imaging. The biofilm harvesting procedure involved stopping the pump for a minute to allow all liquid culture to drain from the fabric, and then scraping as much biomass as possible off the fabric with a plastic spatula.

#### **4.3.5 Biofilm imaging and quantitative image processing**

Biofilm imaging was performed with the Nikon A1 Confocal Microscope operated by NIS-Elements Microscope Imaging Software, version 4.13 (Nikon, Japan) to demonstrate the biofilm formation and development on the coated blend fabric fibres, as well as to assess the amount of biomass remaining on the fabric after harvesting. The biofilms were imaged weekly before and after harvesting. The procedure involved cutting out a used fabric sample approximately 0.7 mm x 0.7 mm in dimension. The location of the cut within the reactor channel was randomly selected each week. Fabric samples covered by biofilms were stained with Hoechst 33342 nucleic acid stain solution in water, washed, and dried at room temperature. Each fabric sample was then imaged by confocal microscopy at three randomly selected locations within the sample.

These 3-dimensional confocal images were further processed with ImageJ (Fiji) software to quantify the approximate density of attached microalgal cells. First, a common biofilm depth to be analysed was selected for all samples by considering the number of z stacks and the sizes of each step. The selected biofilm depth for each image was  $37 \pm 1 \mu\text{m}$ . Then, the corresponding number of z stacks was compressed (**Figure 4.2**), and chlorophyll autofluorescence of the attached *N. oceanica* was quantified by analysing the red channel with ImageJ (Fiji). Similarly, stained fibre availability was quantified using the blue channel.

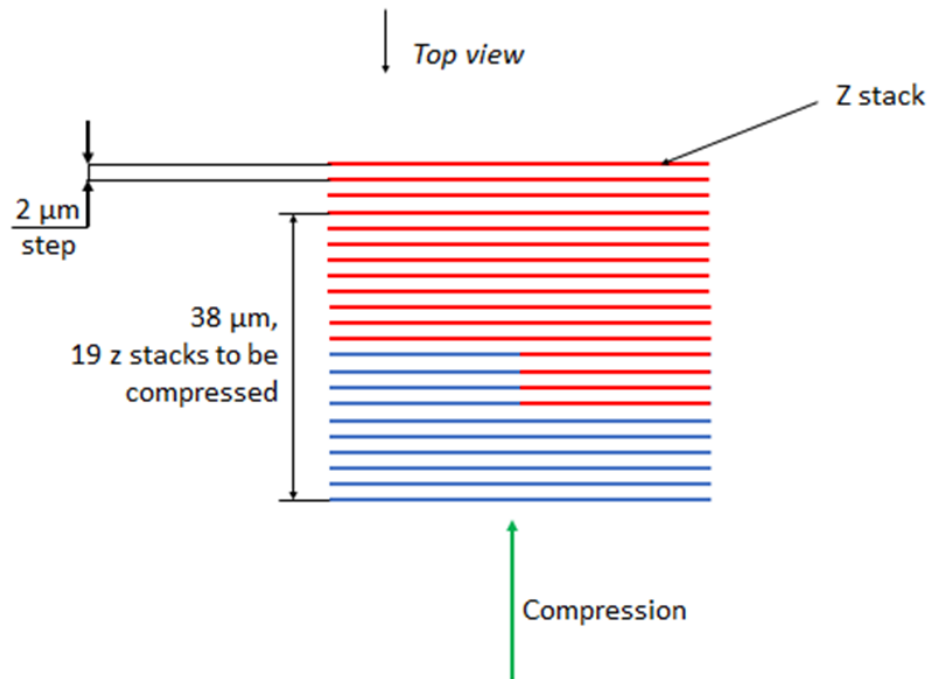


**Figure 4.2** Confocal image compression for the quantification of attached microalgal autofluorescence and stained fibre fluorescence in reactor A after 14 days (2 weeks) of cascade system operation: red stacks represent layers covered by algal cells; blue stacks represent underlying fibres.

The attached microalgal cell density estimate was divided by the total number of fibres that were available for attachment in each image. **Figure 4.3** shows confocal microscopy images of microalgal biofilms before and after harvesting, where the stacks were compressed with ImageJ (Fiji) software.

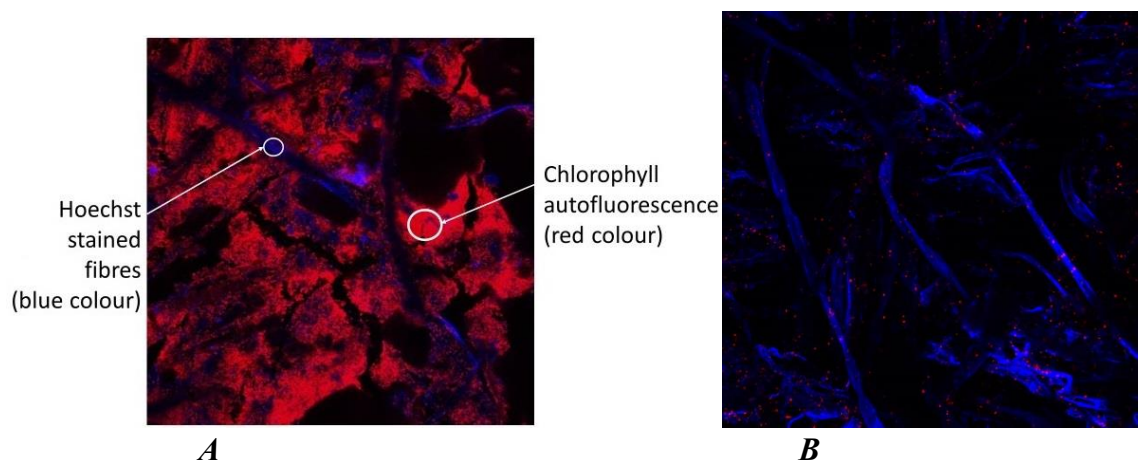


**Figure 4.3** Compressed confocal images of a biofilm before and after harvesting: red colour – chlorophyll autofluorescence; blue colour – Hoechst 33342 stained fabric

fluorescence; *A* – reactor A, 14 days/2 weeks of cascade system operation, before harvesting; *B* – reactor B, 21 days/3 weeks of cascade system operation, after harvesting.

The highest values of chlorophyll autofluorescence and Hoechst 33342 stained fabric fluorescence were set to unity, and all other confocal images were normalised against those values.

The confocal images of biofilms after harvesting were processed in the same way to quantify the amount of biomass remaining after scraping. Percentage of biofilm biomass harvested for every week was calculated from the difference between the amount of attached biomass before and after scraping for each biofilm.

#### 4.3.6 Mass fraction of biomass to water and biomass productivity

*N. oceanica* biofilms were harvested into pre-weighted aluminium containers and weighted (Sartorius Quintix<sup>®</sup> Analytical Balance 220 g x 0.1 mg). The scraped microalgal sludge was then dried in an oven (Labec Pty Ltd, Australia) overnight at 100°C, cooled in a desiccator for 2 hours and weighted again. The mass fraction of biofilm biomass to water (fx/w, g kg<sup>-1</sup>) was calculated as the ratio of dry biomass weight (DW) to wet biomass weight. Aerial productivity ( $P_x$ , g m<sup>-2</sup> d<sup>-1</sup>) was determined from the following equation (Blanken et al. 2014):

$$P_x = \frac{DW}{t \times A}, \text{ where}$$

*t* – growth/harvesting cycle (days);

*A* – biofilm surface area, m<sup>2</sup>.

#### 4.3.7 Statistical analysis

Two-tailed unpaired *t*-tests were applied to test the null hypothesis that there was no difference in the amount of microalgal autofluorescence and stained fabric fluorescence between week 1 vs week 3, week 1 vs week 4, and week 1 vs week 5 of the biofilm cultivation in the cascade system. The results were considered significant at  $p < 0.05$ .

#### 4.4 Results and discussion

The laboratory-scale cultivation of *N. oceanica* biofilms on coated blend fabric in the cascade system was aimed at testing biomass productivity and fabric durability after multiple growth/harvesting cycles; visualising the biofilms and quantifying harvesting efficiency. This experimental study was carried out over 5 weeks (Day 0 – Day 34). The microalgal biofilm in cascade reactor B at different timepoints is shown in **Figure 4.4**.

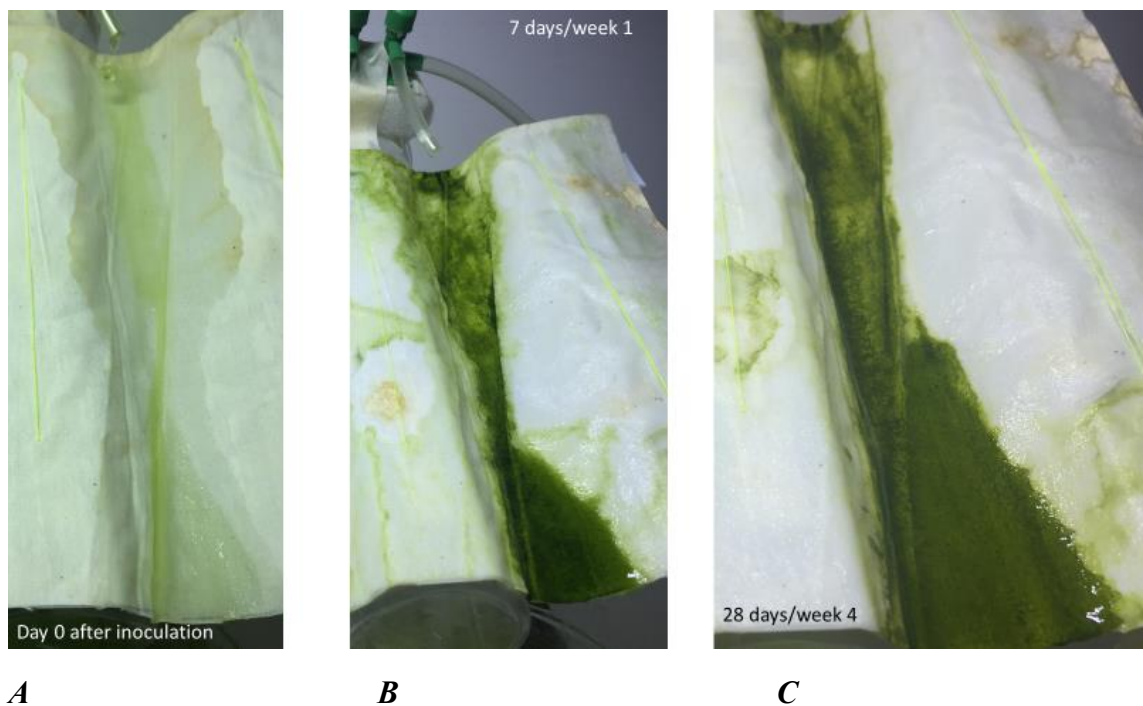


**Figure 4.4** *N. oceanica* biofilm in reactor B at different timepoints of cascade system operation: **A** – initial cell settlement immediately after inoculation on Day 0; **B** – initial attachment (7 days, week 1); **C** – third biofilm growth/harvesting cycle (28 days, week 4).

Measurements of suspended culture OD were performed daily for the first week of cascade system operation (initial cell attachment and biofilm formation, Day 0 – Day 6). A steady decrease in suspended cell density was recorded for both cascade reactors, which was attributed to cell entrapment in the coating and fibres of the coated blend fabric (**Supplement 4.2**). The biofilms were also becoming visually greener every day. After Day 6, the suspended microalgal culture was replaced with fresh F/2 medium. Suspended algal cell density remained steady at OD 0.05-0.20 during further biofilm growth/harvesting cycles. The presence of some cells in the growth medium could be

explained by biofilm sloughing at the trickle feed locations and at the lower ends of the channels. Gravity-driven downward movement of cells was observed, creating thicker biofilms at the edges of the channels (**Figure 4.4B, C**).

Microalgal biomass concentration is an important parameter that determines whether expensive dewatering and drying steps need to be implemented (Wang et al. 2018). The mass fraction of biofilm biomass to water ( $f_{x/w}$ ) was calculated for every week of cascade system operation. Dry biomass content in a typical suspended microalgae cultivation system is 1-10 g kg<sup>-1</sup> (Blanken et al. 2014), and an additional dewatering step (Fasaei et al. 2018) needs to be added to increase the mass fraction of biomass to water to 150-250 g kg<sup>-1</sup> (Blanken et al. 2014). In this study, dry biomass concentration of the harvested sludge did not decrease below 150 g kg<sup>-1</sup> following the initial biofilm formation period of 14 days (**Table 4.1**). An extra dewatering step is therefore not required.

Due to the large variety of bioreactor designs, microalgal species used and environmental parameters tested, it may be difficult to compare biomass productivity between different systems described in the literature (Terry & Raymond 1985; Berner, Heimann & Sheehan 2015). In this study, aerial productivity of biofilms in cascade reactors ( $P_x$ ) was between 15.3 g m<sup>-2</sup> d<sup>-1</sup> and 25.2 g m<sup>-2</sup> d<sup>-1</sup> following initial attachment (**Table 4.1**). This result is comparable with the productivity of the given species grown as a suspension in a raceway pond (Vree et al. 2015). It also correlates with the productivity that is usually reported for thin-layer cascade systems, which is between 4.5 and 25 g m<sup>-2</sup> d<sup>-1</sup> (Torzillo et al. 2010; De Marchin, Erpicum & Franck 2015; Apel et al. 2017; Benavides et al. 2017). The biofilm biomass productivity measured in this experiment is above average for attached growth bioreactors. For *Nannochloropsis* sp. biofilms, the productivity ranges between <5 g m<sup>-2</sup> d<sup>-1</sup> (Naumann et al. 2013) and 20 g m<sup>-2</sup> d<sup>-1</sup> (Shen et al. 2014).

**Table 4.1** Mass fractions of biomass to water (fx/w) and aerial productivity (Px) of the biofilms in the cascade system.

Day/week	fx/w (g kg <sup>-1</sup> )		Px (g m <sup>-2</sup> d <sup>-1</sup> )	
	Reactor A	Reactor B	Reactor A	Reactor B
14/2	110.7	89.8	8.0	8.2
21/3	68.1	168.3	5.3	15.3
28/4	151.7	213.1	25.2	22.6
35/5	152.9	208.9	22.4	22.7

Lower aerial productivity in the first 14 days of system operation was anticipated due to extensive evidence that initial cell attachment to a fresh attachment material requires more time and results in lower yields (Holmes 1986; Hodoki 2005; Irvin & Allen 2011; Schnurr & Allen 2015). The final biomass in the first prolonged growth/harvesting cycle (week 2) was also comparatively moist. Biofilm biomass productivity for reactor B nearly doubled in the second cycle (week 3), as did mass fraction of biomass to water. The two subsequent growth/harvesting cycles (week 4 and week 5) were characterised by similar aerial productivity for both reactors, with the mean value of 23.2 g m<sup>-2</sup> d<sup>-1</sup>, which is a promising result for attached biomass cultivation in a cascade reactor.

Biomass productivity and mass fraction of biomass to water of one of the biofilms in reactor A was low during week 3 of operation (5.3 g m<sup>-2</sup> d<sup>-1</sup>; 68.1 g kg<sup>-1</sup>). The biofilm changed colour to yellow/light brown, and the attachment was visually lower compared to the biofilms in reactor B. However, the affected biofilm recovered its green colour and growth rate within two days following week 3 of biomass harvesting.

The coated blend fabric was examined visually after every harvest for each biofilm, and no signs of damage were recorded at any timepoint of this study. Similar experiments conducted with *N. oceanica* using cotton fabric showed considerable fabric damage. The first signs of fraying were visible after three weeks of biofilm growth on cotton in every experimental run (**Figure 4.5**).



**Figure 4.5** Cotton fabric damage after 4 weeks of growing *N. oceanica* biofilms in a cascade system under laboratory conditions.

Hence, the coated blend is a superior microalgal biomass attachment material to cotton due to its lightweight nature, lower manufacturing cost and increased durability in saltwater.

Confocal laser scanning microscopy was used to demonstrate the spatial distribution of *N. oceanica* cells on the coated blend fabric over this 5-week experiment. **Figure 4.6A** shows the structure of one of the biofilms in reactor B after 7 days of cascade system operation. At this time, the microalgal cells were predominantly attached to the plastic polymer coating of the fabric. Algal attachment followed the irregular contours of the polymer coating. A similar configuration was observed on day 14, at the end of the initial attachment cycle (**Figure 4.6B**). The coated fractions of the fabric were more densely populated with microalgae, whereas the single uncoated fibres remained mainly bare. In general, the fabric coverage at later times was considerably higher (**Figure 4.6C, D**). These images are representative of all biofilms produced during this experiment.

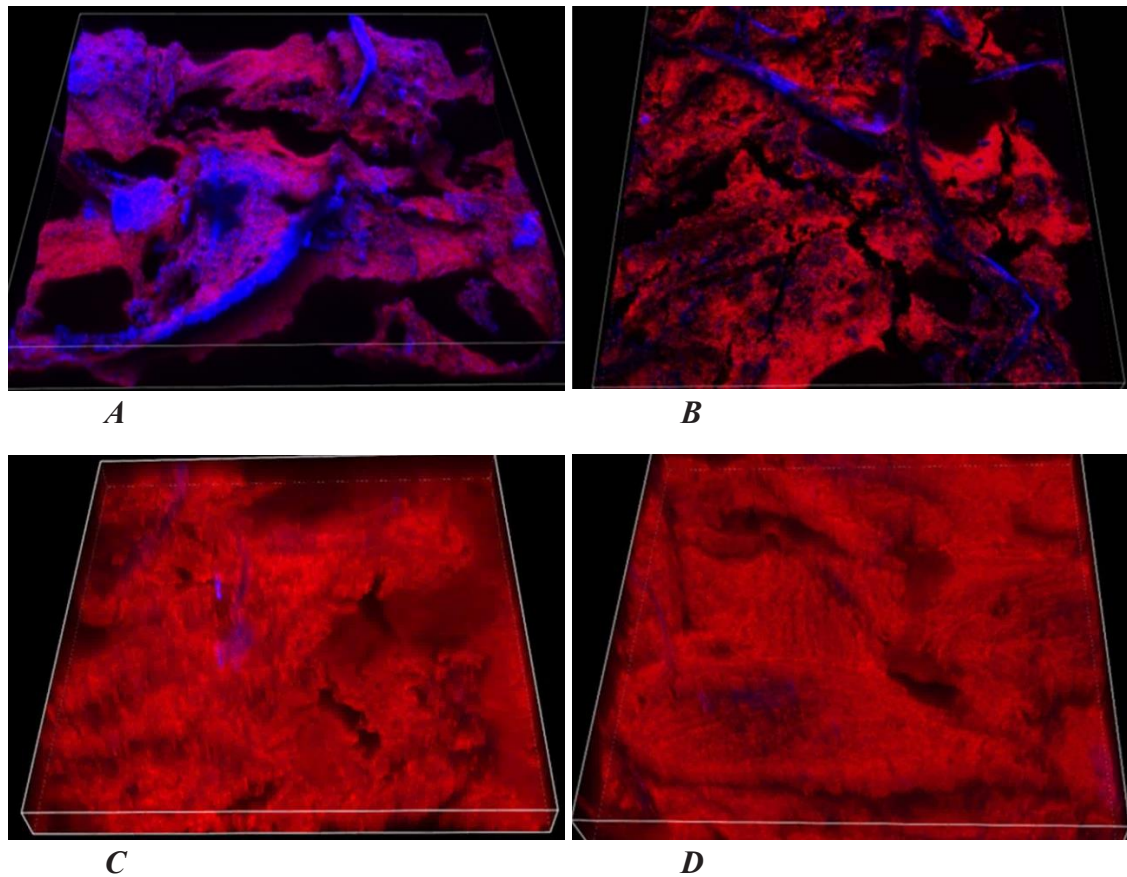
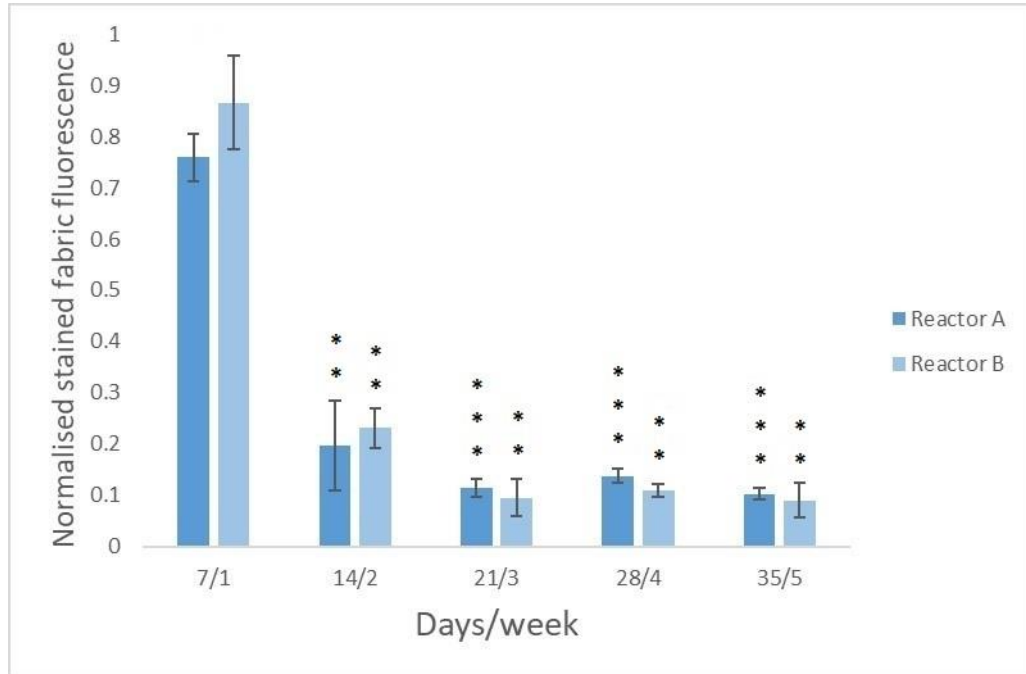


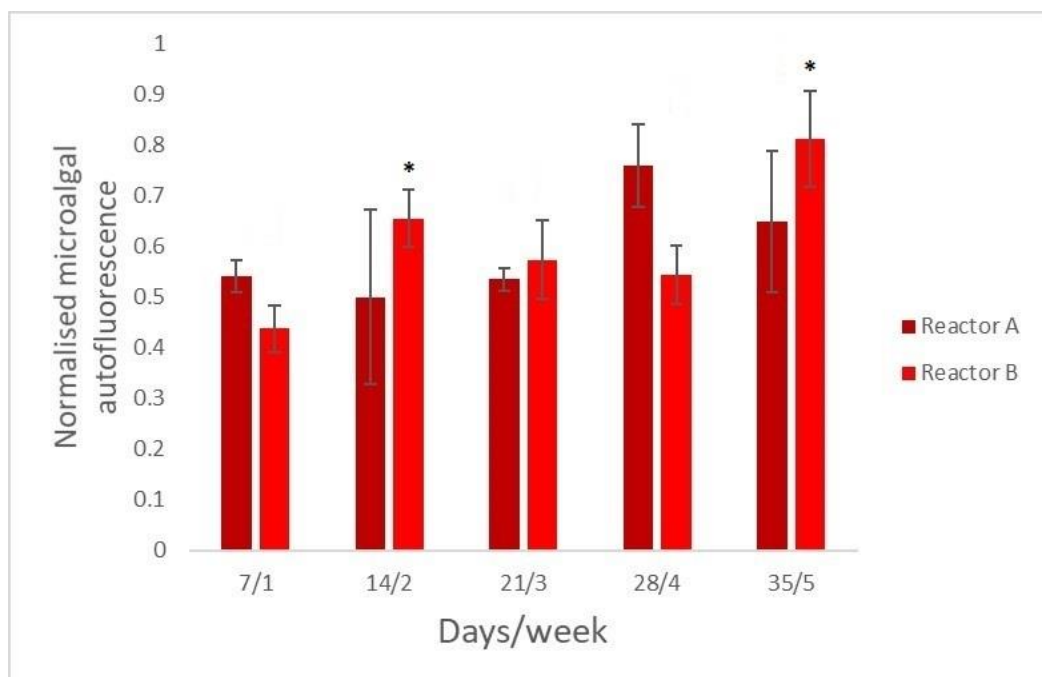
**Figure 4.6** Spatial distribution of microalgal cells on the coated blend fibres in reactor B: red colour – chlorophyll autofluorescence; blue colour – Hoechst 33342 stained fabric fluorescence; imaged square size 600  $\mu\text{m}$  x 600  $\mu\text{m}$ , variable depths; **A** – *N. oceanica* biofilm after 7 days/1 week of cascade system operation; **B** – *N. oceanica* biofilm after 14 days/2 weeks of cascade system operation; **C** – *N. oceanica* biofilm after 28 days/4 weeks of cascade system operation; **D** – *N. oceanica* biofilm after 35 days/5 weeks of cascade system operation.

Analysis of these confocal microscopy images was performed using ImageJ (Fiji) software to quantify the ratio of microalgal autofluorescence (red channel) to stained fibre fluorescence (blue channel). The amount of fibres imaged after the first seven days of biofilm formation in the cascade system was approximately four times higher than during the weeks post initial cell attachment (**Figure 4.7A**). The red channel autofluorescence, however, remained in the same range with a slight increase in its amount after the initial attachment (**Figure 4.7B**). The sharp decrease in the amount of the blue channel fluorescence compared to the first week could indicate the coverage of the fibres with microalgal biomass. The biofilms were becoming thicker due to cell

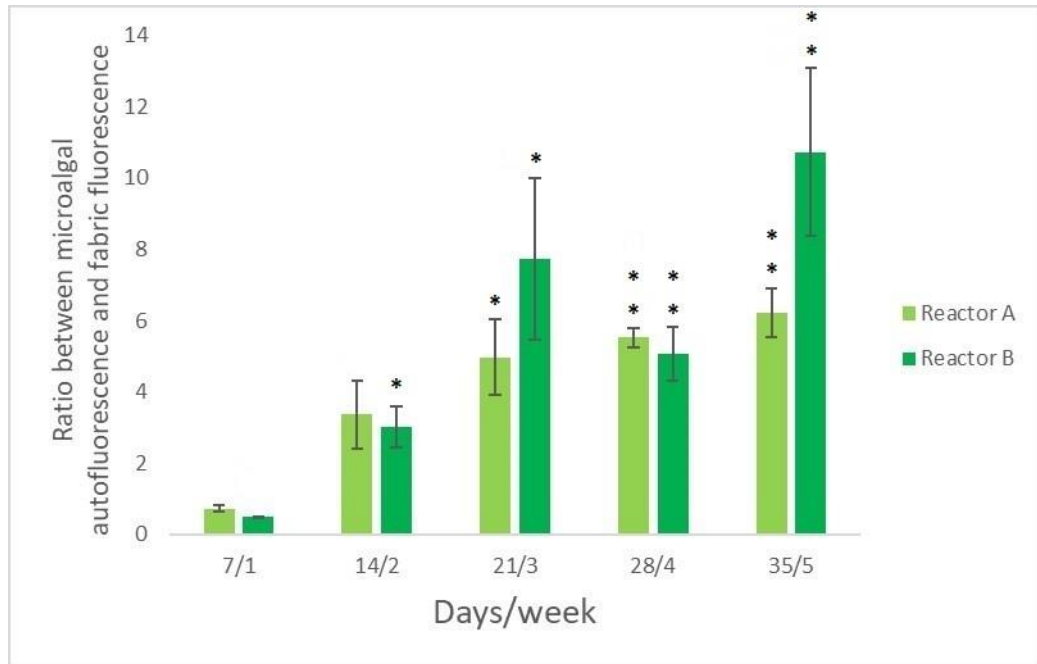
division, which could not be detected from chlorophyll fluorescence as the cells were theoretically forming sequential layers.



**A**



**B**



**C**

**Figure 4.7** Quantification of Hoechst 33342 stained fabric fluorescence (*A*) and attached microalgal fluorescence (*B*), and the ratio between these values (*C*). \* $p < 0.05$ ; \*\* $p < 0.01$ ; \*\*\* $p < 0.001$ .

The ratio between the amount of the imaged microalgal biomass and the stained fabric fibres is reflected in **Figure 4.7C**. Overall, it showed an upward trend that reflected the increase of attached cell density after first seven days of initial attachment.

Visual analysis of the biofilms revealed considerable spatial variability in microalgal cell attachment. The yellow/brown biofilm from week 3 (see **Table 4.1**) was not used for confocal imaging; a green biofilm from the other reactor channel was chosen instead.

Biomass scraping with a plastic spatula proved to be an efficient method of biofilm harvesting in the cascade system. For each of the three weeks post initial attachment, the percentage of biomass removed from the fabric attachment materials was between 95.2% and 98.7% (**Table 4.2**).

**Table 4.2** Percentage of attached biofilm biomass harvested by scraping.

Day/week	% harvested	
	Reactor A	Reactor B
21/3	95.8 %	98.0 %
28/4	96.6 %	95.2 %
35/5	95.4 %	98.7 %

In the future, a fully automated harvester for attached biomass production in cascade systems needs to be designed.

## 4.5 Summary

The potential of microalgal biofilm cultivation in a cascade system was studied by carrying out *N. oceanica* biomass growth/harvesting cycles over 5 weeks. The maximum aerial productivity achieved in the system was  $25.2 \text{ g m}^{-2} \text{ d}^{-1}$ , and the mass fraction of biomass to water of the harvested microalgal sludge was above  $150 \text{ g kg}^{-1}$ , which is comparable to dewatered and concentrated biomass from suspended systems. The coated blend fabric used as the microalgal cell attachment material did not show any signs of damage after four harvesting cycles performed by scraping. Hence, its light weight, the ability to promote and sustain high microalgal cell attachment and biofilm development, and durability in saltwater recommend it as an attachment material for attached microalgal growth systems. Confocal laser scanning microscope images of *N. oceanica* biofilms revealed that the fabric coating was the predominant location of initial microalgal cell attachment, as opposed to the uncoated fibres. Mechanical scraping of attached biomass was highly efficient, with harvesting efficiency of up to 98.7% achieved. In the future, an economical and fully automated microalgal biomass harvesting method needs to be developed. With further optimisation, microalgal cultivation as biofilms in a cascade system could be a viable method of large-scale biomass production due to competitive aerial productivity, high mass fraction of biomass to water and economical harvesting of microalgal biomass.

## 4.6 References

- Apel, A.C., Pfaffinger, C.E., Basedahl, N., Mittwollen, N., Göbel, J., Sauter, J., Brück, T. & Weuster-Botz, D. 2017, 'Open thin-layer cascade reactors for saline microalgae production evaluated in a physically simulated Mediterranean summer climate', *Algal Research*, vol. 25, pp. 381–90.
- Benavides, A.M.S., Ranglová, K., Malapascua, J.R., Masojídek, J. & Torzillo, G. 2017, 'Diurnal changes of photosynthesis and growth of *Arthrospira platensis* cultured in a thin-layer cascade and an open pond', *Algal Research*, vol. 28, pp. 48–56.
- Berner, F., Heimann, K. & Sheehan, M. 2015, 'Microalgal biofilms for biomass production', *Journal of Applied Phycology*, vol. 27, no. 5, pp. 1793–804.
- Bernstein, H.C., Kesaano, M., Moll, K., Smith, T., Gerlach, R., Carlson, R.P., Miller, C.D., Peyton, B.M., Cooksey, K.E., Gardner, R.D. & Sims, R.C. 2014, 'Direct measurement and characterization of active photosynthesis zones inside wastewater remediating and biofuel producing microalgal biofilms', *Bioresource Technology*, vol. 156, pp. 206–15.
- Blanken, W., Janssen, M., Cuaresma, M., Libor, Z., Bhajji, T. & Wijffels, R.H. 2014, 'Biofilm growth of *Chlorella sorokiniana* in a rotating biological contactor based photobioreactor', *Biotechnology and Bioengineering*, vol. 111, no. 12, pp. 2436–45.
- Borowitzka, M.A. 1999, 'Commercial production of microalgae: ponds, tanks, tubes and fermenters', *Journal of Biotechnology*, vol. 70, no. 1–3, pp. 313–21.
- Borowitzka, M.A. & Moheimani, N.R. (eds) 2013, *Algae for Biofuels and Energy*, vol. 5, Springer Netherlands, Dordrecht.
- Brennan, L. & Owende, P. 2010, 'Biofuels from microalgae - A review of technologies for production, processing, and extractions of biofuels and co-products', *Renewable and Sustainable Energy Reviews*, vol. 14, no. 2, pp. 557–77.
- Cao, J., Yuan, W., Pei, Z.J., Davis, T., Cui, Y. & Beltran, M. 2009, 'A preliminary study of the effect of surface texture on algae cell attachment for a mechanical-biological energy manufacturing system', *Journal of Manufacturing Science and Engineering*, vol. 131, no. 6, p. 064505.
- Christenson, L.B. & Sims, R.C. 2012, 'Rotating algal biofilm reactor and spool harvester for wastewater treatment with biofuels by-products', *Biotechnology and Bioengineering*, vol. 109, no. 7, pp. 1674–84.

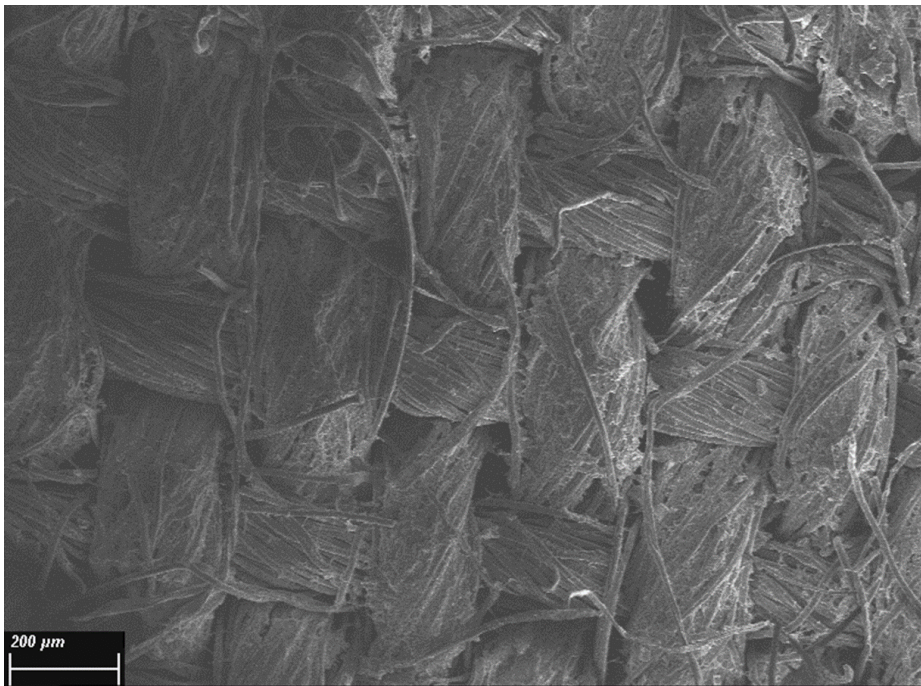
- Cui, Y. & Yuan, W.Q. 2013, 'Thermodynamic modeling of algal cell-solid substrate interactions', *Applied Energy*, vol. 112, pp. 485–92.
- Cui, Y., Yuan, W.Q. & Cao, J. 2014, 'Effect of surface texturing on microalgal cell attachment to solid carriers', *International Journal of Agricultural and Biological Engineering*, vol. 7, no. 2, pp. 82–91.
- Davis, R., Aden, A. & Pienkos, P.T. 2011, 'Techno-economic analysis of autotrophic microalgae for fuel production', *Applied Energy*, vol. 88, no. 10, pp. 3524–31.
- De Assis, L.R., Calijuri, M.L., Do Couto, E.D.A. & Assemany, P.P. 2017, 'Microalgal biomass production and nutrients removal from domestic sewage in a hybrid high-rate pond with biofilm reactor', *Ecological Engineering*, vol. 106, pp. 191–9.
- De Marchin, T., Erpicum, M. & Franck, F. 2015, 'Photosynthesis of *Scenedesmus obliquus* in outdoor open thin-layer cascade system in high and low CO<sub>2</sub> in Belgium', *Journal of Biotechnology*, vol. 215, pp. 2–12.
- Doucha, J. & Lívanský, K. 2009, 'Outdoor open thin-layer microalgal photobioreactor: potential productivity', *Journal of Applied Phycology*, vol. 21, no. 1, pp. 111–7.
- Ekelhof, A. & Melkonian, M. 2017, 'Microalgal cultivation in porous substrate bioreactor for extracellular polysaccharide production', *Journal of Applied Phycology*, vol. 29, no. 3, pp. 1115–22.
- Fasaei, F., Bitter, J.H., Slegers, P.M. & van Boxtel, A.J.B. 2018, 'Techno-economic evaluation of microalgae harvesting and dewatering systems', *Algal Research*, vol. 31, pp. 347–362.
- Gao, F., Yang, Z.H., Li, C., Zeng, G.M., Ma, D.H. & Zhou, L. 2015, 'A novel algal biofilm membrane photobioreactor for attached microalgae growth and nutrients removal from secondary effluent', *Bioresource Technology*, vol. 179, pp. 8–12.
- Genin, S.N., Aitchison, S.J. & Allen, G.D. 2014, 'Design of algal film photobioreactors: Material surface energy effects on algal film productivity, colonization and lipid content', *Bioresource Technology*, vol. 155, pp. 136–43.
- Gross, M., Henry, W., Michael, C. & Wen, Z. 2013, 'Development of a rotating algal biofilm growth system for attached microalgae growth with in situ biomass harvest', *Bioresource Technology*, vol. 150, pp. 195–201.
- Gross, M., Jarboe, D. & Wen, Z. 2015, 'Biofilm-based algal cultivation systems', *Applied Microbiology and Biotechnology*, vol. 99, no. 14, pp. 5781–9.
- Gross, M. & Wen, Z. 2014, 'Yearlong evaluation of performance and durability of a

- pilot-scale Revolving Algal Biofilm (RAB) cultivation system', *Bioresource Technology*, vol. 171, pp. 50–8.
- Gross, M., Zhao, X., Mascarenhas, V. & Wen, Z. 2016, 'Effects of the surface physico-chemical properties and the surface textures on the initial colonization and the attached growth in algal biofilm', *Biotechnology for Biofuels*, vol. 9, no. 1, p. 38.
- Guillard, R.R.L. & Ryther, J.H. 1962, 'Studies of marine planktonic diatoms: I. *Cyclotella nana* Hustedt, and *Detonula confervacea* (Cleve) Gran', *Canadian journal of microbiology*, vol. 8, no. 2, pp. 229–39.
- Hodoki, Y. 2005, 'Bacteria biofilm encourages algal immigration onto substrata in lotic systems', *Hydrobiologia*, vol. 539, no. 1, pp. 27–34.
- Holmes, P.E. 1986, 'Bacterial enhancement of vinyl fouling by algae. Applied and environmental microbiology', vol. 52, no. 6, pp. 1391–3.
- Huang, Y., Zheng, Y., Li, J., Liao, Q., Fu, Q., Xia, A., Fu, J. & Sun, Y. 2018, 'Enhancing microalgae biofilm formation and growth by fabricating microgrooves onto the substrate surface', *Bioresource Technology*, vol. 261, pp. 36–43.
- Irving, T.E. & Allen, D.G. 2011, 'Species and material considerations in the formation and development of microalgal biofilms', *Applied Microbiology and Biotechnology*, vol. 92, no. 2, pp. 283–94
- Johnson, M.B. & Wen, Z. 2010, 'Development of an attached microalgal growth system for biofuel production', *Applied Microbiology and Biotechnology*, vol. 85, no. 3, pp. 525–34.
- Kesaano, M., Gardner, R.D., Moll, K., Lauchnor, E., Gerlach, R., Peyton, B.M. & Sims, R.C. 2015, 'Dissolved inorganic carbon enhanced growth, nutrient uptake, and lipid accumulation in wastewater grown microalgal biofilms', *Bioresource Technology*, vol. 180, pp. 7–15.
- Lee, Y.K. 2001, 'Microalgal mass culture systems and methods: their limitation and potential', *Journal of Applied Phycology*, vol. 13, no. 4, pp. 307–15.
- Liu, T., Wang, J., Hu, Q., Cheng, P., Ji, B., Liu, J., Chen, Y., Zhang, W., Chen, X., Chen, L., Gao, L., Ji, C. & Wang, H. 2013, 'Attached cultivation technology of microalgae for efficient biomass feedstock production', *Bioresource Technology*, vol. 127, pp. 216–22.
- De Marchin, T., Erpicum, M. & Franck, F. 2015, 'Photosynthesis of *Scenedesmus obliquus* in outdoor open thin-layer cascade system in high and low CO<sub>2</sub> in

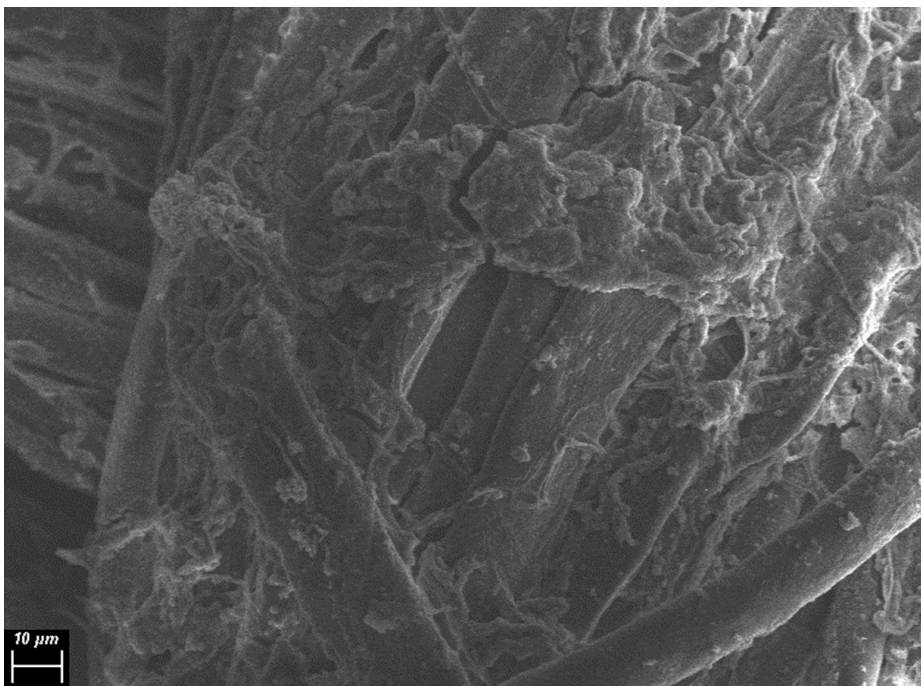
- Belgium', *Journal of Biotechnology*, vol. 215, pp. 2–12.
- Narala, R.R., Garg, S., Sharma, K.K., Thomas-Hall, S.R., Deme, M., Li, Y. & Schenk, P.M. 2016, 'Comparison of microalgae cultivation in photobioreactor, open raceway pond, and a two-stage hybrid system', *Frontiers in Energy Research*, vol. 4, p.29.
- Naumann, T., Çebi, Z., Podola, B. & Melkonian, M. 2013, 'Growing microalgae as aquaculture feeds on twin-layers: A novel solid-state photobioreactor', *Journal of Applied Phycology*, vol. 25, no. 5, pp. 1413–20.
- Norsker, N.H., Barbosa, M.J., Vermuë, M.H. & Wijffels, R.H. 2011, 'Microalgal production—a close look at the economics', *Biotechnology Advances*, vol. 29, no. 1, pp. 24–27.
- Ozkan, A. & Berberoglu, H. 2013, 'Cell to substratum and cell to cell interactions of microalgae', *Colloids and Surfaces B: Biointerfaces*, vol. 112, pp. 302–9.
- Ozkan, A., Kinney, K., Katz, L. & Berberoglu, H. 2012, 'Reduction of water and energy requirement of algae cultivation using an algae biofilm photobioreactor', *Bioresource Technology*, vol. 114, pp. 542–8.
- Pruvost, J., Cornet, J.F. & Pilon, L. 2016, 'Large-scale production of algal biomass: photobioreactors', in F. Bux & Y. Chisti (eds), *Algae Biotechnology*, Springer, Cham (pp. 41–66).
- Schnurr, P.J. & Allen, D.G. 2015, 'Factors affecting algae biofilm growth and lipid production: a review', *Renewable and Sustainable Energy Reviews*, vol. 52, pp. 418–429.
- Schnurr, P.J., Espie, G.S. & Allen, D.G. 2013, 'Algae biofilm growth and the potential to stimulate lipid accumulation through nutrient starvation', *Bioresource Technology*, vol. 136, pp. 337–44.
- Schultze, L.K.P., Simon, M.V., Li, T., Langenbach, D., Podola, B. & Melkonian, M. 2015, 'High light and carbon dioxide optimize surface productivity in a twin-layer biofilm photobioreactor', *Algal Research*, vol. 8, pp. 37–44.
- Sekar, R., Venugopalan, V.P., Satpathy, K.K., Nair, K.V.K. & Rao, V.N.R. 2004, 'Laboratory studies on adhesion of microalgae to hard substrates', *Hydrobiologia*, vol. 512, pp. 109–16.
- Šetlík, I., Šust, V. & Málek, I. 1970, 'Dual purpose open circulation units for large scale culture of algae in temperate zones. I. Basic design considerations and scheme of a

- pilot plant', *Algological Studies/Archiv für Hydrobiologie, Supplement Volumes*, pp. 111–64.
- Shayan, S.I., Agblevor, F.A., Bertin, L. & Sims, R.C. 2016, 'Hydraulic retention time effects on wastewater nutrient removal and bioproduct production via rotating algal biofilm reactor', *Bioresource Technology*, vol. 211, pp. 527–33.
- Shen, Y., Xu, X., Zhao, Y. & Lin, X. 2014, 'Influence of algae species, substrata and culture conditions on attached microalgal culture', *Bioprocess and Biosystems Engineering*, vol. 37, no. 3, pp. 441–50.
- Taylor, A.P.A., Holden, P.J., Finnie, K.S. & Bartlett, J. 2005, *Membrane bioreactor*, Patent 2005243606, Australian Intellectual Property Trademark Database.
- Taylor, A.P.A. 2006, *Sewage Treatment*, Patent 2006315091, Australian Intellectual Property Trademark Database.
- Terry, K.L. & Raymond, L.P. 1985, 'System design for the autotrophic production of microalgae', *Enzyme and Microbial Technology*, vol. 7, no. 10, pp. 474–87.
- Torzillo, G., Giannelli, L., Martinez-Poldan, A., Verdone, N., De Filippis, P., Scarsella, M. & Bravi, M. 2010, 'Microalgal culturing in thin-layer photobioreactors', *Chemical Engineering*, vol. 20, pp. 265–70.
- Vree, J.H., Bosma, R., Janssen, M., Barbosa, M.J. & Wijffels, R.H. 2015, 'Comparison of four outdoor pilot-scale photobioreactors. Biotechnology for biofuels', vol. 8, no. 1, pp. 215–27.
- Wang, J.H., Zhuang, L.L., Xu, X.Q., Deantes-Espinosa, V.M., Wang, X.X. & Hu, H.Y. 2018, 'Microalgal attachment and attached systems for biomass production and wastewater treatment', *Renewable and Sustainable Energy Reviews*, vol. 92, pp. 331–42.
- Wijihastuti, R.S., Moheimani, N.R., Bahri, P.A., Cosgrove, J.J. & Watanabe, M.M. 2017, 'Growth and photosynthetic activity of *Botryococcus braunii* biofilms', *Journal of Applied Phycology*, vol. 29, no. 3, pp. 1123–34.
- Zhao, X., Kumar, K., Gross, M.A., Kuntz, T.E. & Wen, Z. 2018, 'Evaluation of revolving algae biofilm reactors for nutrients and metals removal from sludge thickening supernatant in a municipal wastewater treatment facility', *Water Research*, vol. 143, pp. 467–78.

## Supplement 4.1



*A*



*B*

**Figure S4.1** 65% polyester and 35% cotton with plastic polymer coating fabric (coated blend).

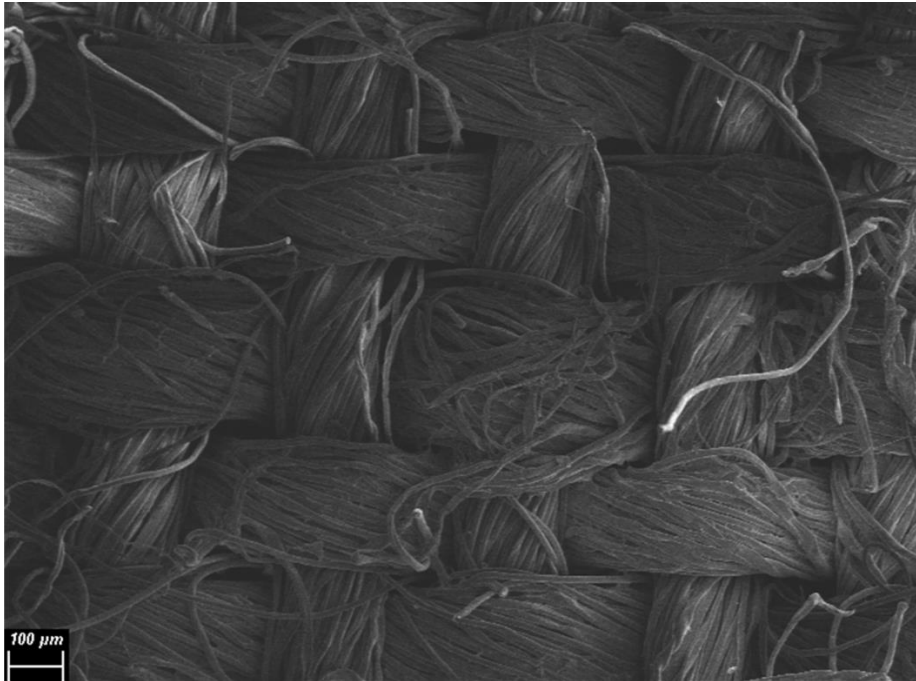


**Figure S4.2** 65% polyester and 35% cotton without coating.

## Supplement 4.2

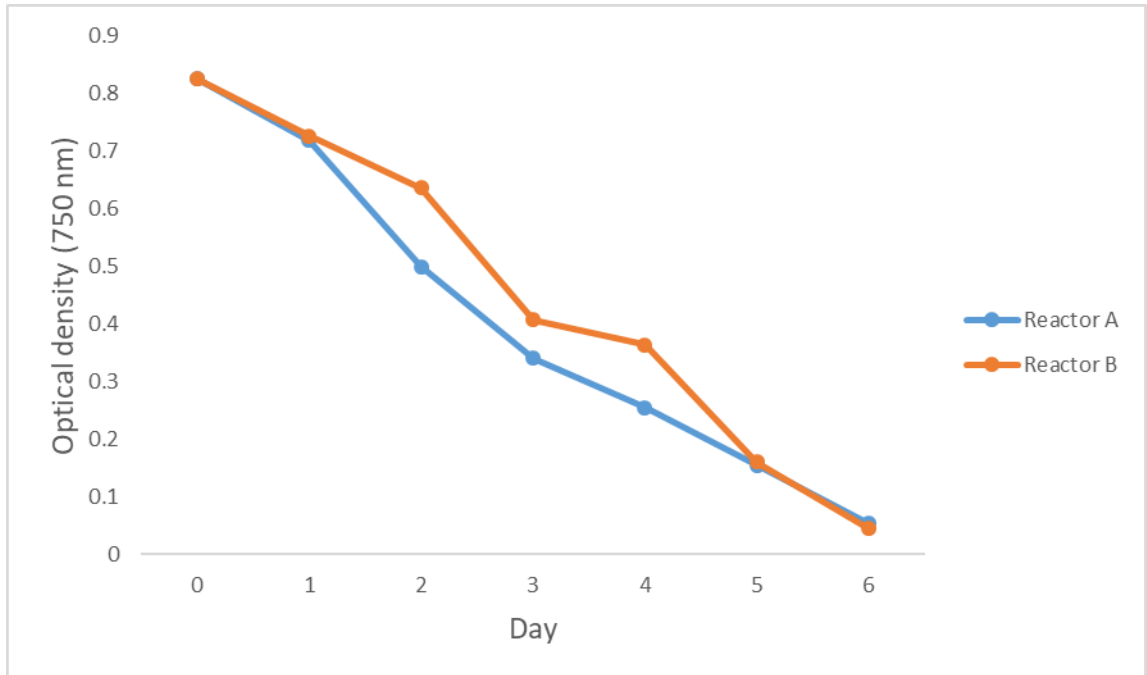


**Figure S4.3** Cell density of the suspended biomass during the first week of the cascade system operation. The steady decrease in the suspended biomass density was recorded due to cell attachment to the fabrics and biofilm formation.

## **CHAPTER 5. GENERAL CONCLUSIONS AND PERSPECTIVES FOR FUTURE RESEARCH**

Harvesting is one of the major bottlenecks in the large-scale production of microalgal biomass (Molina Grima et al. 2003; Laamanen, Ross & Scott 2016). Conventional harvesting methods are uneconomical due to the high energy cost of processing large liquid volumes, and they are time-consuming resulting in long biomass production downtime (Chen et al. 2011; Zeng et al. 2016). My thesis addressed this challenge by growing microalgal biofilms aggregated on an attachment material. This method of biomass harvesting reduced the energy requirement for separation of microalgal cells from the growth medium and enabled the regrowth of biomass after harvesting with short re-inoculation/system downtime.

Two major knowledge gaps in the attached microalgal biomass cultivation were addressed: (i) the selection of an appropriate cell attachment material, and (ii) the design of a suitable biofilm bioreactor.

Considerable changes in biofilm system productivity depending on the choice of a cell attachment material have been experimentally confirmed by many studies (Christenson & Sims 2012; Gross et al. 2013; Tao et al. 2017; Melo et al. 2018). Theoretical approaches proposed to explain and predict the efficiency of an attachment material in biofilm formation (Irving & Allen 2011; Christenson & Sims 2012; Ozkan & Berberoglu 2013; Cui & Yuan 2013; Genin, Aitchison & Allen 2014; Gross et al. 2016; Zheng et al. 2016) have not defined a specific group of materials that would be beneficial for most biofilm system configurations. In my thesis, this hurdle was overcome by introducing a fabric that promotes cell adsorption in biofilm systems of various designs. Several fabrics were investigated as a flexible and inexpensive attachment material for microalgal cell attachment (**Figure 5.1**). Their surface structure was imaged by scanning electron microscopy (SEM) and biofilm attachment was analysed by confocal laser scanning microscopy (CLSM).

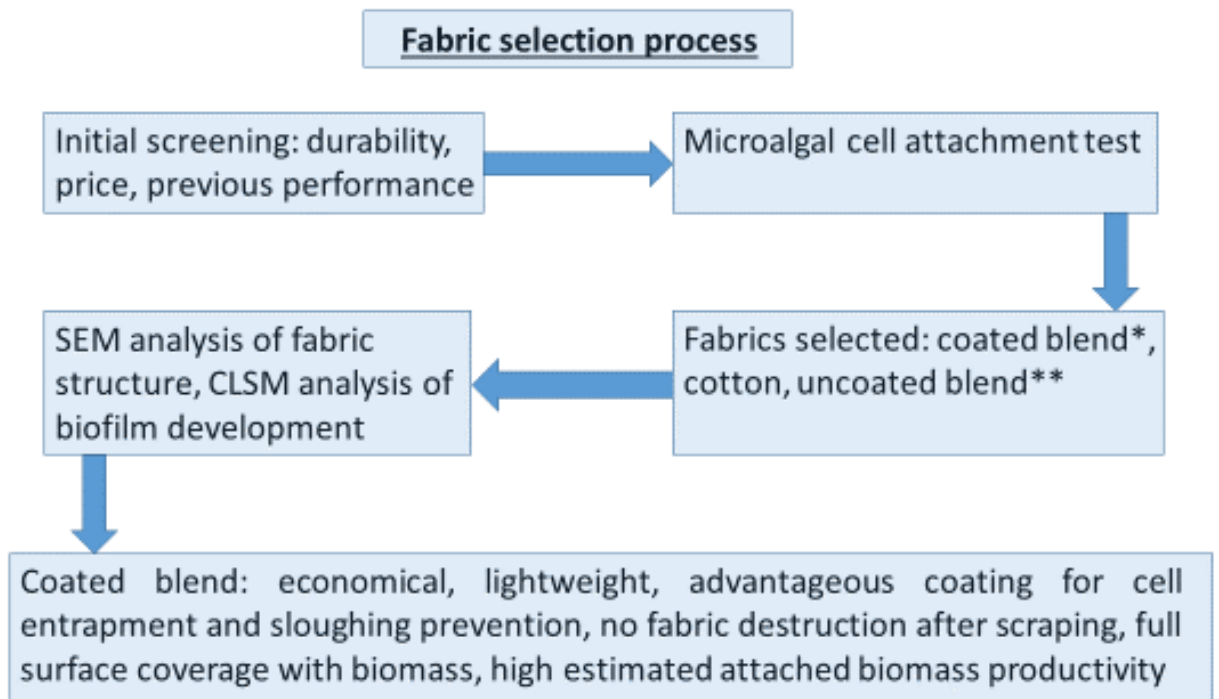


**Figure 5.1** Steps undertaken in my thesis to select the most beneficial fabric for microalgal cell attachment.

\*65% polyester and 35% cotton blend with plastic polymer coating applied to enhance cell attachment and fabric durability.

\*\*65% polyester and 35% cotton blend without coating.

The superior performance of coated blend fabric at both laboratory and pilot scales was attributed to its increased surface roughness, which was created by plastic polymer coating. Previous research indicated that surface roughness is a determining factor for initial cell adsorption efficiency to a material (Irving & Allen 2011; Cui, Yuan & Cao 2014; Cao et al. 2009; Gross, Jarboe & Wen 2015; Huang et al. 2018). My results showed that the porous web-like structure of coated blend fabric created an excellent environment for cell entrapment compared to plain uncoated fabrics, which had different feature geometries. Biofilm formation hotspots appeared on coated blend, and their location coincided with the location of the coating, which was inhomogeneous. This pattern of cell attachment was observed during biofilm cultivation in different bioreactors, for both freshwater and seawater microalgal species. Thus, the attachment pattern of microalgae is primarily determined by the surface features of the attachment material, and it does not change significantly with bioreactor geometry. Moreover, the higher initial cell attachment on this fabric led to more stable and plentiful biofilm

surface coverage at later stages of biofilm development. The microalgal biofilm on coated blend was stable and it did not wash off easily. The low cost, durability, lightweight nature and flexibility of coated blend make it an excellent choice as an algal biofilm attachment material.

A pilot-scale microalgal biofilm system was designed and retrofitted into a conventional raceway pond with suspended microalgal culture. Biofilm fabrics were mounted onto the vanes of paddlewheels to take advantage of their rotational motion so that the biofilm accesses nutrient medium followed by atmospheric CO<sub>2</sub> and sunlight upon each rotation (Christenson & Sims 2012; Gross et al. 2013; Blanken et al. 2014; Sebestyén et al. 2016). This biofilm system was simple to manufacture and operate, and the light and nutrient gradients inherent to suspended cultures and measured in my thesis in the raceway pond were alleviated by rotational biofilm cultivation. Biofilms were substantially denser at the fabric liquid-air interface, which was caused by the partial submersion of the paddlewheel vanes in the suspended culture. This important observation was valid for all fabric attachment materials both at laboratory and at pilot scales. Thus, biofilm bioreactor design should exploit this phenomenon by increasing the attachment material area at the liquid-air interface for enhanced productivity.

Thin-layer cascade bioreactors were also modified to include a stationary biofilm attachment material for attached biomass growth and harvesting. Cascade systems, which already facilitate high microalgal growth rates and volumetric productivity (Pruvost, Cornet & Pilon 2016; Apel et al. 2017), were further enhanced with coated blend fabric. This resulted in dry biomass content of 150 g kg<sup>-1</sup> in the harvested sludge, which is similar to dry biomass content of suspended cultivation followed by dewatering, which is between 150-250 g kg<sup>-1</sup> (Blanken et al. 2014). Besides, a high aerial biomass productivity of 25.2 g m<sup>-2</sup> d<sup>-1</sup> was achieved in this novel system, which is comparable with suspended biomass productivity in a raceway pond for the same microalgal species (Vree et al. 2015). No visible damage to coated blend fabric was observed over 5 weeks of biofilm growth and harvesting, which confirmed the fabric durability. Attached biomass harvesting by scraping achieved up to 98.7% cell removal efficiency from the fabric surface. Although the biofilms on coated blend are stable and resistant to washing off, this fabric also facilitates easy biomass harvesting at the end of the growth cycle.

Experiments confirmed that both the retrofitted paddlewheel system and the modified cascade system are promising bioreactors for attached microalgal biomass production (Table 5.1).

**Table 5.1** Main results from biofilm systems operation.

<b>Paddlewheel system in the raceway pond</b>	
Suspended batch culture growth limitations	CO <sub>2</sub> from day 5; light from day 10; nitrate from day 20.
Biomass harvesting potential	Rapid attachment of cells to fabrics, considerable decrease in suspended cell density after fabrics introduction.
Biofilm formation on paddlewheel vanes	Highest cell attachment at the liquid-air interface of an attachment material.
Coated blend durability	No visible changes to fabric structure at outdoor conditions under UV rays.
<b>Cascade system retrofitted for biofilm cultivation</b>	
Mass fraction of harvested biomass to water	>150 g kg <sup>-1</sup>
Maximum aerial biomass productivity	25.2 g m <sup>-2</sup> d <sup>-1</sup>
Percentage of biomass removed by scraping	95.2% and 98.7%
Coated blend durability	No visible changes to fabric structure after multiple harvestings.

Based on the findings discussed in my thesis, a generalised model to predict the performance of a growth material in a biofilm system could be developed. To assess the potential of the prospective growth material, the following steps must be taken:

1. Assess the structural properties of the material. Determine how lightweight and flexible the material is when dry and after being soaked in water. Test the material for its resistance to tear under both dry and wet conditions and observe whether it keeps its shape when stretched.
2. Perform an initial attachment test. As discussed in Chapter 2, assess the ability of the material to promote initial algal cell settlement on its surface.
3. Study surface roughness. If the material performed well in the initial cell attachment test, proceed to study the microtopography of its surface by SEM. Depending on the roughness of the material, predict the stability of the biofilm

grown on its surface. Based on the experiential results discussed in my thesis, a web-like surface with a multitude of microscopic pores promotes stable cell attachment and helps the biofilm withstand shear stress.

Several aspects of the experiments carried out in my thesis could be improved in the future.

The initial cell attachment experiment to select appropriate fabrics for biofilm development should use several freshwater and seawater microalgal species. This would allow for a quick comparison of fabrics performance with different species at identical biofilm formation conditions. CLSM could be employed at this stage to provide more insights into biofilm formation patterns and attached biomass productivity.

The accuracy of CLSM imaging of biofilm development and attached biomass quantification could be improved by replication. The number of locations within a biofilm sample could be increased to provide a more precise spatial assessment of biofilm development on the fabrics.

Surface roughness of fabrics was not measured in my thesis. In the future, scanning electron microscopy could be used to image surface topography and measure roughness of growth substrates. Generally, surface roughness is measured with a profilometer, such as an interferometer or by confocal laser scanning microscopy, which could also be a useful tool to quantify the widths and depths of pores on a fabric surface. Alternatively, there is a number of other contact and non-contact methods to measure surface roughness of a fabric.

A rural area, as opposed to a city downtown district, should be the location of choice for construction and operation of pilot-scale raceway ponds. Firstly, this would eliminate heavy industrial pollution that can frequently cause microalgal culture death, up to complete termination of all experimentation. Secondly, no light reflection from neighbouring buildings that interferes with irradiance measurements in the pond would be experienced. In addition, to further decrease light reflection, neutral colours must be chosen for raceway pond construction materials, as opposed to bright white surfaces. When designing a pond, the height of its walls should be appropriate for the chosen suspension depth to prevent sunlight shading.

Overall, my thesis has developed a novel attached biomass harvesting process that uses a promising fabric attachment material (cotton blend) across two different bioreactor configurations. Future work in this space should be directed at in-depth analysis of biofilm formation dynamics on the coated blend fabric, optimisation of layouts and growth conditions in the biofilm bioreactors, the design of automated biomass scrapers and scaling up the attached biomass production process.

At this stage, the main priority would be to investigate the long-term stability of the plastic polymer coating that increases porosity on the surface of coated blend. Changes to coated blend performance in the case of coating alteration/destruction need to be accounted for. SEM and CLSM techniques are useful tools for this research. Further studies of microalgal biofilm formation and development patterns on coated blend need to be carried out by labelling and imaging other crucial biofilm components, such as extracellular polymeric substances and bacteria. Studying changes in bacterial communities within biofilms would provide more information about their structure and stability. These microbial assemblages can affect microalgae in both positive and negative ways, having a major impact on biomass productivity and composition for both suspended and attached cultures (Fukami et al. 1997; Fuentes et al. 2016). It has already been shown that the presence of a bacterial biofilm on an attachment material promotes initial settlement of microalgal cells (Schnurr & Allen 2015). Studying the changes in the composition of these bacterial mats during the course of multiple biofilm harvesting and regrowth cycles and their influence on microalgal biomass productivity is the next important step in microalgal biofilm research.

For the paddlewheel biofilm system designed in my thesis, speed of rotation of the vanes in a raceway pond must be adjusted to establish a balance between the shear stress experienced by the biofilms and the frequency of their submersion in liquid to prevent drying out. Despite the biggest advantage of the paddlewheel system, which is easy retrofitting into the existing raceway pond infrastructure, the cascade system modified for biofilm cultivation is considered the more beneficial system for attached biomass cultivation at this stage. The cascade system has a simpler layout that enables easier biomass harvesting; it is less sophisticated in construction and operation; and it can be installed as an independent unit both indoors and outdoors.

The general requirement for a biomass scraper in a biofilm reactor is that it must not introduce system downtime, and its material must be rigid enough to remove biomass without damaging the fabric. Polymers, specifically synthetic rubbers, could hypothetically be beneficial for scraper manufacturing due to a certain degree of elasticity, affordability, and abrasion and heat resistance. For harvesting of biofilms in the cascade system, a scraper could represent a bar with a sharp knife-like edge stationary positioned at the elevated end of the sloping surface. The bar should be mounted above the sloping surface to allow unobstructed nutrient flow. During harvesting, the sharp edge of the bar should be lowered to contact the fabric, and moved all the way down across the sloping surface. In such a way, biomass would be scraped into a supplementary collection gutter installed below the sloping surface. Then, the bar should be lifted and moved back to its initial position. If a corrugated sloping surface is used, the bar edge can be manufactured to replicate the geometry of the corrugated profile.

Evaporation in cascade reactors can serve as a means of temperature control or for rapid increase in salinity for contamination reduction (Apel et al. 2017). However, the freshwater requirement to replace the liquid loss can be expensive. One of the prospective ways to minimise evaporation is covering the sloping surface of the modified cascade reactor with a transparent plastic sheet. This sheet would not obstruct the medium flow as the microalgal biofilms grow in channels on the sloping surface. It would also reduce system pollution by preventing the settlement of dust particles and fungal spores. The disadvantage of this method is that the possible condensation on the sheet could reduce light availability for the microalgal cells. Additional light sources could be mounted on the sheet to increase photon flux density in case of condensation, or to change the light/dark cycles. Besides, temperature control measures could be needed for this system configuration. These measures could include placing the medium containers in shaded areas or underground. The underground option is also beneficial for locations where space is limited, and it could decrease suspended biomass growth due to insufficient illumination.

In general, to reduce suspended microalgal growth, the cascade bioreactor and its ancillary medium containers should be opaque. To harvest the microalgal cells that flow into the containers after being caught in the tubing and other structural components of a cascade system, the properties of polar fleece fabric could be exploited. In my thesis, it

was found that once submerged in a microalgal suspension, polar fleece entraps microalgal cells within its fibres acting as a filter. No stable biofilm formation is observed, and the biomass can be easily harvested by squeezing the fabric. Thus, stripes of polar fleece could be mounted in the containers so that they are fully submerged in the liquid medium. Turbulence created by the pump operation would hypothetically agitate the liquid, moving the cells towards the filters. The fabric stripes can be reused multiple times after squeezing.

Using multiple species for biofilm formation could be beneficial in terms of initial cell attachment to a fabric. If cells of different shapes and sizes were used, they could get entrapped in a larger number of crevices within the rough surface of the substrate, thus providing a higher surface coverage.

Additionally, it would be advantageous to exploit the liquid/air interface of the attachment material, which promotes considerably higher microalgal cell attachment. For the rotating paddlewheel system, this could be practically implemented by constructing the reactor with an adjustable paddlewheel submersion depth. Altering the level of the vane submersion in the pond at multiple timepoints during the day would change the location of the liquid-air interface on the fabric. Once the residence times have been optimised, this should result in a thick biofilm formation across the entire surface of the vanes. In the modified cascade system, the sequential exposure of the attachment material to liquid and gaseous phases could be achieved by interrupting the flow of liquid medium on the sloping surface. The liquid could be delivered to the biofilms in batches; however, the frequency of attachment material irrigation needs to be determined to prevent the biofilm from drying out.

## 5.1 References

- Apel, A.C., Pfaffinger, C.E., Basedahl, N., Mittwollen, N., Göbel, J., Sauter, J., Brück, T. & Weuster-Botz, D. 2017, 'Open thin-layer cascade reactors for saline microalgae production evaluated in a physically simulated Mediterranean summer climate', *Algal Research*, vol. 25, pp. 381–90.
- Blanken, W., Janssen, M., Cuaresma, M., Libor, Z., Bhajji, T. & Wijffels, R.H. 2014, 'Biofilm growth of *Chlorella sorokiniana* in a rotating biological contactor based photobioreactor', *Biotechnology and Bioengineering*, vol. 111, no. 12, pp. 2436–45.
- Cao, J., Yuan, W., Pei, Z.J., Davis, T., Cui, Y. & Beltran, M. 2009, 'A preliminary study of the effect of surface texture on algae cell attachment for a mechanical-biological energy manufacturing system', *Journal of Manufacturing Science and Engineering*, vol. 131, no. 6, p. 064505.
- Chen, C.Y., Yeh, K.L., Aisyah, R., Lee, D.J. & Chang, J.S. 2011, 'Cultivation, photobioreactor design and harvesting of microalgae for biodiesel production: A critical review', *Bioresource Technology*, vol. 102, no. 1, pp. 71–81.
- Christenson, L.B. & Sims, R.C. 2012, 'Rotating algal biofilm reactor and spool harvester for wastewater treatment with biofuels by-products', *Biotechnology and Bioengineering*, vol. 109, no. 7, pp. 1674–84.
- Cui, Y. & Yuan, W. 2013, 'Thermodynamic modeling of algal cell-solid substrate interactions', *Applied Energy*, vol. 112, pp. 485–92.
- Cui, Y., Yuan, W.Q. & Cao, J. 2014, 'Effect of surface texturing on microalgal cell attachment to solid carriers', *International Journal of Agricultural and Biological Engineering*, vol. 7, no. 2, pp. 82–91.
- Fuentes, J., Garbayo, I., Cuaresma, M., Montero, Z., González-del-Valle, M. & Vilchez, C. 2016, 'Impact of microalgae-bacteria interactions on the production of algal biomass and associated compounds', *Marine Drugs*, vol. 14, no. 5, p.100.
- Fukami, K., Nishijima, T. & Ishida, Y. 1997, 'Stimulative and inhibitory effects of bacteria on the growth of microalgae', *Hydrobiologia*, vol. 358, no. 1–3, pp. 185–91.
- Genin, S.N., Aitchison, S.J. & Allen, G.D. 2014, 'Design of algal film photobioreactors: Material surface energy effects on algal film productivity, colonization and lipid content', *Bioresource Technology*, vol. 155, pp. 136–43.

- Gross, M., Henry, W., Michael, C. & Wen, Z. 2013, 'Development of a rotating algal biofilm growth system for attached microalgae growth with in situ biomass harvest', *Bioresource Technology*, vol. 150, pp. 195–201.
- Gross, M., Jarboe, D. & Wen, Z. 2015, 'Biofilm-based algal cultivation systems', *Applied Microbiology and Biotechnology*, vol. 99, no. 14, pp. 5781–9.
- Gross, M., Zhao, X., Mascarenhas, V. & Wen, Z. 2016, 'Effects of the surface physico-chemical properties and the surface textures on the initial colonization and the attached growth in algal biofilm', *Biotechnology for Biofuels*, vol. 9, no. 1, p. 38.
- Huang, Y., Zheng, Y., Li, J., Liao, Q., Fu, Q., Xia, A., Fu, J. & Sun, Y. 2018, 'Enhancing microalgae biofilm formation and growth by fabricating microgrooves onto the substrate surface', *Bioresource Technology*, vol. 261, pp. 36–43.
- Irving, T.E. & Allen, D.G. 2011, 'Species and material considerations in the formation and development of microalgal biofilms', *Applied Microbiology and Biotechnology*, vol. 92, no. 2, pp. 283–94.
- Laamanen, C.A., Ross, G.M. & Scott, J.A. 2016, 'Flotation harvesting of microalgae', *Renewable and Sustainable Energy Reviews*, vol. 58, pp. 75–86.
- Melo, M., Fernandes, S., Caetano, N. & Borges, M.T. 2018, 'Chlorella vulgaris (SAG 211-12) biofilm formation capacity and proposal of a rotating flat plate photobioreactor for more sustainable biomass production', *Journal of Applied Phycology*, pp. 1–13.
- Molina Grima, E., Belarbi, E.H., Acien Fernández, F., Robles Medina, A. & Chisti, Y. 2003, 'Recovery of microalgal biomass and metabolites: process options and economics', *Biotechnology Advances*, vol. 20, no. 7, pp. 491–515.
- Ozkan, A. & Berberoglu, H. 2013, 'Cell to substratum and cell to cell interactions of microalgae', *Colloids and Surfaces B: Biointerfaces*, vol. 112, pp. 302–9.
- Pruvost, J., Cornet, J.F. & Pilon, L. 2016, 'Large-scale production of algal biomass: photobioreactors', in F. Bux & Y. Chisti (eds), *Algae Biotechnology*, Springer, Cham (pp. 41–66).
- Schnurr, P.J. & Allen, D.G. 2015, 'Factors affecting algae biofilm growth and lipid production: a review', *Renewable and Sustainable Energy Reviews*, vol. 52, pp. 418–429.
- Sebestyén, P., Blanken, W., Bacsa, I., Tóth, G., Martin, A., Bhajji, T., Dergez, Á., Kesserű, P., Koós, Á. & Kiss, I. 2016, 'Upscale of a laboratory rotating disk

biofilm reactor and evaluation of its performance over a half-year operation period in outdoor conditions', *Algal Research*, vol. 18, pp. 266–72.

Tao, Q., Gao, F., Qian, C.Y., Guo, X.Z., Zheng, Z. & Yang, Z.H. 2017, 'Enhanced biomass/biofuel production and nutrient removal in an algal biofilm airlift photobioreactor', *Algal Research*, vol. 21, pp. 9–15.

Vree, J.H., Bosma, R., Janssen, M., Barbosa, M.J. & Wijffels, R.H. 2015, 'Comparison of four outdoor pilot-scale photobioreactors. *Biotechnology for biofuels*', vol. 8, no. 1, pp. 215–27.

Zeng, X., Guo, X., Su, G., Danquah, M., Chen, X. & Lin, L. 2016, 'Harvesting of Microalgal Biomass', in F. Bux & Y.Chisti (eds), *Algae Biotechnology*, Springer, Cham, pp. 77–89.

Zheng, Y., Huang, Y., Liao, Q., Zhu, X., Fu, Q. & Xia, A. 2016, 'Effects of wettability on the growth of *Scenedesmus obliquus* biofilm attached on glass surface coated with polytetrafluoroethylene emulsion', *International Journal of Hydrogen Energy*, vol. 41, no. 46, pp. 21728–35.